**International Scientific-Theoretical and Production Journal**

# ADVANCES IN ELECTROMETALLURGY

3, 2007

Quarterly

English translation of the quarterly «Sovremennaya Elektrometallurgiya» journal published in Russian since January 1985

***Founders:*** *E.O. Paton Electric Welding Institute of the NASU*
*International Association «Welding»*

***Publisher:*** *International Association «Welding»*



*Editorial and advertising offices are located at PWI:*
International Association «Welding»,
E.O. Paton Electric
Welding Institute of the NASU,
11, Bozhenko str., 03680,
Kiev, Ukraine
Tel.: (38044) 287 67 57,
529 26 23,
Fax: (38044) 528 04 86
E-mail: journal@paton.kiev.ua
http://www.nas.gov.ua/pwj

*Subscriptions:*
4 issue per year;
**184$** — regular, **150$** — for subscription agencies, **100$** — for students;
postage and packaging included.
Back issues available.



# CONTENTS

# PRODUCTION OF INCREASED STRENGTH TITANIUM BY ITS DOPING WITH OXYGEN IN PROCESS OF CHAMBER ELECTROSLAG REMELTING

**A.D. RYABTSEV**[1], **S.I. DAVYDOV**[2], **A.A. TROYANSKY**[1], **L.Ya. SHVARTSMAN**[2], **O.A. RYABTSEVA**[1], **V.V. PASHINSKY**[1] and **K.L. FEOFANOV**[2]
[1]National Technical University, Donetsk, Ukraine
[2]Company «ZTMK», Zaporozhie, Ukraine

Possibility of using oxygen-containing master alloy for controllable introduction of oxygen to titanium for the purpose of increasing its strength characteristics is shown. The method of chamber electroslag remelting of the composite consumable electrode is used.

*Keywords: titanium, oxygen, additional alloying, chamber ESR, hardness, structure*

Titanium is one of the most distributed elements in the nature. Despite the fact that this metal was discovered as long as in 1791, it's application as of independent structural material and basis of alloys started just a little more than fifty years ago after successes achieved in the field of metallurgy of active metals and alloys.

Titanium alloys are used in the fields of technology, where high specific strength and resistance to impact loads are needed. At present in national and foreign machine building commercial titanium and (to a greater degree) its low-alloyed alloys are used because of higher strength characteristics.

In addition to improvement of the technology for production of the titanium sponge as an initial feedstock, quality of titanium and its alloys was improved. Due to sharp reduction of harmful impurities, in particular gases, plasticity and toughness of titanium and titanium-base alloys increases. However, high-purity titanium is not always widely used as a structural material, because at high plasticity it has low strength.

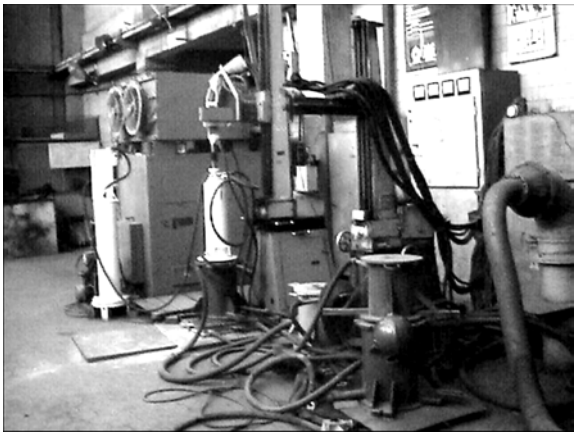

**Figure 1.** General view of ESR chamber furnace

Significant strength increase is achieved by alloying of titanium using different elements, in particular, aluminium and vanadium. So, lately titanium-base alloys, having strength which exceeds 4–5 times that of the iodide titanium, are used.

At the same time, in case of application of the titanium alloys for items of the medical equipment the most important requirements are corrosion resistance and biocompatibility. At present for this purpose the VT6S-type titanium alloys are used. However, presence of vanadium (the alloying component) in the alloy can cause under certain conditions [1] formation of unsafe for a human organism chemical compounds. That's why development of the titanium alloys, alloyed by safe elements, is a rather actual task.

In this respect oxygen, as a titanium-strengthening element, is of interest. At high temperatures it easily dissolves both in $\alpha$-Ti and $\beta$-Ti [2], forming interstitial solutions. Maximal solubility of oxygen in titanium constitutes about 30 at.%. Oxygen effects most noticeably mechanical properties of titanium at its content in the metal up to 0.6 wt.% [3], whereby significant increase of strength characteristics at relatively insignificant worsening of plastic properties was registered.

So, by controlling content of oxygen in titanium one can effect its mechanical properties to a significant degree, whereby it is necessary to keep in mind that compounds of oxygen with titanium are harmless for a human organism and used in pharmaceutics and medicine [4].

Production of titanium, doped by oxygen, requires for development of a reliable metallurgical technology for introduction of oxygen into the metal and ensuring of its uniform distribution over height and section of the ingots and casts.

Such technology can be developed on the basis of the special electrometallurgy processes, in particular chamber electroslag remelting (CESR). The latter

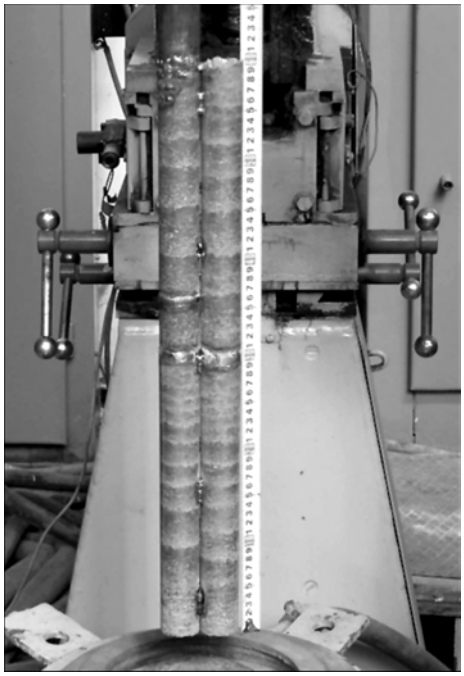

**Figure 2.** Pressed consumable built-up electrode

one in addition to the known flexibility in additional alloying allows ensuring high purity, as well as structural and chemical homogeneity of the material, due to uniform melting of the consumable electrode with the master alloy and simultaneous solidification of the ingot in the controllable atmosphere [5–8].

It is suggested to use so called titanium-oxygen master alloy as the oxygen-containing material. Sweepings of the reaction mass from the retort cover, subjected to a special seasoning in air for the purpose of their saturation with oxygen and nitrogen and then to vacuum separation for removal of magnesium and chlorine residues, are initial feedstock for its production [9]. From this material satellite-electrodes for CESR were made by the pressing method.


**Figure 3.** ESR ingot from TG-110 titanium sponge (melt 1)

Remelting was performed in the chamber electroslag furnace, developed on basis of the A-550 unit (Figure 1). The unit allows degassing the working space down to the residual pressure 665–1330 Pa at low inflow of the atmospheric air and performing remelting in the inert gas at normal and excessive (up to the level $(3–5)\cdot10^4$ Pa values of the pressure, which ensures exclusion of atmospheric air suction into the furnace melting space and preservation of the getter activity of condensate of the flux metal component.

The water-cooled chamber was installed directly on flange of the mould upper part, and before melting it was pumped off and then filled with argon. In the course of melting excessive pressure of argon (about 15 kPa) was maintained in the system for compensation of its possible losses.

The billets, pressed separately from the grade TG-110 titanium sponge and from sweepings of the reaction mass of 40 mm diameter and 300 mm length, were argon-arc welded into the consumable electrodes of 600 mm length (Figure 2).

The produced built-up electrodes were remelted into copper water-cooled mould of 115 mm diameter

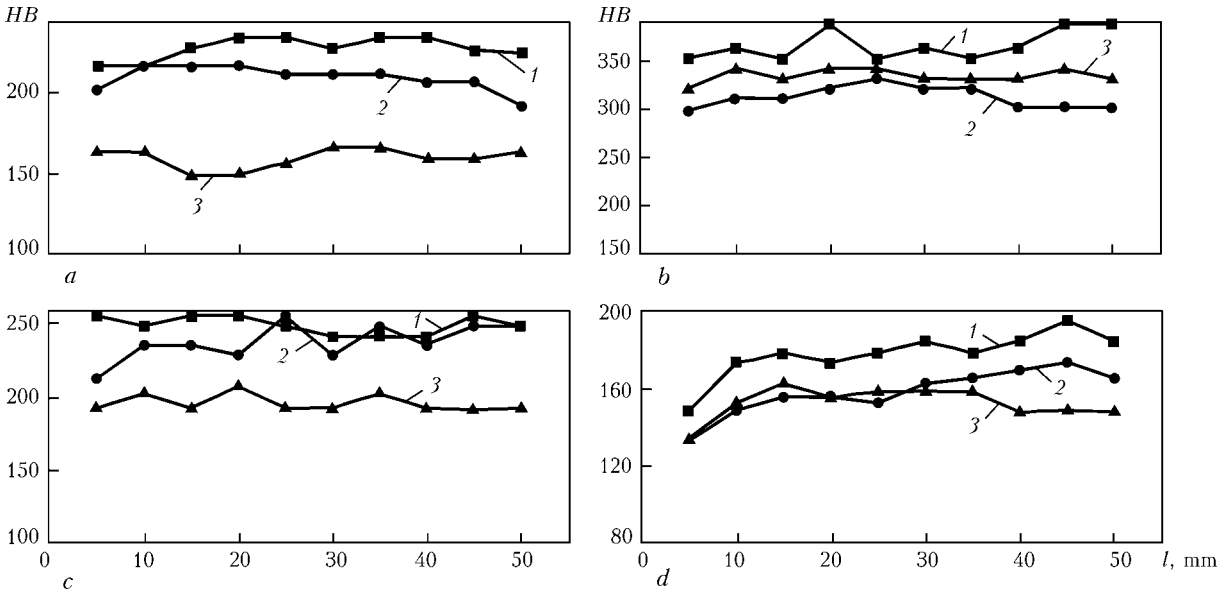


**Figure 4.** Distribution of hardness over section of samples: *a–d* — melt 1–4, respectively; *1* — bottom; *2* — middle; *3* — head; *l* — distance from center of ingot

Results of experimental metal investigation

| Type of electrode | Slag composition | Weight share of impurities, % | | | | | | *HÂ* | $\sigma_t$, MPa | δ, % |
|---|---|---|---|---|---|---|---|---|---|---|
| | | Fe | Si | Ni | Ñ | N | Î | | | |
| TG-110 titanium sponge | – | 0.056 | 0.003 | 0.032 | 0.004 | 0.011 | 0.044 | 105 | – | – |
| Melt 1 (TG-110) | $CaF_2$ | 0.090 | 0.002 | 0.032 | 0.015 | 0.055 | 0.100 | 150–200 | 438 | 12.0 |
| Melt 2 (RM) | $CaF_2$ | 0.090 | 0.003 | 0.018 | 0.016 | 0.098 | 0.400 | 300–360 | 708 | – |
| Melt 3 (50 % TG-110 + 50 % RM) | $CaF_2$ | 0.080 | 0.004 | 0.019 | 0.011 | 0.110 | 0.300 | 200–260 | 637 | 10.8 |
| Melt 4 (TG-110) | $CaF_2$ + Ca | 0.044 | 0.003 | 0.034 | 0.015 | 0.033 | 0.070 | 135–180 | 480 | 16.0 |

and 500 mm length. The following versions were considered: melt 1 –– electrode from 100 % TG-110 titanium sponge; melt 2 –– electrode from 100 % reaction mass (RM); melt 3 –– built-up electrode from 50 % TG-110 titanium sponge and 50 % RM; melt 4 –– electrode from 100 % TG-110 titanium sponge.

Powder of calcium fluoride $CaF_2$ of grade Ch (TU 6-09-5335–88), calcinated at the temperature 973 K for 3 h, and metal calcium were used as the flux-forming materials. The flux was melted directly in the mould using «solid» start. Remelting was performed using flux from pure $CaF_2$ (melts 1–3) and flux of the $CaF_2$ + Ca system (melt 4). Electrical parameters were maintained at the constant level ($U$ = 47 V, $I$ = = 3 kA), ensuring good quality of surface formation of the ingots being melted.

The ingots were cooled in the mould for about 30 min and then they were «undressed». They had smooth side surface (Figure 3). Slag cap and skull separated easily. The ingots were subjected to ultrasonic control (USC) at the frequency 5 MHz using the Krautkramer Branson instrument USN 52, then they were cut along longitudinal axis, and samples were taken for investigation of chemical composition and structure of the metal in the cast state. The structure was investigated at magnifications 50–500 on the microscopes «Neophot-21» and «Neophot-2». The samples were photographed by digital camera, and the digitized file was analyzed using computer program Image Tool for obtaining quantitative characteristics of the structure. Hardness was measured on the Rockwell instrument according to *HRC* scale and then using the tables converted into *HB*. Gas content in metal of the samples was determined on the LECO instrument.

The results of chemical analysis and mechanical tests of the metal of experimental ingots are presented in the Table. Hardness values are presented in Figure 4.

It is established that hardness of the metal of experimental ingots increases as content of oxygen in them gets higher. So, the highest hardness is characteristic of the specimens with 0.4 wt.% O (melt 2),

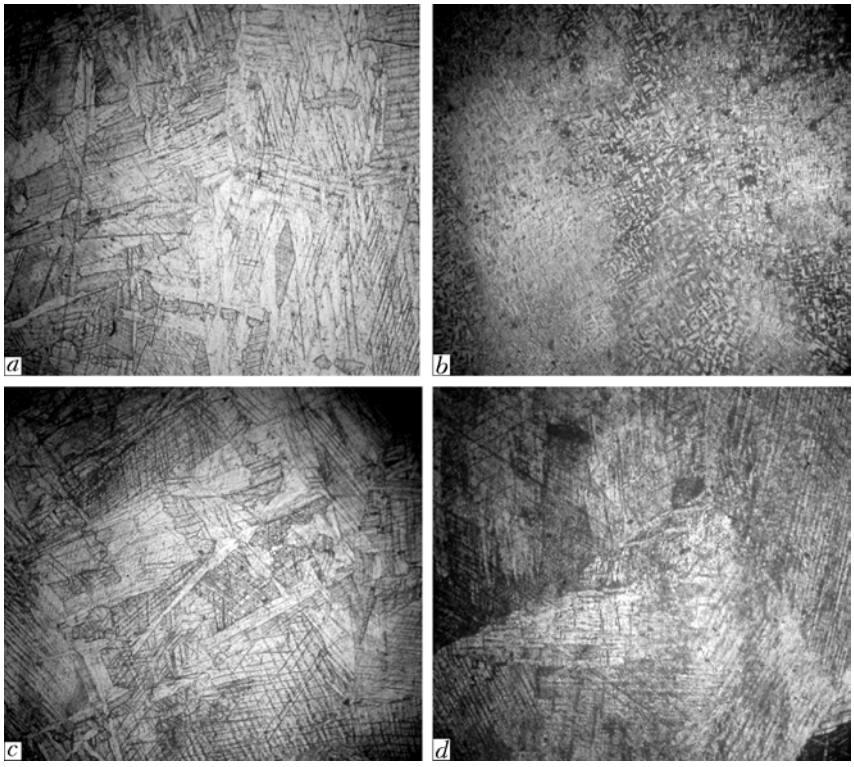


**Figure 5.** Metal microstructure: *a*–*d* –– melt 1–4, respectively (×50)

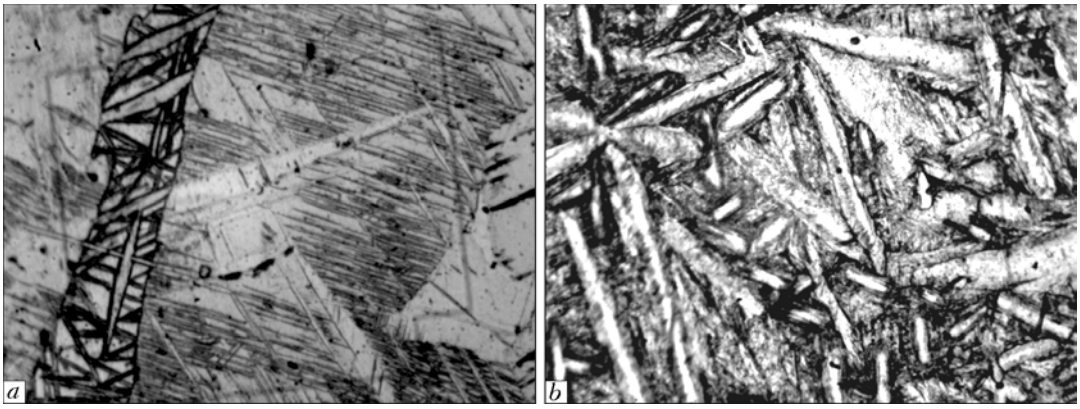

**Figure 6.** Metal microstructure: *a* — melt 4; *b* — melt 2 (×500)

and the lowest — with 0.07 wt.% O (melt 4), whereby in the radial direction (from the surface to the center) hardness in all ingots at all levels remains approximately constant, which proves uniform distribution of the impurities over horizontal section of the ingots. At the same time, the trend was registered of hardness increase from head of the ingot to its bottom. This is connected with transition of the impurities from the flux into the metal at initial stages of the ingot formation.

Microstructure of metal of the sample, cut out from the middle of the ingots, is presented in Figures 5 and 6.

As one can see from the Figures, the metal of all melts has single-phase α- or α′-structure, dispersity of which depends upon weight share of oxygen. Microstructure of the metal, when content of oxygen in it constitutes 0.1 % (melt 1), is typical for the commercial titanium. Increase of weight share of oxygen up to 0.3 % (melt 3) does not cause significant change of the α-phase morphology. Increase of dispersity of the α-phase packages was registered.

At further increase of oxygen content in titanium up to 0.4 % (melt 2) the microstructure acquires a typical acicular character, which allows its classifying as α′-phase. Formation of this structure is accompanied by sharp increase of hardness. At low weight share of oxygen (0.07 %) in titanium, which can be ensured by CESR using the flux containing metal calcium (melt 4), the microstructure close to the typical one for commercial titanium is formed similar to the metal structure of melts 1 and 3.

Results of the tests (see the Table) show that changes of mechanical characteristics correlate with the structural ones. In the metal with increased content of oxygen (0.3–0.4 %) significant increase of the strength characteristic values was discovered. At the same time, in melt 3 level of ductility, close to that of the commercial titanium, is preserved, while formation of α′-phase in the metal of melt 2 causes complete loss of ductility.

So, analysis of presented microstructures of the experimental metal proves influence of oxygen content in titanium within considered range on change of their morphology and formation of phases.

## CONCLUSIONS

1. It is established that oxygen may be used as economically doping element that allows significant increasing strength level of titanium due to reduction of the natural reserve of its plastic characteristics.

2. It is shown that the CESR as a metallurgical process makes it possible to introduce by means of the additional alloying necessary amount of oxygen into titanium and ensure in this way chemical homogeneity of the ingot metal.


1. (1978) *Concise chemical reference book*. Ed. by V.A. Rabinovich. Leningrad: Khimiya.
2. (1999) *Constitution diagrams of binary metal systems*: Reference Book. Ed. by N.P. Lyakishev. Vol. 3. Book 1. Moscow: Mashinostroenie.
3. (1979) *Metallurgy and technology of welding of titanium and its alloys*. Ed. by S.M. Gurevich. Kiev: Naukova Dumka.
4. Nikolaev, G.I. (1987) *Metal of century*. Moscow: Metallurguiya.
5. Ryabtsev, A.D., Troyansky, A.A. (2001) Production of ingots of titanium, chrome and alloys on their base in chamber furnaces using the «active» metal-containing fluxes. *Problemy Spets. Elektrometallurgii*, **4**, 6–10.
6. Ryabtsev, A.D., Troyansky, A.A. (2005) Electroslag remelting of metals and alloys using the fluxes containing active additives in furnaces of chamber type. *Elektrometallurguiya*, **4**, 25–30.
7. Ryabtsev, A.D., Troyansky, A.A., Korzun, E.L. et al. (2002) Metal alloying with nitrogen from gas phase in ESR process. *Advances in Electrometallurgy*, **4**, 2–6.
8. Ryabtsev, A.D., Troyansky, A.A., Pashinsky, V.V. et al. (2002) Application of electroslag technology for refining titanium and titanium alloys from nitrogen-rich inclusions. *Ibid.*, **3**, 8–11.
9. Davydov, S.I., Shvartsman, L.Ya., Ovchinnikov, A.V. et al. (2006) Some features of titanium alloying with oxygen. In: *Proc. of Int. Sci.-Techn. Conf. on Ti-2006 in CIS Countries* (Suzdal, Russia, May 21–24, 2006). Kiev: Naukova Dumka, 253–257.

# PRODUCTION OF VANADIUM-CONTAINING HARDENERS WITH APPLICATION OF ELECTROSLAG TECHOLOGY

**F.K. BIKTAGIROV, B.I. KHUDIK, M.L. ZHADKEVICH, K.K. PROKHORENKO, V.A. SHAPOVALOV, A.D. KOROSTIN** and **V.M. MURATOV**
E.O. Paton Electric Welding Institute, NASU, Kiev, Ukraine

Investigations were carried out and highly efficient technology for melting by the method of silicothermic reduction in electroslag furnace from the converter vanadium slag of the vanadium-containing hardener was developed. Weight share of vanadium in the produced hardener was 17–22 % and silicon — 4–7 %. The degree of vanadium recovery into the metal achieved 92–95 % at residual content of $V_2O_3$ in the waste slag being up to 0.5 %.

*Keywords: vanadium slag, electroslag melting, silicothermic reduction, degree of recovery, vanadium-containing hardener*

Vanadium is one of efficient alloying elements widely used in production of cast iron, steels and alloys. So, according to certain forecasts, by mid-XXI century from 20 to 30 % of the whole world production will constitute steels alloyed by vanadium.

The main vanadium-containing material in metallurgy is ferrovanadium with weight share of vanadium 35–80 %. Such ferrovanadium is the product of igneous metallurgical conversion of the commercial vanadium pentoxide (75–95 % $V_2O_5$) produced by the hydrometallurgical method from the slag, used in converter removal of vanadium from the cast iron melted in blast furnaces from the enriched vanadium-containing titanium-magnetite ores.

Production of the vanadium converter slag in the territory of CIS is mainly concentrated at Nizhny Tagil Metallurgical Works (NTMK). It has the following average chemical composition, %: 18–22 $V_2O_5$; 14–18 $SiO_2$; 8–11 MnO; 7–10 $TiO_2$; 2–4 $Cr_2O_3$; 1–4 CaO; 2–4 MgO; 1–3 $Al_3O_3$; 0.03–0.06 P; 26–32 $Fe_{total}$ (in the form of oxides). In addition, this slag contains metal inclusions (iron) in the form of entrapped cold shots in the amount 8–12 % (above 100 %) [1].

Due to multistage processing of the titanium-magnetite ores, containing 0.1–1.5 % $V_2O_3$, complete recovery of vanadium from the iron-vanadium concentrate up to ferrovanadium constitutes less than 50 %, whereby the highest losses occur at the stage of recovery from the vanadium slag of vanadium pentoxide. This fact and significant labor input and energy consumption predetermine high cost of ferrovanadium, which often constrains production of the vanadium-containing steels. That's why mastering of different technologies, which ensure more rational recovery of vanadium, is of great importance in complex processing of mentioned titanium magnetite.

One of such technologies is production of the vanadium-containing hardeners directly from the NTMK converter slag, which allows significant reducing of losses. These hardeners are quite applicable for alloying with vanadium of the majority of developed vanadium steels, especially taking into account the fact that content of vanadium in them is 0.03–0.20 %.

In studies [2–6] data are presented on the processes of carbo-, silico- and alumothermic reduction and melting in ore heat-treating furnaces from the NTMK converter slag of vanadium hardeners with weight share of vanadium from 8 to 15 %, among which the most acceptable from the economic viewpoint are two first mentioned methods.

Carbothermic method allows fuller recovering of vanadium from the slag, but in this case manganese, titanium and silicon are reduced to a significant degree, due to which weight share of the latter in the hardener constitutes 35–40 %. In addition, in the course of this process vanadium, titanium and chromium carbides inevitably form that causes production of the alloy with increased content of carbon.

Silicothermic method has much less shortcomings of this kind, but the developed technologies ensure comparatively low degree of vanadium recovery — approximately 70 % [4].

For successful reduction of vanadium oxides by silicon, especially of the lowest $V_2O_3$ and VO, it is necessary to reduce activity of silica being formed. That's why in silicothermic processing of the vanadium slags their basicity is increased by the lime additives, and reduction process is described by the following reactions:

$$2/5V_2O_5 + Si + XCaO = 4/5V + XCaO \cdot SiO_2; \quad (1)$$

$$2/3V_2O_3 + Si + XCaO = 4/3V + XCaO \cdot SiO_2; \quad (2)$$

$$2VO + Si + XCaO = 2V + XCaO \cdot SiO_2. \quad (3)$$

According to the data of studies [7–10] devoted to investigation of thermodynamics of the CaO–$Al_2O_3$–$SiO_2$ system slags, among various calcium-silicon compounds the most negative change of the Gibbs energy occurs in formation of dicalcium silicate, i.e. the best thermodynamic conditions for progress of the reactions (1)–(3) will be at $X = 2$.

So, for binding of silica, which is originally present in the NTMK slag and forms in the reduction reaction, significant additives of calcium oxide are necessary. As a result, silicothermic process is accompanied by oxide melt formation (slag) in large quantitis, whereby multiplicity of the slag may constitute 3.5–4.0, and taking into account triple difference in values of density, physical volume of the slag exceeds more than 10 times volume of the metal, i.e. silicothermic method may be presented as process of the lime-silicate slag melting accompanied by reduction of vanadium. That's why for its implementation not classical ore heat-treating process, but the electroslag one is more acceptable [11].

Successful application of the electroslag technology should be enabled by correspondence of physical properties (toughness and electric conductivity) of the initial converter and final lime-silica slag to the requirements of stable progress of the melting process under conditions of resistance or similar to them (Figure 1). Melting point of the initial vanadium slag is about 1673, and of the final one — 1423–1523 K.

Electroslag processing of the vanadium-containing NTMK slag (hereinafter ShVd-1) was investigated for the purpose of high-efficiency technology development for production of vanadium-containing hardeners. First analysis of thermo-chemical phenomena, which accompany high-temperature treatment of the ShVd-1 slag, was carried out. Reduction of vanadium oxides under real conditions is not limited by progress of the reactions (1)–(3), because in the oxidation-reduction processes simultaneously participate other compounds, as well as formed intermediate products of the reactions — sub-oxides, silicides, carbides, etc., which can be in relation to the vanadium oxides both reducing and oxidizing agents. So, for analysis of the proceeding reactions it is necessary to use a respective mathematical apparatus.

Interaction of substances in the multicomponent systems till they achieve state of equilibrium can be estimated by means of the multi-purpose «Astra-4» software, developed by Moscow Technical University and Institute of High Temperatures of USSR Academy of Sciences on the basis of processing and generalization of all available physical-chemical and thermodynamic constants of the known substances. Respective calculations with application of preset initial data (charge composition, temperature conditions of the process) allow calculating equilibrium composition of the formed substances and ratio of the phases (metal, slag, and gas ones).

Expediency of using this kind of the program for metallurgical calculations is noted in [12], including processes of the vanadium converter slag reduction [13]. At present this program and its versions are widely used by the specialists.

It is necessary to take into account that such calculations do not give absolutely accurate results, because it is impossible to take into account all peculiarities of a specific task. For example, in case of processing of the ShVd-1 slag the program does not take into account presence of vanadium oxides in complex compounds of the spineleid type (Fe, Mn, Mg)O·(V, Fe, Cr)$_2O_3$, which brings certain changes into the character of interaction of the charge components. In addition, any chemical analysis has a certain error, and under real conditions it is impossible to exactly observe the preset temperature. Nevertheless, these calculations allow correct assessing dynamics of various changes and significant reducing number of specifying analyses and experiments.

For calculations according to the «Astra-4» program, composition of the ShVd-1 slag, indicated in its certificate, was preset, %: 20$V_2O_5$; 35FeO; 18$SiO_2$; 7MnO; 5$Cr_2O_3$; 8$TiO_2$; 2CaO; the rest — magnesium and aluminium oxides and other impurities, which were not taken into account in the calculations. As the reducer silicon in the form of 75 % ferrosilicon

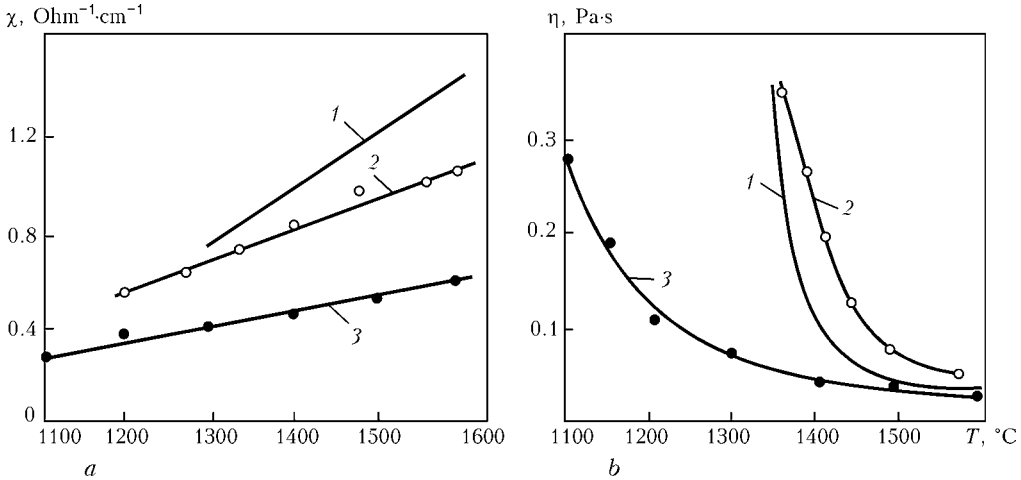


**Figure 1.** Electric conductivity (*a*) and toughness (*b*) of slags: *1* — ANF-6; *2* — initial vanadium; *3* — final lime-silicate

Calculated data of ShVd-1 slag silicothermic reduction

| Additives of ShVd-1 slag mass, % | Weight share of components, % | | | | | | |
|---|---|---|---|---|---|---|---|
| | Metal phase | | | | | | Slag phase |
| | V | $V_5Si_3$ | Mn | Cr | $Cr_3Si$ | $Ti_5Si_3$ | |
| – | – | – | – | – | – | – | $V_2O_3$ — 17.0 %; FeO — 30.0 %; $Fe_3O_4$ — 7.0 %; MnO — 7.0 %; $Cr_2O_3$ — 5.0 %; $TiO_2$ — 7.0 %; $SiO_2$ — 18.0 %; $CaTiO_3$ — 4.0 % |
| 20 FeSi, 80 CaO | 11.8 | 3.5 | 5.5 | 3.6 | – | – | $V_2O_3$ — 3.2 %; $Cr_2O_3$ — 1.6 %; MnO — 2.3 %; $Ca_3Si_2O_7$ — 79.8 %; $CaSiO_3$ — 2.5 %; $CaTiO_3$ — 9.2 % |
| 25 FeSi, 80 CaO | 11.1 | 12.0 | 9.2 | 5.0 | 0.8 | 0.5 | $Ca_3Si_2O_7$ — 85.6 %; $CaSiO_3$ — 3.8 %; $CaTiO_3$ — 9.0 % |
| 30 FeSi, 100 CaO | – | 24.8 | 8.9 | 3.7 | 2.2 | 1.2 | $Ca_3Si_2O_7$ — 81.4 %; $Ca_3Ti_2O_7$ — 8.6 %; CaO — 8.1 % |
| 25 FeSi, 60 CaO | 5.5 | 12.5 | 9.5 | 5.1 | 1.3 | 3.5 | $V_2O_3$ — 3.1 %; $Ca_3Si_2O_7$ — 39.5 %; CàSiO$_3$ — 48.5 %; $CaTiO_3$ — 7.4 % |

and as the flux agent ---- calcium oxide were added to the slag.

Results of certain versions of the calculations for the temperature value 2000 K are presented in the Table. Here in the first line change of the ShVd-1 slag composition in case of its melting without any additives is shown.

According to the calculated data, reduction of the contained in the ShVd-1 slag oxides and composition of the produced metal and slag phases depend upon the amount and the ratio of the introduced reducer and flux agent. In case of lack of silicon (ferrosilicon) in the charge, in the slag phase remain oxides not just of vanadium, but also of manganese and chromium, and in case of a comparatively small amount of calcium oxide only vanadium oxides are reduced not to the full degree. «Free», i.e. not bound with other elements, calcium oxide forms in the final slag in case of presence in the charge of more than 80 % CaO (provided content of silicon is not more than 20 %), that's why the calculations show inexpediency of high amount of its additives.

In case of excess of ferrosilicon, the whole vanadium in the produced hardener binds into silicides, that causes increase of weight share of silicon in the metal. According to the data of these calculations, at the temperature 1900 K amount of the formed gas phase constitutes about 1 % of the whole charge mass. This value gets higher by means of the temperature increase, and at the temperature 2100 K already achieves 9 % (Figure 2), which is mainly stipulated by evaporation of manganese. Simultaneously, but to a lesser degree, losses of chromium and vanadium occur. That's why temperature increase is undesirable for silicothermic processing of the vanadium-containing slag.

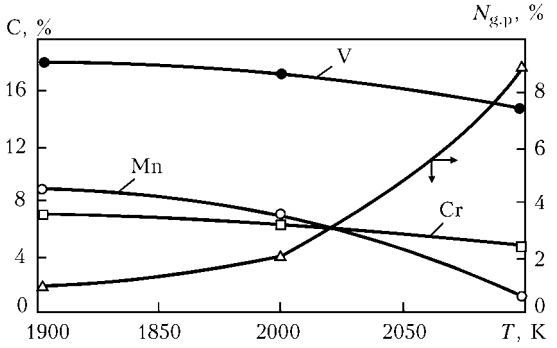


**Figure 2.** Influence of temperature on amount of formed gas phase $N_{g.p}$ and content of vanadium, manganese and chromium in hardener in silicothermic reduction of vanadium-containing slag

Taking into account results of calculations, in the electroslag 260 kW furnace experimental processing melts of the ShVd-1 slag were performed. They were carried out in periodic mode and terminated by pouring of the formed products into the cast iron mould, whereby the produced hardener contained 8–10 % V and about 10 % Si, and in the slag remained up to 3–5 % of vanadium oxides, mainly in the form of $V_2O_3$. Degree of vanadium reduction did not exceed 70 %.

These results (combination of increased amount of silicon in the metal and vanadium oxides in the slag) prove that rate of melting exceeds rate of progress of the reduction processes. That's why in the course of the charge melting not the whole reducer manages to react with the oxides being reduced, and its residue transits into the metal.

Seasoning of melting products in the furnace enables increase of the vanadium recovery degree due to interaction of the available in the metal pool silicon with vanadium oxides, which are present in the slag melt. However, this method causes reduction of the process productivity, increase of power consumption, and additional heat load on structural elements of the furnace.

In [2] in silicothermic processing and melting of the NTMK converter slag in the ore heat-treating furnace the technology was suggested and tested, at which only a portion (a bigger one) of the necessary ferrosilicon was put into the charge, while the rest was fed into the furnace before pouring, which made it possible to improve parameters of the vanadium recovery.

We took steps to increase efficiency of vanadium recovery in the course of electroslag processing of the vanadium-containing slag. They concerned both

preparation of the charge and optimization of the conditions of melting technology, including electrical parameters of the process.

In the produced according to the corrected technology hardener, weight share of vanadium increased up to 12–13 %, and silicon reduced down to 5–7 %. Residual content of $V_2O_3$ in the slag reduced down to 2.0–2.5 %, and degree of vanadium recovery achieved 80–85 %.

As one can see, the results turned out to be significantly better than the previous ones, however significant amount of not completely reduced vanadium remained in the slag. Neither long seasoning of slag and metal melts in the furnace, nor additives of ferrosilicon and even aluminium managed to significantly improve vanadium recovery results.

Difficulty of vanadium oxide recovery from the ShVd-1 slag is, evidently, determined by the fact that they are in complex compounds and bound with other oxides. That's why it is necessary to weaken these bonds by means of the flux components and lime additives.

Carried out investigations showed that increase of basicity of the final processed ShVd-1 slag enabled increased degree of vanadium recovery into the metal (Figure 3). In addition, this improves conditions of refining of the melted material, including refining from sulfur, which is an essential factor in its further application. Additionally for increasing sulfur-absorbing capacity of the formed slag, fluorite was added into the charge [14]. So, at optimal basicity final content of $V_2O_3$ in the waste slag reduces down to 0.5 %, and degree of vanadium recovery increases up to 92–95 %, whereby up to 50 % of vanadium-containing hardener of the following composition is produced from the ShVd-1 slag, %: 17–22 V; 4–7 Si; 2–6 Cr; 5–10 Mn; 2–3 Ti; 0.1–0.4 C; 0.01–0.05 P; 0.02–0.03 S; Fe ---- the rest.

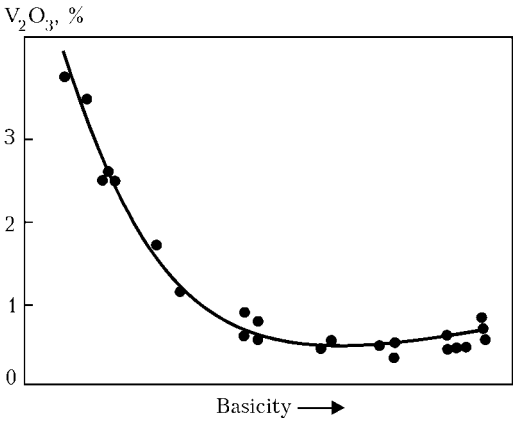


**Figure 3.** Influence of final slag basicity on degree of reduction of vanadium oxide

The developed technology of the converter slag silicothermic reduction passed commercial check in the modernized UO-109 electroslag furnace (design of the PWI Design Office) equipped with power supply sources of up to 1 MW power (Figure 4). The results obtained confirmed efficiency of the technology.

For improvement of the melting conditions and reduction of dust release and losses of the material, the process of the charge briquetting was mastered, which, in addition to reduction of load on the gas cleaning equipment, allowed reducing duration of melting and increasing of productivity. Consumption of electric power for processing of 1 t charge was 700–900 kW, and in recalculation into 1 t of the produced hardener ---- 3500–4500 kW.

At present feasibility study is prepared and design of the workshop is developed, which would allow

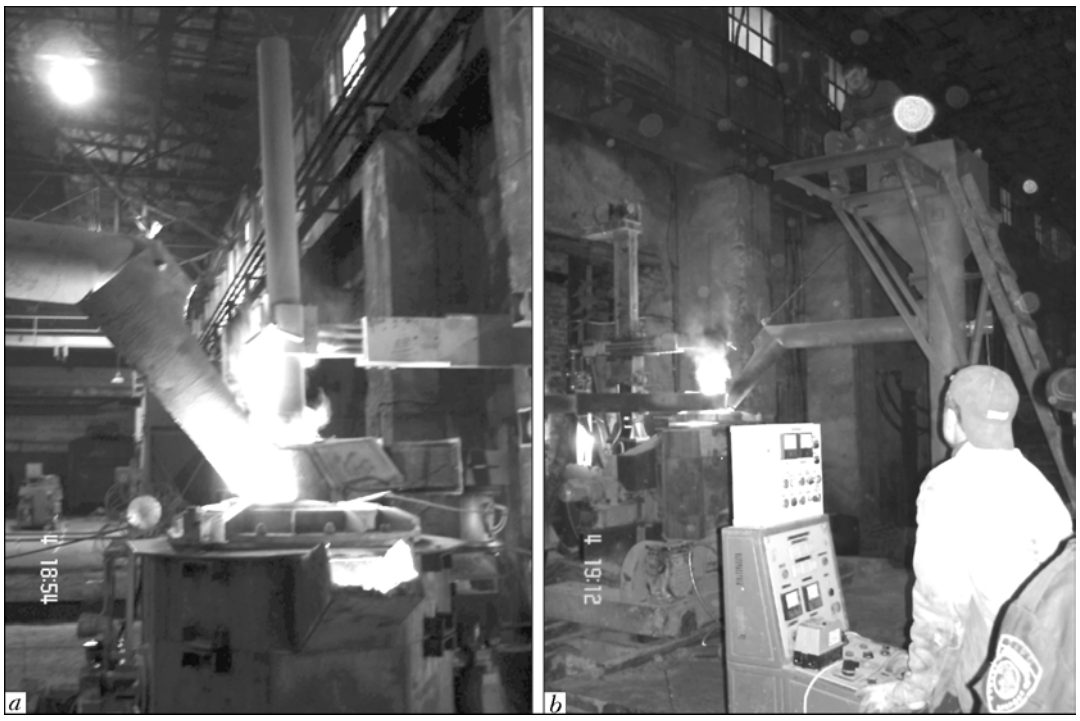


**Figure 4.** Melting of vanadium slag in electroslag furnace: *a* — furnace; *b* — melting process

processing of 10,000 t of the NTMK vanadium-containing slag per year, which is planned to be located at one of the Ukrainian enterprises.

Investigations, connected with vanadium recovery from the ShVd-1 slag, are continued for the purpose of the technology optimization and reduction of the production expenses, in particular by replacement in the charge of a portion of ferrosilicon for coke, i.e. development of a combined single-stage carbosilicothermic process. Similar technology is mentioned in [1], but it lacks data on peculiarities of such process.

One more promising method of the vanadium-containing hardener reduction may by duplex process, i.e. two-stage melting with primary reduction of iron, production of the enriched with vanadium slag, and subsequent melting from it of ferrovanadium with weight share of vanadium from 40 to 50 %.


1. Filippenkov, D.A., Deryabin, Yu.A., Smirnov, L.A. (2001) *Efficient technologies of steel alloying with vanadium*. Ekaterinburg.
2. Bajramov, B.I., Zajko, V.P. (1981) Melting of vanadium-containing master alloys. *Stal*, **7**, 37–39.
3. Ryss, M.A. (1985) *Production of ferroalloys*. Moscow: Metallurgiya.
4. Salnikov, G.I., Kanaev, Yu.P., Lukin, S.V. et al. (1985) Production of vanadium-silicon in industrial ore-smelting electric furnace. *Stal*, **10**, 45–47.
5. Zajko, V.P., Zhuchkov, V.I., Leontiev, L.I. et al. (2004) *Technology of vanadium-containing ferroalloys*. Moscow: Akademkniga.
6. Zhuchkov, V.I., Shiukov, O.Yu., Leontiev, L.I. et al. (2005) Production and application of vanadium-containing ferroalloys. *Tekhnologiya Metallov*, **9**, 2–4.
7. Gasik, M.I., Lyakishev, N.P., Emlin, B.I. (1988) *Theory and technology of ferroalloy production*. Moscow: Metallurgiya.
8. Babushkin, V.I., Matveev, G.M., Mchedlov-Petrosyan, O.P. (1972) *Thermodynamics of silicates*. Moscow: Strojizdat.
9. Emlin, B.I., Gasik, M.I. (1978) *Reference book on electrothermic processes*. Moscow: Metallurgiya.
10. Yakushevich, N.F., Kondratiev, D.V. (2000) Thermodynamics of primary slags in system $CaO$–$Al_2O_3$–$SiO_2$. *Izvestiya Vuzov. Chyorn. Metallurgiya*, **2**, 4–9.
11. Zhadkevich, M.L., Biktagirov, F.K., Shapovalov, V.A. et al. (2005) Application of electroslag melting for production of ferroalloys from mineral raw material. *Advances in Electrometallurgy*, **1**, 10–13.
12. Popel, S.I., Sotnikov, A.I., Boronenkov, V.N. (1986) *Theory of metallurgical processes*. Moscow: Metallurgiya.
13. Marshuk, L.A., Zhuchkov, V.I. (2003) Thermodynamic modeling of reduction process with aluminium of variable composition vanadium converter slag. *Elektrometallurgiya*, **6**, 25–30.
14. Biktagirov, F.K. (2003) Sulphide capacity of oxide-fluoride slags. *Advances in Electrometallurgy*, **4**, 13–15.

# ELECTROSLAG CASTING WITH MELTING TOGETHER
## Review

**M.L. ZHADKEVICH, V.L. SHEVTSOV** and **L.G. PUZRIN**
E.O. Paton Electric Welding Institute, NASU, Kiev, Ukraine

Review of publications, concerning ESC with melting together, is made. Peculiarities of this electroslag casting method are described, and data on quality of the metal of produced billets are presented. It is shown that properties of the metal in the melting together zone are not inferior after heat treatment to those of the cast electroslag metal. Examples of successful application of this kind of electroslag casting for production of billets from different grades of steel are given. The conclusion on expediency of using ESC method with melting together under present economic conditions for manufacturing special-purpose parts of complex shape is drawn.

*Keywords: electroslag casting, melting together, quality of the melting together zone metal, big crankshafts, equipment for NPP, rolls*

Electroslag casting (ESC) is the method for producing special-purpose shaped billets, which are later used in the cast form. Cast electroslag billets are frequently used instead of the forged pieces, because in regard to their service properties they are not inferior to the latter and in certain respects even exceed them [1]. High quality of the electroslag metal is ensured due to refining of the molten metal in the process of remelting and its subsequent directed hardening in the water-cooled casting mould [2].

In ESC the moulds are used, internal configuration of which corresponds with necessary allowances to the shape of the external surface of the future shaped billet. They are made dismountable and have a more complex design than the moulds, used for melting of the conversion ingots by the method of classical electroslag remelting (ESR).

The ESC method differs from ESR not just by the shape of the ingots being melted, but also by a number of technological peculiarities. So, in the course of melting in ESC depth of the slag and the metal pools may significantly change, which exerts significant influence on the electroslag process mode and conditions of structure formation of the billet being melted [3]. In addition, process of the billet core formation differs from that in the places of formation of the branch pipes and other protruding parts [4]. In these places a new solidification front is formed, direction of movement of which does not coincide with the main one, provided additional cooling surfaces are available. In the zone, where these fronts meet, defects of shrinkage origin may form [5].

The ESC method with melting together, in which in the process of electroslag melting of the main billet its connection with the previously fabricated parts takes place, does not have this defect. In this case conditions of solidification of the metal close to the classical ESR are preserved, which stably ensures the highest quality of the cast metal [3].

ESC with melting together makes it possible to fabricate billets of a much more complex shape and bigger dimensions than in case of using conventional ESC. Application of this method allows increasing productivity of casting and reducing consumption of auxiliary materials and electric power. In this method the moulds of simple shape and smaller size are used, which is especially important under present economic conditions.

Indisputable merit of ESC with melting together is possibility of producing composite billets, the parts of which are made from steel of different grades or cast iron. In addition, the billets can be successfully adjusted for application under different conditions of operation of their separate parts, like, for example, composite rolls of rolling mills [6].

Depending upon mutual arrangement of the billet being melted and the parts to be melted to it, three different ESC methods with melting together may be singled out.

According to the first one, parts of the future billet, manufactured in advance, are installed into special holes, made in walls of the dismountable mould.

According to the second method these parts are installed inside the mould.

According to the third method, the prepared parts are placed under or above the mould, in which electroslag melting of the billet is performed.

In ESC with melting together almost always shunting of the working current, which passes through the metal pool, by the parts being melted together is performed. Depth of penetration depends upon the current, which passes through the part being melted together. In development of the ESC technology with melting together it is extraordinary important in many cases to have possibility to control value of this current in order to guarantee quality melting together of a part without its excessive penetration.

Classical example of the first ESC method with melting together is electroslag melting of crankshafts or their separate parts (cranks). Crankshaft is one of

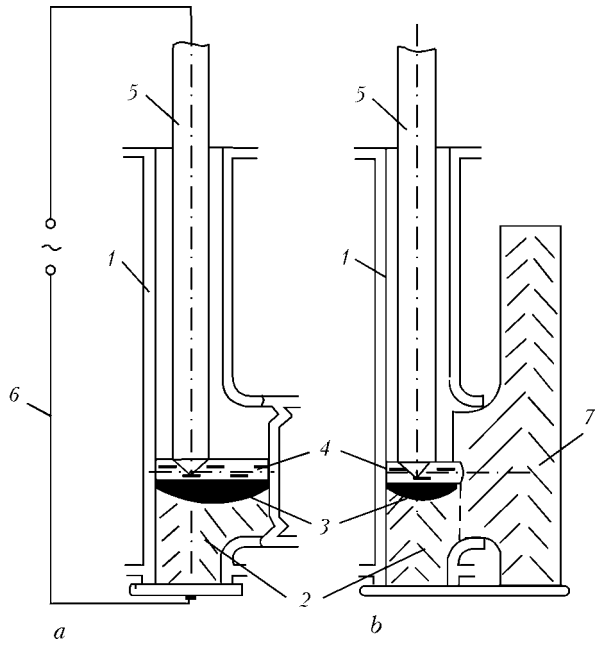


**Figure 1.** Scheme of crankshaft manufacturing: *a* — melting of first chain of crankshaft with crankpin; *b* — melting of second cheek with melting it to crankpin; *1* — mould; *2* — billet being melted; *3* — metal pool; *4* — slag pool; *5* — consumable electrode; *6* — power source; *7* — part being melted together

main parts of piston machines (internal combustion engines, pumps, compressors). Constructively they are made of main journals and crankpins and connecting them cheeks, located in different spatial positions.

At PA «Bryansk Machine-Building Plant» serial production of cranks for crankshafts of powerful ship diesels is mastered according to the technology of E.O. Paton Electric Welding Institute [7]. The cranks for them are fabricated by the ESC method with melting together. Each crank represents two cheeks, interconnected by the crankpin. Mass of electroslag casting billet of the crank is about 5 t, and diameter of the crankpin is about 0.5 m. After heat and mechanical treatments the cranks are assembled into crankshafts on main journals by means of shrink fit.

The cranks are manufactured in the mould, having shape of the cheek with a water-cooled niche in the place of a future crankpin. First billet of the cheek with a crankpin in the form of a boss is melted (Figure 1, *a*). Then the casting is taken from the mould and installed nearby outside the mould in such way that billet of the crankpin entered into the niche. Final operation consists in melting of the second cheek with simultaneous melting to it of the crankpin, manufactured together with the first cheek of the crank (Figure 1, *b*).

It is possible to produce by the ESC method with melting together, using consecutive melting of the cheeks with simultaneous melting to them of the manufactured beforehand crankpins, not just separate cranks but entirely the whole crankshaft, whereby main journals and crankpins are installed into respective holes in walls of the water-cooled mould designed for ESC of the cheeks (Figure 2, *a*). After melting of each second cheek the produced crank is turned around axis of the main journal at the required angle and melting of the next in turn cheek is performed (Figure 2, *b*). This operation is repeated till the whole crankshaft is fully manufactured. In this way crankshafts, designed for gas and engine compressors of several tons mass, are manufactured [8].

At the plant in city of Tientsin (People's Republic of China) similar technology is used for production of the diesel crankshafts of up to 3 m length [9].

By the ESC method with melting together of the pre-manufactured parts, installed into the mould hole, billets of the compressor unit connecting rods from steel 40 [10], cutter holders of big machine tools [11], forks of bulldozer blades for heavy industrial tractors

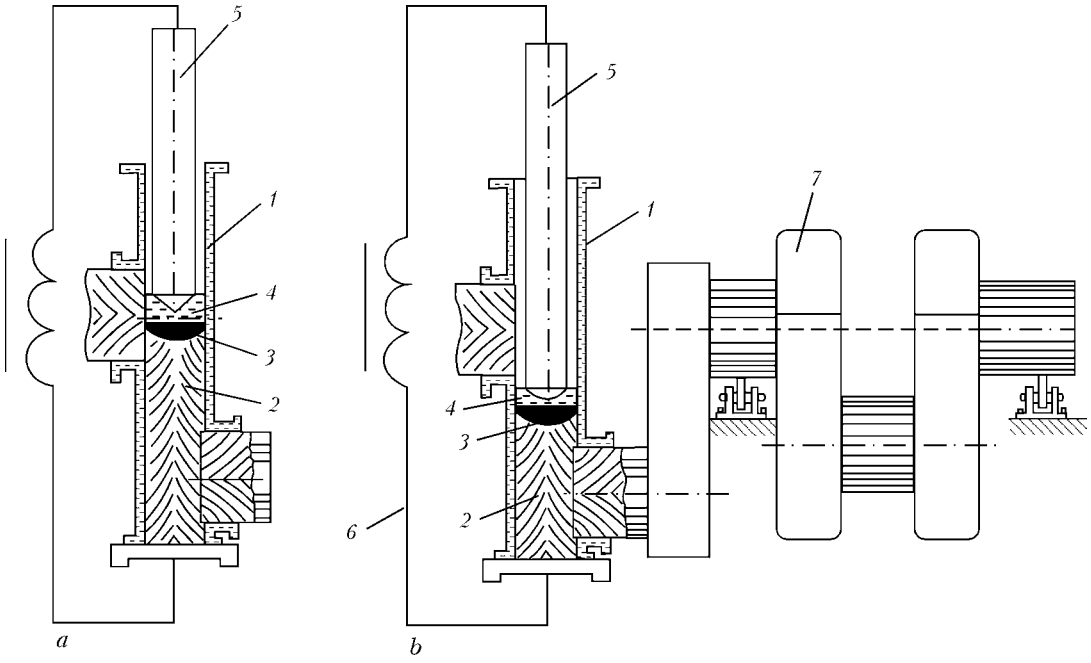


**Figure 2.** Scheme of ESC of entire crankshaft: *a* — melting of first cheek with melting together of crankpins; *b* — melting of crankshaft; *1–6* are the same as in Figure 1; *7* — crankshaft

[12], and a number of other parts of complex shape are produced.

An example of another application of the ESC method with melting together is electroslag cladding (ESCl) by a thick layer of external surface of the rolls or other cylindrical components, which allows not just repairing worn rolls, but manufacturing new bimetal ones. Originally such cladding was performed using an annular mobile mould and consumable electrodes in the form of a paling of bars, installed in the middle of the gap between the mould and the billet being surfaced [13].

In such ESCl method non-uniform penetration was registered in cross-section of the billet being surfaced. Opposite the consumable electrodes penetration was much higher than in intervals between them. This phenomenon can be avoided if to use instead of the paling of bars a continuous tubular consumable electrode [14], manufactured by the method of spun casting, and rolled pipes.

However, when for ESCl any types of consumable electrodes are used, non-uniform penetration over height of the billet being surfaced occurs. As electroslag process progresses, depth of penetration increases, whereby one does not manage to prevent this phenomenon by programmed change of power, because in the classical process with application of the consumable electrodes a direct connection exists between the power, released in the slag pool, and amount of the melted in it metal [14].

It became possible to significantly change energy situation in the slag pool due to application in the course of ESCl of the current-leading mould (CLM), which allows introducing into the slag pool energy irrespective of the amount of the metal being melted in it, and to refuse in this way from application of the consumable electrodes. In ESCl of cylindrical billets the CLM makes it possible to maintain more simply unchangeable depth of penetration over length of the billet being melted [15].

Using CLM ESCl is performed by application of a lumpy additive material in the form of shot, chips, chaff or small chunks (Figure 3, *a*) [16] and by feeding into the slag pool separate portions of molten metal, melted beforehand in another unit, for example, in the induction furnace (Figure 3, *b*) [9].

Using ESC with melting together (the third method) bosses are, as a rule, produced on the semifinished big item in the form of different branch pipes. For this purpose the mould, designed for formation of the cast branch pipe, is installed directly on the body of the future item (Figure 4). Preliminary in the body in the places, where future branch pipes will be located, technological holes are drilled, and above them the mould is coaxially installed. A branch pipe is formed by the method of ESR of a consumable electrode, manufactured from the same steel as the item body. In the process of the branch pipe melting its melting together with the body occurs. In the course of further melting of the produced semifinished

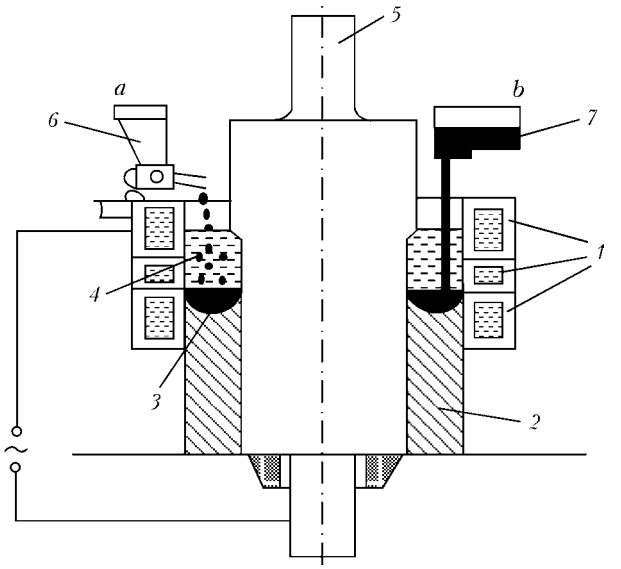


**Figure 3.** ESCl of rolls in CLM: *a* — with feeding into slag pool of lumpy additive material; *b* — with feeding into slag pool of molten metal; *1–4* are the same as in Figure 1; *5* — billet being surfaced; *6* — batcher for lumpy material feeding; *7* — vessel for feeding molten metal

item the holes of necessary diameter are drilled over axis of the branch pipes.

This method of ESR with melting together, developed at the E.O. Paton Electric Welding Institute, is used in serial production of steam separators and pressurizers for nuclear power plants. On one body of a steam separator there are 432 branch pipes of 105 mm diameter from 22K steel, and on the pressurizer body — 108 branch pipes of 150 mm diameter from the same steel. For their melting a special rig is used, which ensures precise positioning of the mould relative axis of the future branch pipe and performance of ESCl in it [17, 18].

In this way branch pipes with flanges are melted on body of the Dn 800 valve from steel 20 for second circuit of the NPP power unit. Preliminary the very

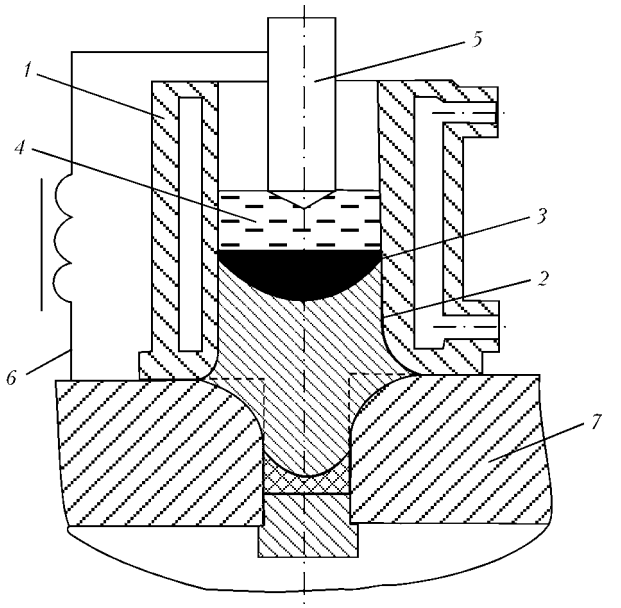


**Figure 4.** Scheme of process for electroslag melting of branch pipes: *1–6* are the same as in Figure 1; *7* — main item

body is melted by the ESC method [10]. In similar way cylindrical branch pipes are melted on covers of Dn 400 valves from steel 20 for pipelines of RBMK 1000 units of NPP and on the cover of the steam chest from 15Kh1M1F steel [19]. In similar way parts of the hub type on a hollow shaft are manufactured from 38KhS steel, for which purpose a manufactured beforehand hollow shaft is installed into the mould and a flange is melted in it with simultaneous melting to the shaft [20].

Wide introduction of special-purpose parts for ship building, chemical, power engineering and other branches of industry, produced by the ESC method with melting together, was enabled by high quality of these items and economic efficiency of their production. Available in the literature data, obtained on the basis of different investigations, and (which is especially important) positive results of operation convincingly confirmed this.

The ESC method with melting together combines in one technological process ESC and ESW. The billets, produced by this method, actually consist of two parts with different structures of the metal (pre-manufactured parts to be melted together and the basic casting) and zone of their connection. Mechanical properties of this billet first of all depend on the joining zone metal quality.

The parts to be melted together have, as a rule, simple shape and are manufactured from forged pieces or rolled metal, which ensures their high quality, and in some cases ---- by the ESC method and even ESC method with melting together.

Quality of cast electroslag metal of the billet core is doubtlessly high, because it was repeatedly confirmed by the most careful and diverse investigations within many decades [1].

Special attention in development of the ESC technological process with melting together is paid to achievement of the required metal properties in the area of connection, including heat-affected zone of metal of the part being melted together. In ESC with melting together mass of the cast part of the billet significantly exceeds mass of the weld in ESW. That's why despite the fact that in casting with melting together significantly higher amount of heat is released than in ESW, rate of melting together is low and, according to our estimates, equals 0.2–0.4 m / h, while in ESW of the metal of 100 mm thickness it is not less than 0.8 m / h [21].

Low rate of melting together enables more stretched in time thermal cycle than in usual ESC and longer stay of the metal of the part being melted together under high temperature conditions. Such thermal cycle causes unfavorable change of metal structure of the transitional layer and requires for additional investigation.

Available data prove that under ESW conditions of low-alloyed and alloyed structural steels, as well as in ESC with melting together of billets from these steels, in the heat-affected zone significant growth of the grain and formation of Widmanstaetten structure and ferrite banks over the grain boundaries were registered. This causes significant reduction of ductility and toughness of the metal in the overheating zone. For restoration of the metal properties in this zone only high-temperature tempering after welding of low-alloyed steels with low content of carbon is sometimes used. However, in majority of cases for achievement of the required properties it is necessary to heat an item up to the temperature of full or partial austenite transformation.

In ESC with melting together the task of ensuring high property parameters in the overheating zone is successfully solved. So, in cranks of crankshafts from 20G steel of powerful ship diesels quality of the ESC metal of the cheeks and crankpins in the melting together zone after annealing and subsequent normalization with tempering significantly exceeds that of the metal of cranks, manufactured by conventional casting, not just in regard to strength, ductility, and toughness [7], but also in regard to fatigue strength [22], whereby properties of the metal in the melting together zone don't differ at all from those of the electroslag cast metal of the cheeks, which was not subjected to overheating. Detailed investigation of quality of the ESC crankshafts after their long operation on ships did not show any defects [23].

In the course of numerous investigations of quality of the transitional zone metal and branch pipes, melted on bodies of NPP equipment from 22K steel, it was registered that on this steel as well full restoration of the metal properties in the overheating zone is achieved after normalization with tempering. Investigations of the transitional zone metal, its mechanical properties, susceptibility to embrittlement and resistance to the low-cycle fatigue showed full identity of properties of the metal of this zone, the base metal of the item body and the cast electroslag metal of the branch pipe [17, 18].

Similar results in regard to removal of consequences of overheating were also achieved in manufacturing by the ESC method with melting together of the hub-type billets from alloyed steel with increased content of carbon of 38KhS grade [20]. After annealing and oil hardening with subsequent tempering mechanical properties of the metal in the fusion zone did not differ from those of the metal in other parts of the billet and exceeded properties, required by the standard for this grade of steel. Moreover, some specimens from the fusion zone had noticeably higher value of impact strength than specimens from areas of the billet, which were not subjected to overheating during manufacturing.

In production of the composite rolls (steel / cast iron) by cladding in CLM of chromic cast iron by the additive in the form of shot [24] values of rates of cladding and melting together in ESC are close (about 0.4 m / h). As far as melting point of the used for surfacing chromic cast iron is lower than that of steel, heat-affected zone of deposit on a steel billet has a

lower maximum temperature, and metal with Widmanstaetten structure was not discovered in it. Mechanical properties of the heat-affected zone metal are not given; just certain increase of its hardness is mentioned.

So, consequences of unfavorable action of the extended thermal cycle of ESC on steel parts being melted together, as shows experience, are removed by heat treatment with heating of the cast above temperature of austenite transformation and subsequent tempering. In many cases it coincides with conditions of heat treatment of the used steel, required for acquisition by it of the necessary properties.

In development of the ESC technology with melting together one has to take into account different sensitivity of steels to action of thermal cycles on them and carefully develop conditions of their heat treatment for achievement of the required level of mechanical properties.

## CONCLUSIONS

1. It is established that the most universal method for producing high-quality massive steel billets of complex shape is ESC with melting together, application of which at present may be very efficient for development of many branches of mechanical engineering.

2. It is shown that the ESC method with melting together guarantees obtaining of mechanical properties of the metal of billets at the level of those made from cast electroslag metal.

3. It is determined that ESC with melting together is the most economical in comparison with other methods of ESC as to the cost of the rigging and auxiliary materials and consumption of electric power and metal.

4. It is shown that in development of technological process for ESC with melting together one has to find possibility to affect level of the working current portion, which is shunted by the parts being melted together.

5. It is determined that for each specific grade of steel, used in manufacturing of billets by the ESC with melting together method, it is necessary to develop conditions of heat treatment, which would ensure obtaining of necessary mechanical properties.


1. (1981) *Electroslag metal*. Ed. by B.E. Paton, B.I. Medovar. Kiev: Naukova Dumka.
2. Medovar, B.I., Latash, Yu.V., Maksimovich, B.I. et al. (1963) *Electroslag remelting*. Moscow: Metallurgizdat.
3. Paton, B.E., Medovar, B.I., Bojko, G.A. (1974) *Electroslag casting. Review*. Moscow: NIIMASh.
4. Shevtsov, V.L., Kumysh, I.I., Marinsky, G.S. et al. (1975) Slag and metal filling of cooled moulds in electroslag casting of complex shape products. *Problemy Spets. Elektrometallurgii*, **2**, 26–31.
5. Shevtsov, V.L., Majdannik, V.Ya., Zhadkevich, M.L. et al. (1998) Electroslag casting of billets of casings of high pressure Christmas tree. *Ibid*., **4**, 3–12.
6. Ksyondzyk, G.V. (1968) Means and prospects of electroslag cladding. In: *New mechanized cladding methods*. Kiev: PWI.
7. Medovar, B.I., Bojko, G.A., Popov, L.V. et al. (1979) Electroslag casting in production of crankshafts of large ship diesels. *Problemy Spets. Elektrometallurgii*, **10**, 37–41.
8. Bezhin, V.V., Dubinsky, R.S., Medovar, B.I. et al. (1983) Production of billets of gas-motor-compressor crankshafts by electroslag casting method. In: *Electroslag technology*. Kiev: Naukova Dumka.
9. Medovar, B.I., Medovar, L.B., Saenko, V.Ya. (1999) Development of electroslag process in special electrometallurgy. *Avtomatich. Svarka*, **9**, 7–12.
10. Alikin, A.P., Bojko, G.A. (1983) Electroslag casting in chemical machine-building. In: *Electroslag technology*. Kiev: Naukova Dumka.
11. Yuzhanin, Zh.I. (1976) Combined (ESR + rolling) tool holder billets of heavy turning mills. *Problemy Spets. Elektrometallurgii*, **5**, 45–46.
12. Mironov, Yu.M. (2005) *Electroslag furnaces for melting and casting*: Manual. Cheboksary: ChGU.
13. Ksyondzyk, G.V. (1966) Circular electroslag cladding of cylindrical parts in vertical position. *Avtomatich. Svarka*, **5**, 63–67.
14. Ksyondzyk, G.V. (1973) Some principles of parent metal penetration in circular electroslag cladding. In: *High-performance processes of cladding and consumables*. Kommunarsk.
15. Kuskov, Yu.M. (1999) Cladding in current-carrying mould: the prospective direction of electroslag technology development. *Avtomatich. Svarka*, **9**, 76–80.
16. Kuskov, Yu.M. (2005) *Electroslag process and technology of cladding by discrete materials in current-carrying mould*: Syn. of Thesis for Dr. of Techn. Sci. Degree. Kiev: PWI.
17. Paton, B.E., Tupitsyn, L.V., Sobolev, Yu.V. et al. (1977) New advanced technological process for production of branch pipes on equipment bodies. *Energomashinostroenie*, **1**, 27–29.
18. Fojta, A., Rozkoshny, K. (1988) Experience of electroslag melting of pressurizer branch pipes. *Problemy Spets. Elektrometallurgii*, **1**, 37–43.
19. Kriger, Yu.N., Nechaev, E.A., Karpov, O.S. (1985) Electroslag melting in power engineering. *Ibid*., **3**, 24–28.
20. Tsygurov, L.G., Kovalev, V.G., Bojko, G.A. (1991) Technological diagrams of ESC of part billets of hub type. *Ibid*., **1**, 11–15.
21. (1980) *Electroslag welding and cladding*. Ed, by B.E. Paton. Moscow: Mashinostroenie.
22. Goncharov, I.T., Egorov, S.P. (1984) Study of fatigue strength of cranks of ship diesel crankshafts made by electroslag casting method. In: *Special electrometallurgy*, Issue 21, 39–41.
23. Popov, L.V., Antsiferov, S.S., Bojko, G.A. et al. (1983) Experience of application of electroslag casting technology at the Production Association «Bryansk Machine-Building Plant». In: *Coll. on Electroslag Technology*. Kiev: Naukova Dumka.
24. Ksyondzyk, G.V. (1984) Transition zone in electroslag shot cladding of chromium cast iron on steel. In: *Coll. on New Surfacing Processes, Properties of Deposited Metal and Transition Zone*. Kiev: PWI.

# ELECTRON BEAM METHOD OF GRAPHITE EVAPORATION AND PRODUCTION OF CONDENSATES FREE FROM TUNGSTEN IMPURITIES

**Yu.A. KURAPOV** and **B.A. MOVCHAN**
E.O. Paton Electric Welding Institute, NASU, Kiev, Ukraine

Regularities of evaporation and condensation of carbon in case of its electron beam evaporation through tungsten melt under conditions of direct and reflected vapor flows are investigated. Owing to separation of the vapor flow carbon condensate without tungsten impurities was produced.

*Keywords: electron beam evaporation, tungsten melt, evaporation and condensation of carbon, tungsten impurities, direct vapor flow, reflector, reflected vapor flow, re-evaporation, critical temperature of condensation*

In study [1] results of investigation of certain regularities of electron beam evaporation and condensation of carbon from the tungsten melt are considered. Due to difference of pressure of vapors mainly carbon is released from the pool. This allows significant increasing rate of electron beam evaporation of carbon and producing sufficiently powerful vapor flow of this material. Shortcoming of this method of producing carbon-containing materials is presence in the condensate of a small amount of refractory impurities. Concentration of tungsten in evaporation of carbon through the tungsten melt may constitute from 2.5 to about 10 wt.%, depending upon conditions of evaporation [1, 2].

Cleaning of the carbon-containing materials from impurities, and first of all from refractory metals, is a labor-consuming process, which in a number of cases may cause destruction of structural components of the material. On the other hand, for a number of fields of application, for example electronics and medicine, sufficiently clean carbon-containing materials with nanosize structure are necessary. In this connection rather actual task is cleaning of the vapor flow of carbon from impurities of tungsten directly in the process of production of the carbon-containing materials.

This problem can be solved by using the technique of application of coatings by reflected molecular beams. So, in [3] the method of application of a coating by the molecular beam reflected from the concave screen, is proposed. Tin and zinc, i.e. materials with low melting point, were used as evaporating materials.

Investigations of the evaporation processes in vacuum condensation of copper, nickel, iron and titanium are presented in [4, 5]. Condensation of these materials is performed up to a certain critical temperature $T_{cr}$ of the substrate, above which the process is absent. Influence of the melting point of the metal being condensed on $T_{cr}$ is determined. As melting point of the metal being condensed increases, $T_{cr}$ gets higher. For copper, nickel, iron and titanium condensates $T_{cr} = (0.75–0.79)T_{melt}$. Effect of critical condensation temperature is stipulated by the fact that average time of life of the adsorbed atom on the surface (before re-evaporation) reduces as temperature of the substrate increases [6–8]. At the substrate temperature above $T_{cr}$ atoms of the metal being condensed differ by the energy, necessary for overcoming of potential relief of the substrate and evaporation from its surface.

Proceeding from results of investigations of dependence of the carbon coating condensation factor upon the molybdenum substrate temperature, critical temperature $T_{cr}$ = 1150 °C was calculated in [9]. Relatively low critical temperature under presented conditions is explained by the fact that vapor flow of carbon evaporated through the tungsten pool consists of clusters of approximately 1–2 nm size.

The goal of this work consists in investigation of regularities of carbon evaporation and condensation under conditions of direct and reflected vapor flows in case of its electron beam evaporation from the molten tungsten pool.

The experiments were carried out in the UE-150 electron beam unit. Vacuum in the working chamber was $1.33 \cdot 10^{-2}$ Pa, internal diameter of crucible —– 50 mm. Evaporated rod of 48.5 mm diameter and 200 mm length was made from fine-grain graphite of MG-1 grade. On consumable end of the graphite rod a washer of 48.5 mm diameter from tungsten of VCh grade of 125 g mass was placed. Condensation of vapor flow of carbon was performed according to two schemes (Figure 1). As substrates (Figure 1, *a*) and a reflector (Figure 1, *b*) 210 × 170 × 4 mm molybdenum plates were used; as a substrate for condensation of the reflected vapor flow (Figure 1, *b*) a sheet tray from iron of 500 × 500 × 1 mm size was used.

Evaporation of graphite was performed at different values of the electron beam power within 27–42 kW (current of the beam corresponded to 1.15; 1.3; 1.5; 1.7 A) at fixed acceleration voltage 24 kV. Mass of

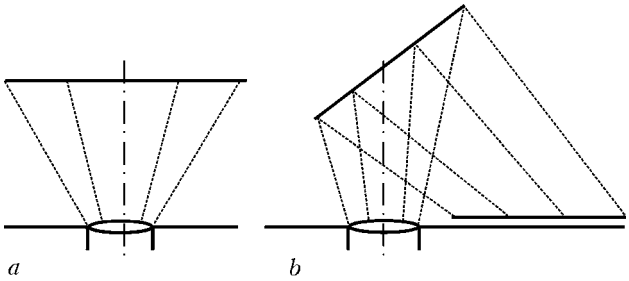


**Figure 1.** Scheme of electron beam evaporation and condensation of vapor flow of carbon: *a* — direct; *b* — reflected

the tungsten shot was maintained at the constant level.

Dependences of the rate of condensation of direct flow of carbon upon rate of its evaporation and temperature of the substrate are presented in Figure 2, where dashed line shows similar dependence obtained in [2] for 1000 °C temperature of the substrate. Rate of condensation was determined proceeding from thickness of the condensates produced under different conditions of evaporation. Analysis of these data proves reduction of the carbon condensation rate on the molybdenum substrate as temperature of the latter increases, which matches data of [9], where dependence of the carbon condensation factor upon temperature of the molybdenum substrate in the area of critical temperature was studied.

Dependences of the condensation rate of direct and reflected vapor flows of carbon upon rate of its evaporation are presented in Figure 3. Direct vapor flow was condensed on the molybdenum substrate heated up to the temperature 1200 °C (see Figure 1, *a*). Reflected vapor flow produced by means of the reflector, heated up to the temperature 1200 °C, was condensed on the iron tray at the temperature 400 °C (see Figure 1, *b*). Experimental results prove that rate of condensation of the reflected vapor flow is 5–6 times lower than that of the direct flow.

During evaporation (Figure 1, *b*) content of tungsten impurities in the condensates, produced on the reflector and the substrate, was controlled. Weight share of tungsten in the condensate was determined using the CamScan scanning microscope with the INCA-200 Energy X-ray attachment. Samples for

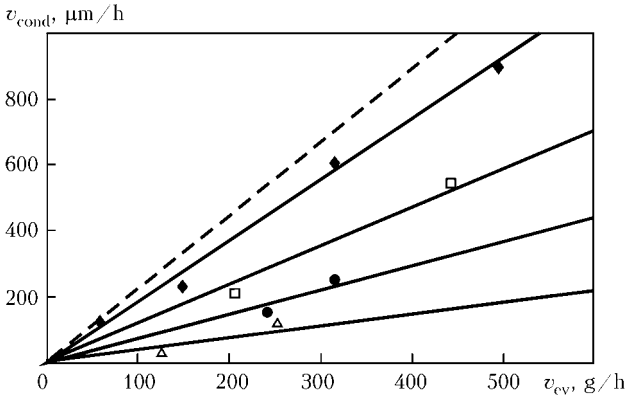


**Figure 2.** Dependence of rate of condensation of direct flow of carbon upon rate of evaporation and temperature of substrate (experiment), °C: – — 1000 [1]; ◆ — 1200; ❒ — 1350; ● — 1500; Δ — 1650

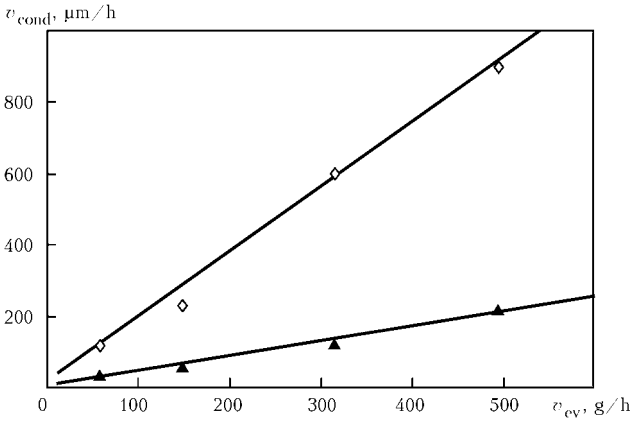


**Figure 3.** Dependence of rate of condensation of direct and reflected vapor flows of carbon upon rates of its evaporation: ◆ — direct flow, $T_s$ = 1200 °C; ▲ — reflected flow, $T_{ref}$ = 1200, $T_t$ = 400 °C

analysis were taken from center of the reflector and at the distance 60 mm from the center, and from central area of the tray (Figure 4).

Process of the tungsten amount reduction in the reflector condensate at low rate of the graphite evaporation is connected [1] with increase of the carbon weight share in the tungsten melt due to its dissolution and delivery on the reaction surface by convective flows, taking into account increase of the tungsten pool volume and area of the melt contact with solid carbon.

Increase of the graphite evaporation rate up to 180 g / h, when power of heating increases, enables saturation of the melt with carbon due to stabilization of the pool size and establishment of a constant area of the molten tungsten contact with solid carbon, owing to which a certain equilibrium content of tungsten is achieved according to the constitutional diagram W–C [2]. As rate of graphite evaporation increases up to 500 g / h, reduction of weight share of tungsten in the condensate (in peripheral areas of the reflector) stops and increases only in center of the reflector. At the same time content of tungsten in carbon condensate on the tray reduces practically by one order (0–0.92 wt.%).

Dependences of weight share of tungsten in condensates of the reflector and the tray upon temperature of the reflector heating, presented in Figure 5,

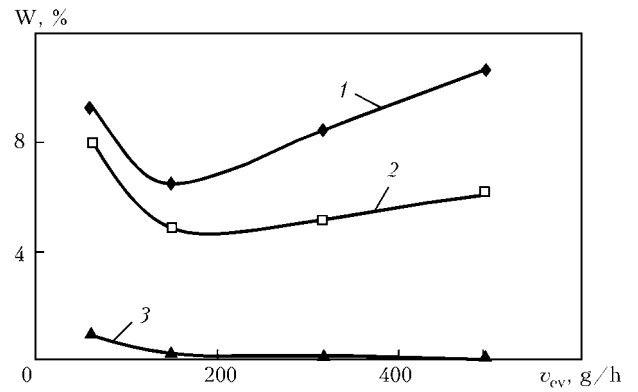


**Figure 4.** Dependence of content of tungsten in condensate upon rate of graphite evaporation (see Figure 1, *b*): *1* — in center of reflector, $T_{ref}$ = 1200 °C; *2* — at distance 60 mm from the center of reflector; *3* — on tray, $T_t$ = 400 °C

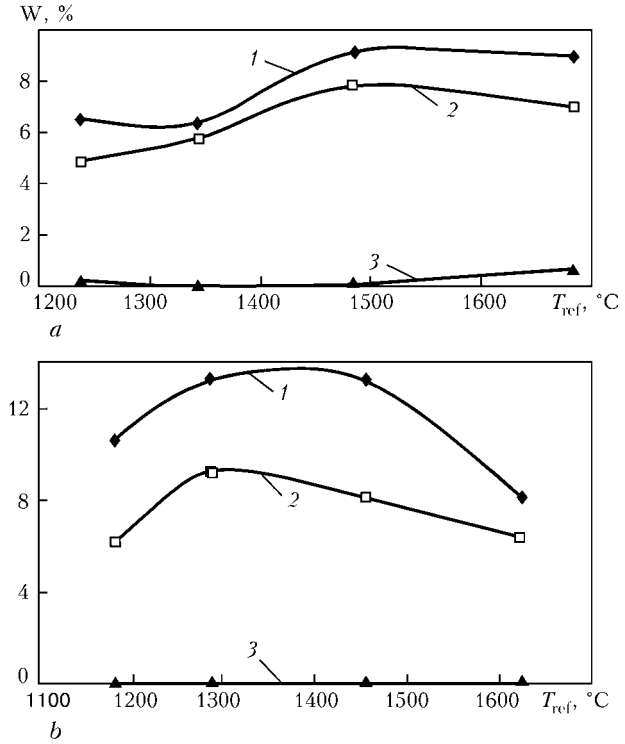


**Figure 5.** Dependence of tungsten content in reflector and tray condensates upon temperature of reflector heating at values of carbon evaporation rate of 150 (*a*) and 500 (*b*) g / h: *1* — in centre of reflector; *2* — at distance 60 mm from the center of reflector; *3* — on tray

are obtained for two rates of carbon evaporation — 150 and 500 g / h. Investigation of the re-evaporation factor influence, i.e. temperature of the reflector heating, on content of tungsten impurities in condensates of the reflector and the tray showed that while under weak conditions of evaporation (150 g / h, Figure 5, *a*) weight share of tungsten in the reflector condensates monotonously increases from 5–6 to 7–9 % as the reflector temperature grows from 1200 to 1700 °C, in the tray condensates content of tungsten impurities changes from 0.22 to 0.68 %, respectively.

Under intensive conditions of carbon evaporation (500 g / h, Figure 5, *b*) content of tungsten in the reflector condensate is characterized by the run-up 6–10 % with maximum 9–13 %, whereby significant difference in its amount over the reflector surface is mainly explained by separation of the vapor flow by masses and change of the melt pool surface profile. At the same time condensates of the tray under all conditions of the reflector temperature change do not contain tungsten impurities at intensive evaporation of carbon (Figure 5, *b*).

It is probable that in the process of condensation on a more heated surface of the reflector a certain share of particles of the carbon vapor flow will be repelled from the reflector surface, participating in this way in the process of re-evaporation. For example, experimental factor of carbon condensation on the reflector, determined as a ratio of obtained by us rate of carbon condensation at $T_{ref}$ = 1200 °C to the rate of carbon condensation, obtained in [9] for $T_s$ = = 1000 °C (see Figure 2, dashed line), equals 0.82, which matches results of investigations of [9]. In this case 18 % of vapor flow of carbon should re-evaporate and condensate on the tray, which is confirmed by experimental data (see Figure 3).

Significant portion of tungsten atoms, when they get on surface of the reflector heated below $T_{cr}$ for tungsten, are condensed on it, and cluster flow of carbon (for which $T_{cr}$ = 1150 °C [9]) is reflected partially from the reflector, taking into account factor of re-evaporation determined by temperature of the reflector heating. So, the reflector, fulfilling in this case function of a separator, cleans vapor flow of carbon from tungsten and allows obtaining condensates with low content of tungsten impurities or even without the latter.

Results of carried out investigations prove possibility of full cleaning of the carbon vapor flow from tungsten impurities and obtaining pure carbon condensates.


1. Movchan, B.A., Kurapov, Yu.A., Krushinskaya, L.A. (2007) Investigation of a number of regularities of electron beam evaporation and condensation of carbon. *Advances in Electrometallurgy*, **1**, 6–8.
2. Chujkov, Yu.B., Movchan, D.A., Grechanyuk, N.I. (1987) Some regularities of electron beam evaporation of carbon through molten tungsten pool. In: *Special electrometallurgy*, Issue 63, 43–48.
3. Palatnik, L.S., Grishchenko, Yu.I. (1967) Reflector for condensation of films with predetermined thickness distribution. *Zavod. Laboratoriya*, **7**, 774–776.
4. Movchan, B.A., Ushakova, S.E., Lyakhov, V.I. (1980) Investigation of re-evaporation processes in vacuum condensation of copper, nickel, iron and titanium. *Problemy Spets. Elektrometallurgii*, **13**, 66–69.
5. Movchan, B.A., Ushakova, S.E., Lyakhov, V.I. (1981) Investigation of reflection of nickel and copper vapor flows from heated surfaces. *Ibid.*, **15**, 49–52.
6. Komnik, Yu.F. (1964) Typical temperatures of thin film condensation. *Fizika Tv. Tela*, 6(**10**), 2897–2908.
7. Palatnik, L.S., Komnik, Yu.F. (1960) On critical temperature of Bi, Sb and Pb condensation. *Doklady AN SSSR*, 134(**2**), 337–340.
8. Semenov, N.N. (1930) On theory of adsorption and condensation. *Zhurnal Fiz-Khim. Obrab. Materialov*, **62**, 33–39.
9. Movchan, B.A., Badilenko, G.F., Chujkov, Yu.B. et al. (1992) Structure of carbon materials produced by electron beam evaporation and vacuum condensation. In: *Special electrometallurgy*, Issue 70, 39–42.

# INVESTIGATION OF DISTRIBUTED CHARACTERISTICS OF ELECTRON BEAM FORMED BY RING CATHODE IN ELECTRON BEAM ZONE MELTING

**V.F. DEMCHENKO, E.A. ASNIS, A.B. LESNOJ, S.P. ZABOLOTIN** and **N.E. SHEGELSKY**
E.O. Paton Electric Welding Institute, NASU, Kiev, Ukraine

Distribution of the electron current density on surface of a cylindrical metal specimen was investigated by the split anode method, and width of the heating zone and effective efficiency of the heat source in electron beam crucible-free zone melting were estimated.

*K e y w o r d s : electron beam, zone melting, electron current, split anode*

**Theoretical substantiation of the experiment.** In order to analyze heat state and size of the melted zone during growing of a single crystal of silicon by the method of electron beam crucible-free zone melting (EBZM) it is necessary to have quantitative data on characteristics of the electron beam heating source, namely width of the heating zone, efficiency, and density of the heat source distribution on the specimen surface. In EBZM with ring cathode a cylindrical specimen (anode) is heated by the electron beam, which in the process of melting moves along the specimen at a constant speed $v$. The specimen being heated and walls of the chamber represent the anode, that's why a portion of the electron flow generated by the cathode interact with the specimen, while the other portion of electrons fall on walls of the vacuum chamber. In correspondence with this the anode current $I_A$ may be presented in the form of two summands: $I_A = I_{sp} + I_{ch}$, where $I_{sp}$, $I_{ch}$ are the components of the anode current, which act on the specimen and walls of the vacuum chamber, respectively.

Let $z$ be axial coordinate, $i(z, t)$ — distribution of tape density of electron current in the specimen at the instant $t$ (under tape density of current the current is meant, which acts on the area of ring surface of the specimen of a unit length). In order to find $i(z, t)$ we use idea of the split anode method. For this purpose let us consider the anode, built-up from two coaxial cylindrical specimens 1 and 2 (total length $L$ of the split anode equals length of the whole anode).

Between two parts of the split anode during the assembly a narrow slot was arranged in order to exclude flowing of current between parts of the split anode (Figure 1).

Specimen 1 has a direct electrical contact with the vacuum chamber walls, and specimen 2 closes on the chamber wall via resistance $R$ parallel with voltmeter $V$. During processing of the experiment results voltage $U$ was measured, which according to Ohm's law was recalculated into current, which passes through specimen 2. At arbitrary position of the electron beam relative the slot between specimens 1 and 2 it may be written as

$$I_{sp}(t) = I_{sp}^{(1)}(t) + I_{sp}^{(2)}(t), \quad (1)$$

where $I_{sp}^{(1)}(t)$, $I_{sp}^{(2)}(t)$ are the anode current components, which act on specimens 1 and 2, respectively. In this ratio fall of the electron beam on the specimen at the angle 80° is taken into account, that's why at small width of the slot one may disregard flowing of electrons through the slot. Efficiency of the electron beam heating calculated relative the anode current share, which flows through the specimen, may be presented in the form

$$\eta = \frac{I_{sp}}{I_A}. \quad (2)$$

In order to determine the efficiency it is necessary to measure $I_{sp}$ and $I_A$, but it is not sufficient for estimating the heating zone width and distribution of the heat flux density on the specimen surface.

Main idea of the split anode method consists in measurement of one of the components of current $I_{sp}^{(1)}(t)$ or $I_{sp}^{(2)}(t)$ at different positions of electron beam relative the slot, and then in restoration by the measured characteristics of the tape density distribution of electron current over surface of the specimen. During performance of the experiment current $I_{sp}^{(2)}(t)$ was registered and additionally anode current $I_A$ was measured, which in the course of melting was maintained at constant level. Let us designate through $\zeta$ coordinate of the built-up specimen slot. Then at arbitrary position of the beam relative the slot one may write

$$I_{sp}^{(2)}(t) = \int_{\zeta}^{L} i(z, t)dz. \quad (3)$$

Length of specimen 2 and initial position of the cathode carriage were selected in such way that current $I_{sp}^{(2)}(t)$ in specimen 2 at the initial instant of time

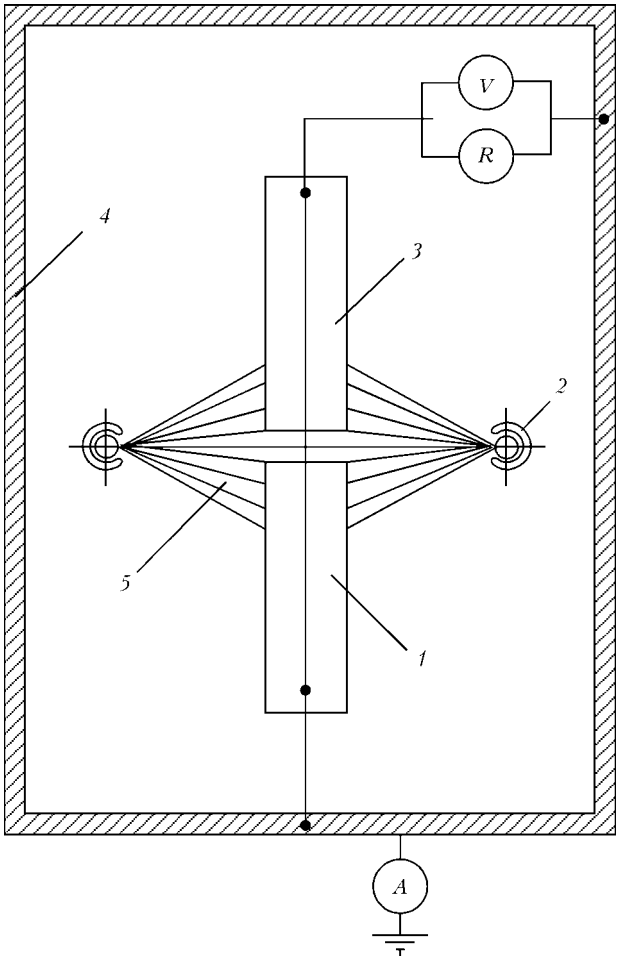


**Figure 1.** Scheme of split anode and arrangement of measuring instruments: *1*, *3* — specimen 1 and 2; *2* — ring cathode; *4* — vacuum chamber wall; *5* — electron beam

$t = 0$ was absent. Then the carriage moved at a constant speed $v$ in direction of specimen 2, and in each position of the carriage current $I_{sp}^{(2)}(t)$ was measured as function of time $t$. Tape density of current in specimen 2 during continuous movement of the carriage is function of two variables — spatial coordinate $z$ and time $t$, i.e. $i = i(z, t)$. Taking into account absence of any dynamic processes, which can affect distribution of tape density of current, function $i(z, t)$ satisfies condition of quasi-stationarity, which may be determined in the following way. For any $z$, $t$ and time increment $dt$ function $i(z, t)$ satisfies the condition

$$i(z + v\,dt,\ t) = i(z,\ t). \tag{4}$$

It follows from expression (4) that full differential of function $i(z, t)$ equals zero. As far as $i(z + v\,dt,\ t + dt) = i(z,\ t) + v\,\dfrac{\partial i}{\partial z}\,dt + \dfrac{\partial i}{\partial t}\,dt$, from formula (4) follows condition of quasi-stationarity of distribution of current density $i(z, t)$

$$v\,\frac{\partial i}{\partial z} = \frac{\partial i}{\partial t}. \tag{5}$$

Let us integrate equation (5) over length of specimen 2 in the range $[\xi, L]$:

$$v[i(L,\ t) - i(\zeta,\ t)] = -\frac{d}{dt}\int_{\zeta}^{L} i(z,\ t)\,dz. \tag{6}$$

Let us take into account expression (3), then equation (6) may be written in the form

$$\frac{dI_{sp}^{(2)}}{dt} = v[i(\zeta,\ t) - i(L,\ t)]. \tag{7}$$

It follows from (7) that it is expedient to select length of specimen 2 as big that in case of full shift of the beam to specimen 2 (i.e. provided $I_{sp}^{(1)} = 0$) tape density of current on end $z = L$ of specimen 2 be equal zero. As it turned out during performance of the experiment, a standard specimen of 100 mm length, cut into two equal parts, fully satisfies this condition.

Let $l(t) = vt$ be movement of the beam within time $t$. Then, taking into account the fact that $dl = v\,dt$, equation (7) may be written in the form

$$i(\zeta,\ l) = \frac{dI_{sp}^{(2)}}{dl}. \tag{8}$$

From this ratio, having preliminary measured $I_{sp}^{(2)}(l)$, it is possible to determine by differentiation of $I_{sp}^{(2)}(l)$ distribution of tape density of the current in spot of the specimen heating by the electron beam. Dependence $I_{sp}^{(2)} = I_{sp}^{(2)}(l)$ allows also estimating effective width of a spot of the specimen heating by the electron beam. For determining effective efficiency of the electron beam heater we identify, according to formula (2), anode current of the specimen $I_A$ with the current, measured by the ammeter connected to the vacuum chamber wall–earth circuit (Figure 1).

**Processing and analysis of results of the experimental investigations.** In experimental investigation of distributed characteristics of the ring cathode one has to take into account the fact that they, as well as number of the reflected electrons, may depend upon the anode current $I_A$ and the anode material. It is inexpedient to use silicon as the anode, because within working range of currents liquid phase is formed during heating of silicon that fills the slot, which is an electric isolator between components of the split anode. So, one has to select for the built-up anode more refractory materials with melting point by 200 °C higher than that of silicon. In this connection as a material for the split anode niobium and titanium were used, whereby the latter may be considered as a simulator of anode from silicon. The investigations were carried out for three versions of the current: 20, 25, and 30 mA. For split anode from niobium two former conditions were used, and in titanium anode the anode current equal to 30 mA was maintained. Values $I_{sp}^{(2)}(t)$ were registered each 30 s, speed of the carriage movement $v$ for all versions equaled $2 \cdot 10^{-3}$ cm / s.

In order to analyze influence of the anode material and current on change of the electron current in the specimen the results of experimental measurements

were processed relative dimensionless current $\bar{I}(l) = \frac{I_{sp}^{(2)}(l)}{I_A}$. With an error, indistinguishable in graphic construction, the results of three experiments, expressed in the dimensionless form, are identical (Figure 2).

This proves the fact that the anode material and values of the anode current $I_A$ practically do not affect efficiency, size of the anode spot and distribution of the anode current on the specimen surface (in the latter case with accuracy up to the constant multiplier proportional to the anode current).

Presented in Figure 2 data prove that efficiency of the electron beam heating source equals 0.83, whereby 17 % of the power constitute losses, connected with reflected electrons and electrons, which miss the specimen and deposit on the vacuum chamber walls.

In order to estimate distribution of the electron current density $i(l)$ on the specimen surface at fixed $\zeta$ it is necessary to calculate in correspondence with expression (8) derivative of the function $I_{sp}^{(2)}(l)$. As follows from [1], the task of numerical restoration of the derivative by measured values of the function is stated incorrectly. Really, measured values of the function $I_{sp}^{(2)}(l)$ may differ from the true values by the measurement error $\delta(l)$, which is certainly non-smooth or even discontinuous function of parameter $l$, that's why despite insignificance of the measurement error, which does not exceed several percent, derivative of the function $\delta(l)$ may be of any high value.

In this connection in order to measure distribution of the current density (or other distributed parameters, for example, density of heat flux) by measured integral characteristics one acts as follows: the law of the current density distribution is postulated in the form of a certain functional dependence with numerical parameters, and then measured current $I_{sp}^{(2)}(l)$ is used for identification of these parameters [2]. The shortcoming of such approach consists in the fact that it may happen that a selected law of distribution of function $i(z)$ would not correspond to the true law of the required function distribution, and, therefore, the calculated data would not always be authentic. In order to avoid errors of this kind it is necessary to stably restore derivative $\frac{dI_{sp}^{(2)}}{dl}$ by measured values of function $I_{sp}^{(2)}(l)$, for which purpose we will use method of regularization of the incorrectly stated tasks suggested in [3]. In correspondence with [1] let us introduce within the interval $[l - \alpha, l + \alpha]$ an averaged function

$$I_\alpha(l) = \int_{l-\alpha}^{l+\alpha} \omega_\alpha(l, \tau)\bar{I}_\alpha(\tau)d\tau,$$

where $\omega_\alpha(l, \tau)$ is the nucleus of averaging;

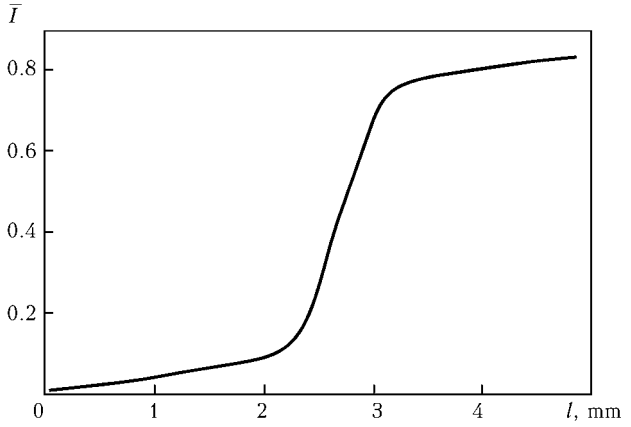


**Figure 2.** Change of dimensionless electron current in specimen 2 depending upon position of carriage of electron beam heater relative slot of split anode

$$\omega_\alpha(l, \tau) = \frac{C_0}{\alpha} \exp \frac{(l - \tau)^2}{(l - \tau)^2 - \alpha^2},$$

where $2\alpha$ is the length of the averaging interval (parameter of regularization). Function $\omega_\alpha(l, \tau)$ transforms into zero at the ends of the averaging interval, and constant $C_0 = 0.82856884$ is selected from the condition $\bar{I}_\alpha(l) = 1$ at $\bar{I}_\alpha(l) \equiv 1$. Approximate derivative from function $I_\alpha(l)$ is calculated according to the formula presented in [1]:

$$\frac{dI_\alpha}{dl} = \int_{l-\alpha}^{l+\alpha} \rho(l, \tau)\bar{I}_\alpha(\tau)d\tau, \qquad (9)$$

where

$$\rho(l, \tau) = \frac{d\omega(l, \tau)}{dl} = \frac{2C_0\alpha(l - \tau)}{[(l - \tau)^2 - \alpha^2]} \exp\left[\frac{(l - \tau)^2}{(l - \tau)^2 - \alpha^2}\right].$$

So, for stable restoration of the derivative using measured values $I_{sp}^{(2)}(l)$ it is sufficient to calculate integral from expression (9). Let $(0, H)$ be an interval of the parameter $l$ change (in this experiment $H = 50$ mm). Function $\bar{I}_\alpha(l)$ was experimentally measured within interval $(0, H)$ in the form of a table of values $\bar{I}_\alpha(l_k)$ for $l = l_k = k\Delta l$, $(k = \overline{0, N}, kN = H)$. In order to increase accuracy of the integral at each interval $[l_k, l_{k+1}]$ function $\bar{I}_\alpha(l)$ was completed by means of the cubic spline, which smoothed noisy data [4]. Integral on the right side of expression (9) was calculated according to Simpson's quadrature formula; number of the completion points $m$ and averaging interval $\alpha$ varied.

In Figure 3 diagrams of distribution of the dimensionless tape current density $\bar{i}_\alpha(l) = \frac{dI_\alpha}{dl}$ calculated for two values of the averaging parameter $\alpha$, are presented. More adequate to physical ideas about law of distribution of the electric current density on the specimen surface should be considered the derivative, restored at the averaging interval, equal to double step $\Delta l$ of measurement of the function $I_{sp}^{(2)}(l)$.

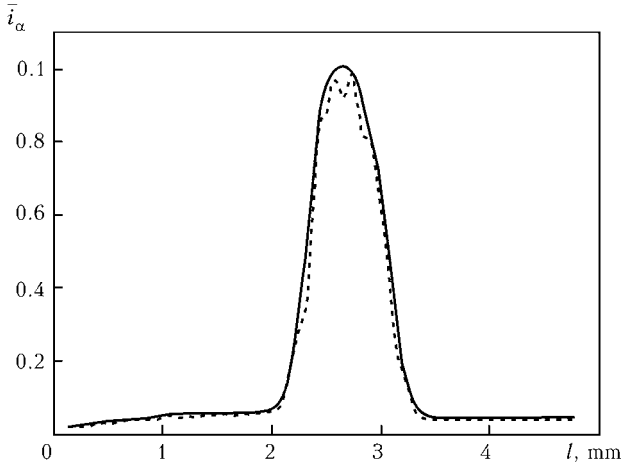


**Figure 3.** Distribution of dimensionless density of electron current on surface of specimen at different values of averaging parameters: dashed line — $\alpha = \Delta l$; solid line — $\alpha = 2\Delta l$

It follows from Figure 3 that it is possible to single out central area in the heating spot, in which function of distribution of the electric current density is well described by normal law of distribution. Peripheral areas have low and practically constant tape density of current. Length of the central area is 14 mm. In this heating zone about 90 % of the electron beam power is released. Figure 3 allows getting information on distribution of surface density of release of the electron beam energy, quantitative data on which are necessary for selection of parameters of the melting conditions, designing of heat baffles, estimation of the electron beam scanning parameters, and calculation of heat processes in formation of a single crystal.

## CONCLUSIONS

1. Methodology for measurement of electric current density on surface of a specimen based on application of the split anode is suggested, and theoretically justified in regard to heating of a cylindrical specimen by an electron beam formed by the ring cathode.

2. It is shown that tape density of current on surface of a specimen equals derivative of the current, which flows in one of the parts of a built-up specimen and changes depending upon shift of the beam axis relative the slot.

3. For calculating derivative using the measured integral characteristic of tape density of the electron current, a version of the method of regularization of incorrect tasks was applied, which allowed stable restortion of the derivative using noisy experimental data.

4. As a result of experimental measurements and their mathematical processing quantitative data on distribution of the electric current density on surface of a specimen being heated and effective efficiency of the source of electron beam heating by ring cathode of direct action were obtained.

1. Belov, Yu.A., Didenko, V.P., Kozlov, N.N. et al. (1982) *Software of complex experiment*. Vol. 1: Measurement processing in study of complex systems. Kiev: Naukova Dumka.
2. Gvozdetsky, V.S., Krivtsun, I.V., Shevelov, M.V. (1984) Procedure of determination of parameters of current density distribution function in anode spot of arc. *Avtomatich. Svarka*, **4**, 6–10.
3. Tikhonov, A.N., Arsenin, V.Ya. (1980) *Methods of solution of incorrect tasks*. Moscow: Mir.
4. Craven, P., Wahba, G. (1979) Smoothing noisy data with spline function. *Numerische Mathematik*, **31**, 377--403.

# RECONSTRUCTION OF ELECTRON BEAM INSTALLATION TICO-15M

**V.I. KOSTENKO[1], P.A. PAP[2], A.N. KALINYUK[2], D.V. KOVALCHUK[2], N.P. KONDRATY[3] and V.B. CHERNYAVSKY[4]**
[1]«Strategiya BM» Ltd, Kiev, Ukraine
[2]NVO «Chervona Khvylya» Ltd, Kiev, Ukraine
[3]«KB VMO» Ltd, Kiev, Ukraine
[4]Physico-Technological Institute of Metals and Alloys, Kiev, Ukraine

Experience of reconstruction of outdated electron beam melting installation with application of the latest developments in the field of electron beam engineering and technology is considered. Reconstruction of the installation with application of new gas-discharge electron guns and control system allowed mastering the new types of products, including those with increased requirements to chemical composition. The carried out works allowed increasing 2.5 times productivity of the equipment and making premises for further development.

*Keywords: titanium, electron beam installation, reconstruction, feeding mechanism, control unit, ingot, oxygen equivalent*

Early in 2006 «Strategiya BM» Ltd bought from the «Fico» company the TICO-15M electron beam remelting installation. Within two months a team of process engineers, engineers and melting operators was established, and in March first ingot of titanium of Grade 2 from spongy titanium fabricated at ZTMK (Zaporozhie, Ukraine) was produced. Dimensions of melted ingots were as follows: diameter 640 mm, length up to 2000 mm, mass up to 2900 kg (Figure 1).

It should be noted that the TICO-15M installation, developed in 1990, earlier never produced more than 20 t ingots per month, and since 2003 did not work at all. That's why the primary task was restoration of its working capacity. For this purpose several structural elements and systems, service life of which was over, were replaced.

Then it became necessary to carry out reconstruction of TICO-15M, which was performed in close cooperation with «KB VMO» Ltd that had great experience in development of the electron beam melting furnaces.

The reconstruction concerned, first of all, feeding mechanism of the consumable billet. The new mechanism envisages application of non-meltable boxes for feeding charge into the melting zone. Mass of possible loading of the charge was increased up to 4.6 t. Asynchronous motors and pulse converters of the «Mitsubishi» company (Japan) with self-control and self-diagnostics systems, allowing their further connecting to the computerized control system of the electron beam installation as a whole, were used for increasing reliability of operation of the drives used for feeding of consumable billets and drawing of the ingots.

Jointly with NTUU «KPI» new PGE-450 electron guns of nominal power 450 kW (acceleration voltage 30 kV), developed at «KB VMO» Ltd, equipped with two focusing and one deviation coils, were installed. The guns are simple in fabrication, convenient in operation, and do not require for additional vacuum pumps for development of working pressure in the working volume. Possibility of installation of the «crucible edge protection mode» sensor is envisaged in them.

A new main control panel of the installation (Figure 2) is installed, which is based on new units of the electron gun control (Figure 3), developed by «Solo» Ltd (Kiev, Ukraine) that fulfill usual func-

**Figure 1.** Ingots from titanium of Grade 2

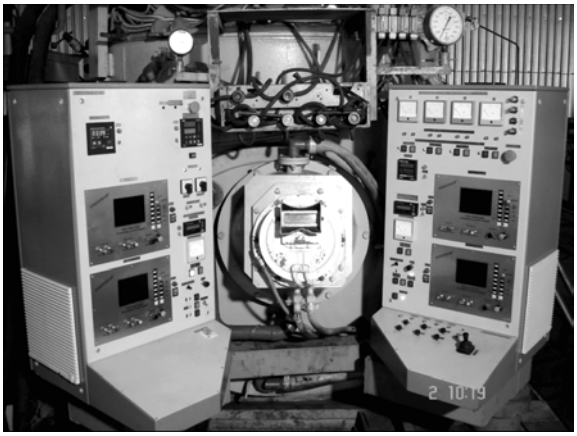

**Figure 2.** Main control panel of TICO-15M installation


**Figure 3.** Control unit of electron gun

**Figure 4.** Malleated slabs of titanium of Grade 2

tions (control movement of the electron beams, focusing of the beams, and operation of the working gas leaks). In addition, the units allow forming and programming from one to six beam configurations with an independent task of one electron gun for creation of the necessary temperature field and control of the system of real-time sweeps by means of a built-in manipulator of the joystick type, storing in the non-volatile memory up to six programmed in advance forms of sweeps, and reflecting on the colored video-terminal established parameters of melting and forms of the sweeps in graphic, symbolic and digital forms. The units ensure so called crucible edge protection mode, which means that electron beam in the process of melting can not get outside real geometric dimensions of the fitting-out. This function of the electron gun control units excludes emergency situations, connected with burning-through of the intermediate unit, mould and cooling systems. The units have built-in resources for ensuring self-control and self-diagnostics conditions and are integrated with a peripheral computer by means of the RS-485 serial channel.

Majority of works, connected with reconstruction of the TICO-15M unit, were carried out without stopping the production. As a result of the reconstruction productivity of the TICO-15M unit is 600 t of ingots per year.

After beginning of the operation more than 650 t ingots of non-alloyed titanium of Grade 1 and Grade 2 ASTM B348 were produced.

One of the ways of increasing efficiency of production under changed conditions of the titanium market is melting of ingots of preset chemical composition, in particular for non-alloyed titanium, and ingots with a certain oxygen equivalent.

More than 200 t of Grade 2 ASTM B348 non-alloyed titanium with oxygen equivalent $O_{eq}$ within 0.17–0.21 were produced from titanium sponge of grades TG-100, TG-110, TG-120 and TG-130. Depending upon content of impurities (nitrogen, iron, carbon), which effect level of $O_{eq}$, ingots of 640 mm diameter and mass up to 2.8 t with oxygen concentration within two ranges (0.11–0.13 and 0.14–0.16 %) were melted. Additional oxygen was introduced into the metal by addition of titanium oxide IV.

Results of chemical and gas analyses showed high homogeneity of composition of the ingots over their height and section. Deviation of oxygen content from the mean value equaled 0.01, nitrogen —- 0.002, iron —- 0.01, carbon 0.002 abs.% for both ranges of concentrations.

Since late 2006 jointly with M.V. Frunze Sumy MNPO the works were carried out, connected with malleating of ingots of 640 mm diameter into flat slabs of 200 and 220 mm thickness (Figure 4).

The malleated slabs were successfully rolled into sheets at the enterprises of Europe. At present specifications are being developed on these products for organization of their serial production.

In near future it is planned to carry out at the enterprise «Strategiya BM» Ltd the next stage of the TICO-15M installation reconstruction, due to which length of the produced ingots will increase up to 3000 mm, mass up to 4.3 t, and annual productivity of the TICO-15M unit will increase up to 900 t.

At the enterprise the quality ensuring system is introduced and works according to requirements of the DSTU ISO 9000 standard. At present the work is carried out, directed at getting a respective certificate in «UkrSEPROZ».

# POWER PARAMETERS OF PROCESS OF PLASMA LIQUID-PHASE REDUCTION OF IRON

**M.L. ZHADKEVICH, V.A. SHAPOVALOV, D.M. ZHIROV, G.A. MELNIK, M.S. PRIKHODKO** and **A.A. ZHDANOVSKY**
E.O. Paton Electric Welding Institute, NASU, Kiev, Ukraine

Volt-ampere characteristics and gradients of voltage of arcs under conditions of plasma liquid-phase reduction of iron are determined. Dependencies of the slag-metal melt temperature upon a number of factors are revealed. Specific power, geometrical and technological parameters of melting reactors on the basis of arc steel-making and ore-smelting furnaces for plasma liquid-phase reduction of iron are suggested and optimized.

*Keywords: reduction of iron, volt-ampere characteristic, voltage gradient, melt temperature, electrical balance, specific power and geometrical parameters of furnaces*

Development of the technology and installations for plasma reduction of iron is impossible without calculation of electrical characteristics of arcs and power parameters of the installation as a whole, necessary for ensuring reliable melting of the charge materials at the required rate, formation of the molten metal and slag pool, progress of the reduction processes, and achievement of necessary temperature of the zone of metallurgical reactions.

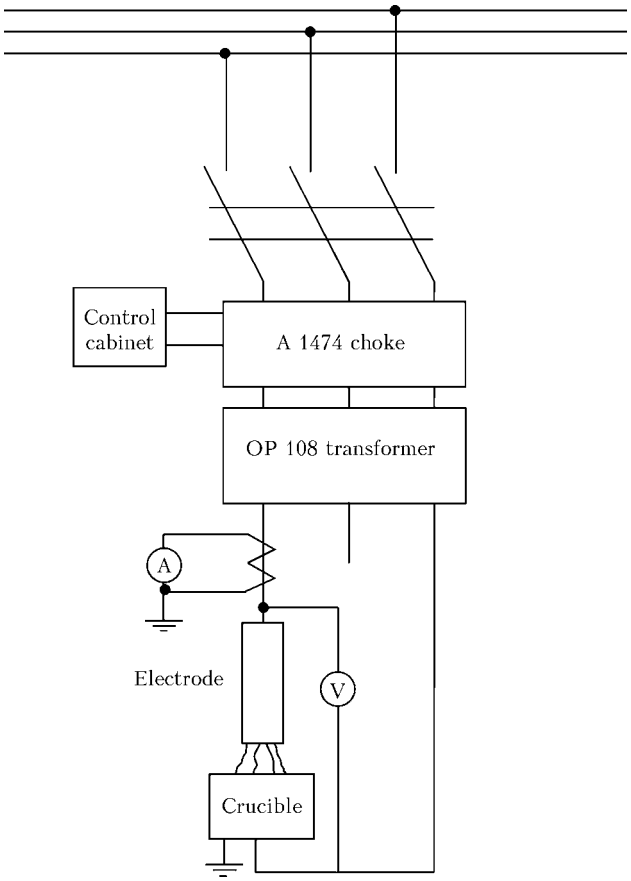


**Figure 1.** Principle scheme of power supply of installation

Arc voltage in the process of the metal melting depends upon many factors: composition of gases, in which the arc burns, current, arc length, etc. Depending upon range of the arc voltage changes the open-circuit voltage of the power source and inclination of its external volt-ampere characteristic (VAC) are selected at certain periods. Specific power parameters depend upon geometrical parameters of the melting zone, position of the electrodes, and density of current on the pool surface.

The goal of this work consisted in investigation of VAC and voltage gradient of the arcs under conditions of plasma liquid-phase reduction of iron, and in determination of heat parameters of the process.

Power parameters were investigated under conditions of plasma liquid-phase reduction of iron from oxidized pellets on the laboratory installation described in [1]. In Figure 1 principal scheme of the power supply is shown. The installation is powered from the 380 V alternative current mains through the saturable choke and isolation transformer with regulated open-circuit voltage. Value of the current is regulated by the A 1474 saturable choke within 600–3000 A, the open-circuit voltage achieves 576 V, VAC steepness is not less than 0.025 V·A.

Experimental VAC in start (argon as the plasma gas) and operation modes (propane-butane and its mixture with air) are presented in Figures 2 and 3. As one can see from the Figures, they are gently growing, their

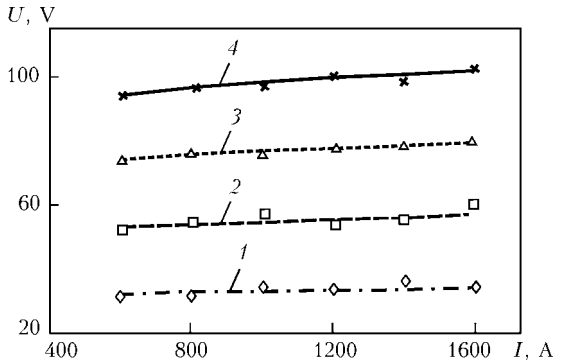


**Figure 2.** VAC of plasma arc in start mode with argon at different values of arc length, cm: *1* — 5; *2* — 10; *3* — 15; *4* — 20

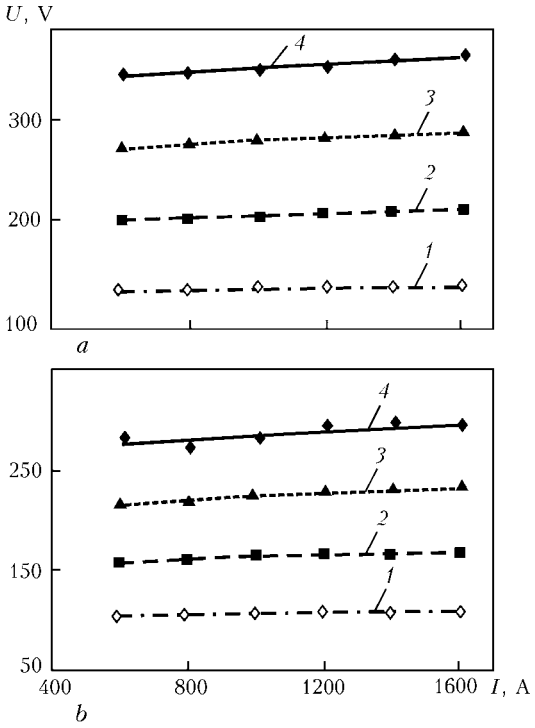


**Figure 3.** VAC of plasma arc in operation mode with propane-butane (*a*) and propane-butane-air mixture (*b*) at different values of arc length: *1–4* are the same as in Figure 2

inclination in the start mode (argon) equals (0.2–0.7)·$10^{-2}$, in the operation mode (propane-butane) —– (0.5–2.0)·$10^{-2}$ and (0.4–1.6)·$10^{-2}$ V·A (propane-butane-air mixture). Big inclination of VAC and a higher general level of the arc voltage (propane-butane or its mixture with air) in comparison with operation on argon are explained by significant consumption of power on dissociation and ionization of the polyatomic gases.

Gradient of the plasma arc voltage during operation in start mode with argon equals approximately 4, in operation mode with propane-butane —– 15, and with propane-butane-air mixture —– 12 V / cm (Figure 4). As current increases, the gradient grows insignificantly. Big gradient in case of application of propane-butane as a plasma gas in comparison with argon can be explained, as well as in regard to VAC,

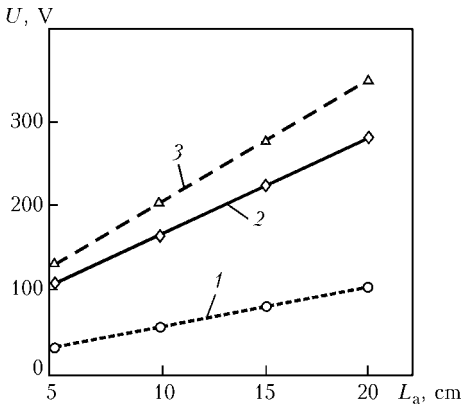


**Figure 4.** Gradient of plasma arc voltage at 1000 A current: *1* —– in start mode with argon; *2* —– in operation mode with propane-butane-air mixture; *3* —– in operation mode with propane-butane

by more significant consumption of power for dissociation and ionization of the polyatomic gases.

It is established after carried out investigations that VAC of the plasma arc under conditions of plasma liquid-phase reduction of iron are described by the empirical dependence for arcs of the three-phase group of plasmatrons or plasma-arc heaters of other types (for example, with hollow graphitized electrodes) [2], which has the following form in case of using argon as a plasma gas:

$$U_a^{Ar} = 1.1[(b\ I_a^m\ L_a) + L_e\ E_c + 10], \quad (1)$$

where $U_a^{Ar}$ is the arc voltage fall in case of operation in argon; $b$ is the coefficient equal to 1.65–1.70; $I_a$ is the arc current, A; $m$ is the index of power equal to 0.065–0.072; $L_a$ is the arc length, cm; $L_e$ is the deepening of the electrode into the nozzle, mm; $E_c$ is the voltage gradient of a portion of the arc column located in the nozzle channel, V / mm.

For calculation of VAC in start mode general view of equation (1) remains unchangeable, but values of certain coefficients in this case should be assumed as follows: $b$ = 1.75–2.20; $m$ = 0.075–0.085.

It is noted in [2] that in case of application of a mixture of gases, arc voltage $U_a^{mix}$ is calculated according to the formula

$$U_a^{mix} = U_a^{Ar}[10^2\{G\}]^n, \quad (2)$$

where G is the volume share of gas in its mixture with argon; $n$ is the index of power depending upon the kind of gas.

As a result of the carried out experiments it is established that value $n$ = 0.35 for propane-butane and $n$ = 0.32 for its mixture with air.

Influence of a number of factors on temperature of the slag-metal melt was investigated. Temperature was measured by the tungsten-rhenium thermocouple. For this purpose in the produced beforehand ingot a hole was drilled parallel to the axis at the distance of 0.5 of its radius (50 mm), through which the thermocouple was introduced from below up to the surface level. Mass of the loaded iron ore pellets was distributed in such way that layer of the slag in the molten state be equal to about 7 mm.

In Figure 5 dependence of the slag-metal melt temperature upon arc power at its length 7 cm is shown that sharply grows when power increases from 70 to 150 kW, and then grows rather slowly, which,

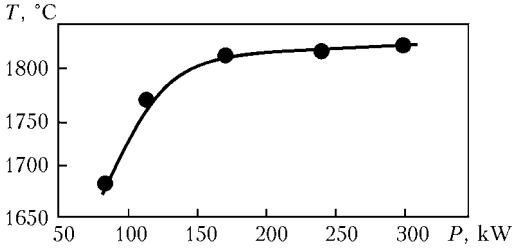


**Figure 5.** Dependence of temperature $T$ of slag-metal melt upon arc power $P$ at its length 7 cm

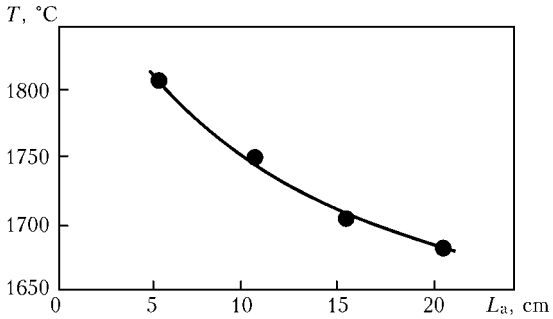


**Figure 6.** Dependence of temperature of slag-metal melt upon arc length at $P$ = 130 kW

evidently, is explained by evaporation of the slag-metal melt at high temperature.

Influence of arc length on the melt temperature at unchangeable 130 kW power was determined (Figure 6). The reason of reduction of power, transferred to the melt as the length increases, consists in increase of heat losses from the arc column due to radiation.

Influence of the plasma gas (propane-butane) consumption on the slag-metal melt temperature within the investigated range is felt weakly, although its reduction as flow rate of the gas increases is clearly seen (Figure 7). Evidently, gas does not manage to be heated up to sufficiently high temperature in arc column, at its high flow rates, which causes certain reduction of the slag-metal melt temperature.

Power balance of the process under different conditions of its progress was drawn. Heat losses in the water-cooled panels and the mould were determined by the method of calorimetric measurements. Tem-

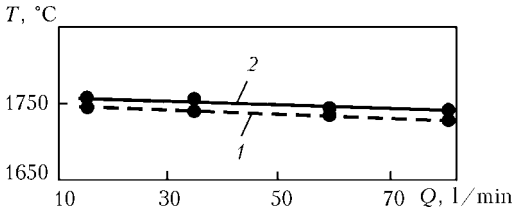


**Figure 7.** Dependence of temperature of slag-metal melt upon flow rate $Q$ of propane-butane at arc power 100 (*1*) and 150 (*2*) kW

perature of waste gases from the reaction space, electrode and graphite crucible was measured by the tungsten-rhenium thermocouple. Heat losses from heated surfaces into ambient space were determined according to the expressions presented in [3]. Distribution of power by items is shown in Table 1.

It should be noted that in case of melting in the graphite crucible, useful power consumed for heating and melting of the charge is, at equal heat inputs, significantly higher than in case of melting in the water-cooled mould. This is explained by lower losses with cooling water at the same arc power. So, increase of the input electric power and arc length cause reduction of efficiency, which matches data on influence of these factors on temperature of the slag-metal melt.

Analysis of the results, obtained under industrial conditions on the DSP 6N2 arc steel-making furnace and the RKZ 1.2 type ore-smelting furnace, as well as described in [4–7], allowed determining such generalized specific power and geometric parameters for calculation of the units for plasma liquid-phase reduction of iron, application of which ensures reduc-

**Table 1.** Power consumption for plasma liquid-phase reduction of iron under different conditions, %

| Item of balance | Water-cooled mould | | | Graphite crucible |
|---|---|---|---|---|
| | 5 cm arc length, 100 kW power | 5 cm arc length, 200 kW power | 20 cm arc length, 200 kW power | 5 cm arc length, 100 kW power |
| Heating and melting of charge (efficiency) | 27 | 17.5 | 12 | 43 |
| Heating of crucible, inoculation and electrode | 15 | 19.0 | 23 | 29 |
| Losses with cooling water | 51 | 55.0 | 55 | 15 |
| Losses with waste gas | 1 | 1.5 | 2 | 3 |
| Losses from heated surfaces into environment | 6 | 7.0 | 8 | 10 |

*Note*. Power input constitutes 100 %.

**Table 2.** Specific parameters of melting reactors for plasma liquid-phase reduction of iron

| Parameters | Recommended | Calculated | |
|---|---|---|---|
| | | DSP-6 | DSP-50 |
| Maximal density of current in electrode section, A / cm$^2$ | 13.8–20.0 | 14 | 17.3 |
| Specific power on hearth surface, kW / m$^2$ | 700–1000 | 670 | 800 |
| Specific active power on area of dissolving of electrodes, kW / m$^2$ | 2500–4400 | 3180 | 6250 |
| Current density on pool surface, A / m$^2$ | 6000–9000 | 6900 | 6250 |
| Ratio of hearth diameter to electrode diameter | 7.4–10.0 | 7.43 | 9.12 |
| Ratio of diameter of electrode dissolving to electrode diameter | 3.00–3.12 | 3.33 | 3.20 |
| Ratio of hearth diameter to diameter of electrode dissolving | 2.50–2.85 | 2.23 | 2.85 |

**Assumed technological parameters of melting reactors for liquid-phase reduction of iron**

| | DSP-6 | DSP-50 |
|---|---|---|
| Arc current, A | 4200–5600 | 15000–21600 |
| Arc voltage, V | 150–200 | 200–290 |
| Open-circuit voltage of transformer, V | 220–281 | 300–407 |
| Working power of furnace, kW | 2500–2600 | 12500–13000 |
| Electrode diameter, mm | 300 | 500 |
| Diameter of cavity in electrode, mm | 40 | 75 |
| Flow rate of natural gas, $m^3$ / h | 420 | 3260 |
| Power consumption, kW·h / t | 1800 | 1200 |
| Duration of melting, h | 4.3 | 4.6 |
| Productivity, t / h | 1.4 | 10.8 |

tion of electric power consumption and increase of the ready product output (Table 2). In addition, here comparative calculated values of specific parameters on the basis of the DSP-6 and DSP-50 melting reactors are presented, applicable to plasma liquid-phase reduction of iron, taking into account application of the waste gases for preliminary solid-phase reduction.

## CONCLUSIONS

1. It is established that VAC of plasma arc under conditions of plasma liquid-phase reduction of iron are described by the established earlier empirical dependence for arcs of the three-phase plasma-arc heaters with specified coefficients for cases of application of propane-butane and its mixture with air.

2. Technical-economic parameters for calculation of reactors for plasma liquid-phase reduction are obtained.

3. Possibility of using arc steel-making furnaces and ore-smelting furnaces as reactors for plasma liquid-phase reduction of iron is shown.


1. Zhadkevich, M.L., Shapovalov, V.A., Melnik, G.A. et al. (2006) Plasma liquid-phase reduction of iron from its oxides using gaseous reducers. *Advances in Electrometallurgy*, **2**, 18–21.
2. Zhadkevich, M.L., Shapovalov, V.A., Melnik, G.A. et al. (2004) Engineering method of calculation of main power parameters of plasma ladles-furnaces. *Ibid*., **3**, 31–33.
3. Smolyarenko, V.D., Kuznetsov, L.N. (1973) *Energy balance of arc steel-making furnaces*. Moscow: Energiya.
4. Gasik, M.I., Lyakishev, N.P., Emlin, B.I. (1988) *Theory and technology of ferroalloy production*. Moscow: Metallurgiya.
5. Egorov, A.V. (1990) *Calculation of power and parameters of electric arc of ferrous metallurgy*. Moscow: Metallurgiya.
6. Nikolsky, L.E., Smolyarenko, V.D., Kuznetsov, L.N. (1981) *Heat operation of arc steel-making furnaces*. Moscow: Metallurgiya.
7. Emlin, B.I., Gasik, M.I. (1978) *Reference book on electrothermal processes*. Moscow: Metallurgiya.

# INVESTIGATION OF DIFFUSION PROCESSES IN MULTILAYER COMPOSITE THERMAL COATINGS

**Yu.S. BORISOV**[1], **L.I. ADEEVA**[2], **G.S. KAPLINA**[2], **A.Yu. TUNIK**[2], **G.N. GORDAN**[2], **I.A. DEMIANOV**[2] and **S.L. REVO**[2]
[1]E.O. Paton Electric Welding Institute, NASU, Kiev, Ukraine
[2]Taras Shevchenko Kiev National University, Kiev, Ukraine

Processes of diffusion interaction at annealing in argon between two layers of coating, applied by the methods of plasma spraying and electric arc metallization, were investigated. The plasma coating layer was produced by spraying of the composite powder $TiSi_2{\cdot}Al_2O_3{\cdot}Ni{\cdot}Cr_3C_2$, above which a layer from aluminium alloy was applied by the method of electric arc metallization. Structure of the coating after annealing at 700 °C within 1.5 h is characterized by absence of the through porosity and increased cohesion strength, which enables increase of its resistance against gas-abrasive wear at 600 °C more than 3 times.

*K e y w o r d s : thermal spraying, multilayer coating, diffusion interaction, structure, gas-abrasive wear*

One of the obstacles on the way to application of plasma coatings at high temperatures under conditions of corrosive environment is possible presence in their structure of the through pores. This may enable penetration of the components of this environment on the coating–base metal interface and development in mentioned zones of active corrosion processes, causing formation of an intermediate layer of the corrosion products and lamination of the coating. For efficient application of such coatings under mentioned conditions it is necessary to remove the through porosity. One of the ways of solution of this task can be application of additional chemical-heat treatment (CHT) of the sprayed layer.

In addition to practical interest, CHT of the plasma coatings also represents scientific interest in connection with peculiarities of the sprayed coating structure [1] ---- laminar, discrete, inhomogeneous character of structure of the coatings, presence of pores and oxide inclusions in them, and presence in the structure, in addition to conventional intergranular boundaries, of different additional boundaries (between particles located in the same layer; interlayer boundaries parallel to the base plane, and, finally, boundaries between the base and the coating), which represent a barrier for progress of the diffusion process. In addition, specificity of the spraying process creates premises for formation of non-equilibrium structures and occurrence of a complex stressed state. Such difference in structures of a coating and a cast material affects processes of the diffusion interaction when CHT of thermal coatings is performed.

Available in the literature data relate mainly to CHT of the coatings, produced by the method of thermal spraying (TS) of powders of metals and metal alloys [2–10] and composite powders [11–16]. Main technological version of CHT is diffusion saturation in powder mixtures in a container with a melting gate or in the shielding environment.

In all kinds of CHT, implemented by application of different technological versions, the goal of this treatment is improvement of certain characteristics of the coating, for example, density, hardness, and strength of cohesion with the base.

In a number of works combination of TS and CHT was performed by application on surface of an item by the metallization method of chromium [17], NiCr [18] and AlSn [19, 20] alloys, or by plasma spraying of silicon [21] with subsequent annealing that caused change of phase composition of the surface layer.

Main peculiarity of the CHT process of the TS coating consists in the need to select CHT conditions, which allow obtaining required characteristics of the coating without reduction of strength of its adhesion to the base and strength properties of the base metal. It is important to avoid in this case Kirkendall's effect, i.e. formation of porosity on the boundary of layers because of different diffusions rates of chemical elements. For forecasting working life of the coatings (taking into account losses of protection properties because of the diffusion resolving) it is necessary to study the diffusion interaction processes, which proceed in a multilayer coating at the temperatures of possible operation.

In this work object of the investigation are composite coatings, containing nickel-bound oxygen and oxygen-free compounds. The most acceptable type of CHT for them, which would cause increase of wear, heat and corrosion resistance, may be alitizing and alumosiliconizing, due to which formation of heat-resistant intermetallics of the Ni–Al system and $Ni_{16}Ti_6Si_7$, $Ti_5Si_4$ silicides should take place. That's why layer of the Al–Si alloy was selected as second upper layer.

**Material and methodology of the experiment.** For plasma spaying composite powder with size of

**Table 1.** Conditions of spraying of two-layer coating

| Type of installation | Voltage, V | Current, A | Plasma gas | Spraying distance, mm | Powder consumption, kg / h | MUF* |
|---|---|---|---|---|---|---|
| *Plasma spraying — first layer* | | | | | | |
| UPU-8M | 55 | 500 | Ar + $N_2$ | 120 | 3.5 | 0.80 |
| *Electric arc metallization — second layer* | | | | | | |
| KDM-2 | 35 | 200 | -- | 200–210 | N / D | 0.75 |

*Material utilization factor.

particles 40–80 μm, produced by the method of self-propagating high-temperature synthesis, of the following composition was used, wt.%: $TiSi_2$ — 30.5; $Al_2O_3$ — 17; Ni — 42.5; $Cr_3C_2$ — 10. For electric arc metallization wire of 95Al–5Si (wt.%) alloy of 2 mm diameter was used.

On the layer, produced by plasma spraying of $TiSi_2 \cdot Al_2O_3 \cdot Ni \cdot Cr_3C_2$ powder on the base from carbon steel (first layer), AlSi coating (second layer) was applied by arc metallization. Conditions of spraying are presented in Table 1. Then annealing at temperature values 700 and 750 °C within 1.5 h in the flow of high-purity argon was performed (GOST 1057–79).

Metallographic investigations of the specimens (polished and after chemical etching in 0.5 % water solution of hydrofluoric acid) were performed on the «Neophot-32» metallographic microscope.

Microhardness of the coatings was determined on the LECO instrument M-400 at the load 0.249 and 0.490 N. Strength of cohesion between the coating and the base was estimated by the glue method.

X-ray diffraction phase analysis (XDPA) was performed on the DRON-UM1 diffractometer in Cu$K_\alpha$ copper radiation. Chemical composition of separate areas of the coating was determined by means of X-ray spectral microanalysis (XSMA) on the Camebax SX-50 instrument.

Wear resistance of the coatings was estimated under conditions of the gas-abrasive wear at high temperature values on a specially designed installation at the following parameters: temperature of the specimen (600 ± 10) °C; pressure of heated air supplied by a compressor through the nozzle equaled 0.5 MPa, which ensured velocity of air flow with the abrasive of 140 m / s; distance from the nozzle edge to the specimen was 50 mm. Powder of $Al_2O_3$ synthetic corundum of 0.6–0.8 mm dispersity was used as the abrasive. Angle of the air-abrasive flow attack was 90°.

Wear of the coating was established by loss of the mass in relation to a unit of the specimen area and 1 kg of the abrasive mass, getting on the specimen, i.e. intensity of the mass wear (mg / ($cm^2 \cdot$kg)) was determined.

**Results and discussion thereof.** As a result of TS dense two-layer coating without cracks and lamination in the zone of connection with the base, having strength of cohesion with the latter 40 MPa, has formed. Porosity of the layer produced by the plasma spraying was 10–12 vol.%; of the layer produced by the electric arc metallization — 4–5 vol.%.

In Figure 1 and Table 2 microstructure and characteristics of the two-layer coating are presented. Structure of the internal layer is of lamellar-granular character. White lamellas of nickel, light orbicular particles, lamellas of titanium silicides of complex composition, fine-dispersed particles of chromium carbide of up to 5 μm size, and dark coarse particles and lamellas of aluminium oxide prevail in it.

External layer of the coating, produced by the method of electric arc metallization, is formed from lamellas of the Al–Si alloy, containing dispersed (up to 1 μm) particles of silicon ($SiO_2$) and aluminium ($\alpha$-, $\gamma$-$Al_2O_3$) oxides.

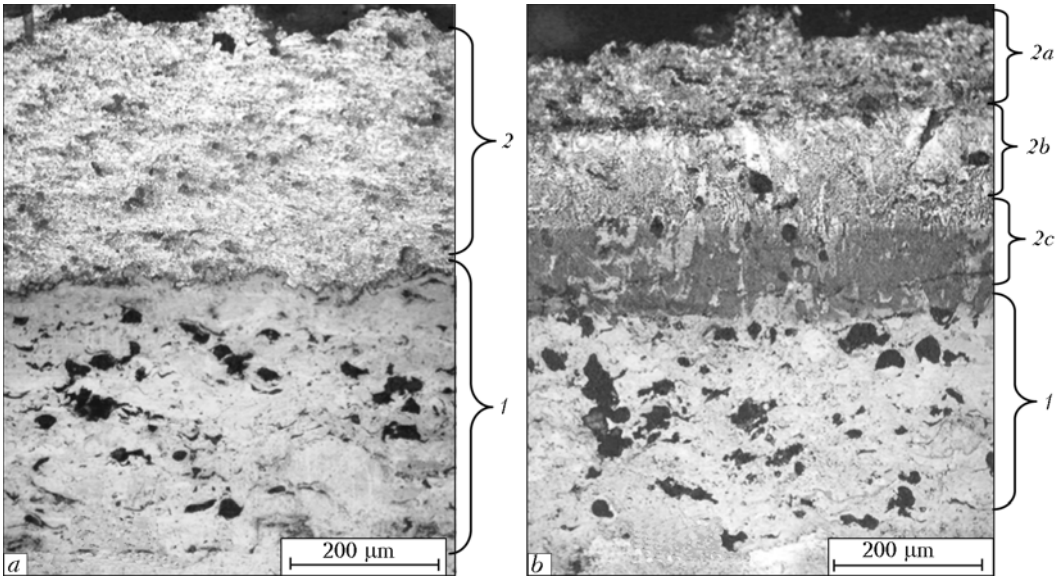


**Figure 1.** Microstructure of multilayer coating (first layer is produced by plasma spraying of $TiSi_2 \cdot Al_2O_3 \cdot Ni \cdot Cr_3C_2$, second — by electric arc metallization of AlSi): *a* — after spraying; *b* — after heat treatment, etched

**Table 2.** Characteristic of multilayer coating

| State of coating | Layer of coating | Thickness of layer, μm | Phase composition | *HV*0.05, GPa |
|---|---|---|---|---|
| After spraying | First | 300 | Ni, $Ni_{16}Ti_6Si_7$, γ-$Al_2$Î$_3$, α-$Al_2$Î$_3$, $TiSi_2$, $Cr_3C_2$, Ñr$_7$Ñ$_3$ | 8.66 ± 1.50 |
| | Second | 350 | Al, Si, α-$Al_2$Î$_3$, γ-$Al_2$Î$_3$, $SiO_2$, halo of 28 ≤ 2θ ≤ 52° | 0.76 ± 0.10 |
| After annealing at 700 °C, 1.5 h | First | 300 | Ni, $Ni_3Ti_2Si$, α-$Al_2$Î$_3$, TiSi, $Ti_5Si_4$, Ñr$_{23}$Ñ$_6$, Ñr$_7$Ñ$_3$, γ-Aλ$_2$Î$_3$ | 8.20 ± 1.00 |
| | Second | 350 | *a* — Al, $Al_3Ni$, α-$Al_2$Î$_3$, γ-$Al_2$Î$_3$, $Al_2SiO_3$, $SiO_2$, halo of 28 ≤ 2θ ≤ 54° | 1.60 ± 0.50 |
| | | | *b* — Al, AlNi, $Al_3Ni$, $Al_{23}Ti_9$, $Ti_5Si_4$, γ-$Al_2$Î$_3$, α-$Al_2$Î$_3$ | 7.86 ± 0.65 |
| | | | *c* — AlNi, $Al_3Ni$, Al, $Al_3Ti$, $Ti_5Si_4$, $(Si, Al)_2Cr$ | 8.69 ± 1.00 |
| After annealing at 750 °C, 1.5 h | First | 300 | Ni, $Ni_3Ti_2Si$, α-$Al_2O_3$, TiSi, $Ti_5Si_4$, $Cr_{23}C_6$, $Cr_7C_3$, γ-$Al_2$Î$_3$ | 8.10 ± 1.00 |
| | Second | 350 | à — Al, $Al_3Ni$, α-$Al_2$Î$_3$, γ-$Al_2$Î$_3$, $Al_2SiO_3$, $SiO_2$, halo of 28 ≤ 2θ ≤ 54° | 1.76 ± 0.50 |
| | | | *b* — Al, AlNi, $Al_3Ni$, $Al_{23}Ti_9$, $Ti_5Si_4$, γ-$Al_2$Î$_3$, α-$Al_2$Î$_3$ | 6.69 ± 0.70 |
| | | | *c* — AlNi, $Al_3Ni$, Al, $Al_3Ti$, $Ti_5Si_4$, $(Si, Al)_2Cr$ | 8.34 ± 1.00 |

*Note*. First layer is produced by plasma spraying of $TiSi_2Al_2O_3$·Ni·$Cr_3C_2$, second layer — by electric arc metallization of $Al_5Si$.

On X-ray photograph of the surface layer diffusion halo within the range of angles 28 ≤ 2θ ≤ 52° was detected, which proves presence of the amorphous component in the structure.

As a result of heat treatment at the temperature 700 °C within 1.5 h processes of intensive diffusion interaction took place between layers of the coating (Figures 1, *b* and 2, Table 2). Diffusion of nickel, chromium and titanium from the plasma-sprayed layer into external aluminium-base layer with formation of nickel and titanium aluminides and complex compounds of aluminium, chromium and silicon was registered.

Sources of nickel and titanium are nickel bonds of the plasma coating and complex silicide $Ni_{16}Ti_6Si_7$, which forms during heating thermodynamic more stable low silicide $Ni_3Ti_2Si$. Chromium carbides $Cr_3C_2$ and $Cr_7C_3$ transformed as a result of heating into the low carbides $Cr_7C_3$–$Cr_{23}C_6$ with reduction of their general amount. By this fact formation of compound $(Si, Al)_2Cr$ in the zone adjacent to the plasma layer (Figure 2, *c*) can be explained. In the zone of con-

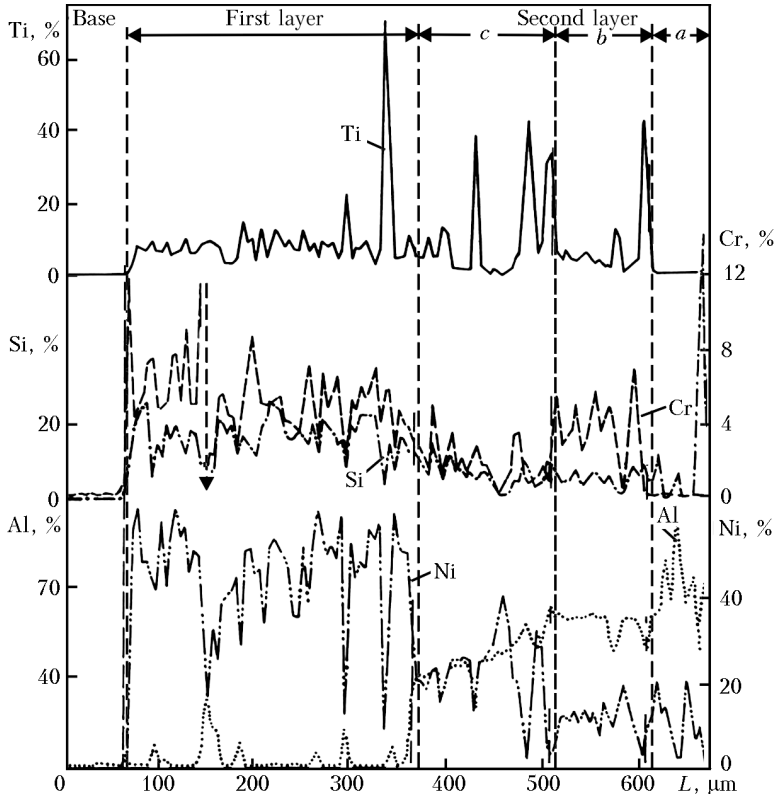


**Figure 2.** Distribution of chemical elements in two-layer coating annealed at temperature 700 °C within 1.5 h in flow of argon: *L* — length of investigated area

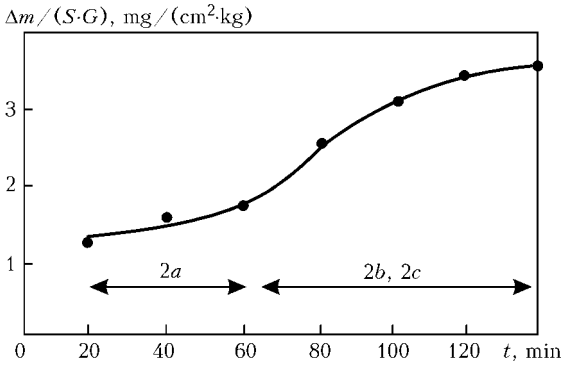


**Figure 3.** Kinetics of gas-abrasive wear of modified multilayer coating at test temperature 600 °C: Δ*m* — loss of multilayer coating mass; *S* — area; *G* — mass of abrasive

nection of two layers microporosity, caused by diffusion of nickel, titanium and chromium, was detected. As a result of diffusion of these elements compaction of the upper metallization layer occurs. At the same time formed microporosity does not cause lamination of the two-layer coatings and does not reduce strength of cohesion with the base.

Cross diffusion of aluminium from external layer into the internal composite one, which is characteristic of aluminide coatings on the bases of nickel and its alloys [22], was not registered. It is, evidently, connected with complex composition and presence of additional boundaries in the composite thermal layer, which acts as a barrier for progress of the diffusion processes.

Microstructure of the external (second) layer, in contrast to the internal (first) one, underwent significant changes: it got compacted and became practically pore-free; three diffusion zones, differed by structure, phase composition and hardness, may be singled out in it (see Figure 1, *b*, Table 2).

In the surface layer 2*a* content of the dispersed strengthening particles has increased in comparison with non-annealed state mainly due to newly formed NiAl nickel aluminides and presence of oxides.

On X-ray photograph of the surface layer, as well as before the annealing, diffusion halo was detected within the same range of angles that proves presence of the amorphous component of the structure. Microhardness of this layer has increased two-fold after the annealing.

Lower located zone 2*b* consists of a light matrix with elongated and columnar crystals of dark color. Direction of growth of the crystals coincides with directed diffusion of nickel, chromium and titanium from first layer into second one. According to the data of layer-by-layer XDPA, nickel and titanium aluminides and titanium silicides are formed as a result of the diffusion interaction between these elements and Al–Si alloy, which causes significant strengthening of this zone. Microhardness of this area has increased by one order (Table 2).

In direct proximity to the plasma layer the hardest dark zone 2*c* is located, which mainly formed from particles of nickel (AlNi, $Al_3Ni$) and titanium ($Al_3Ti$) aluminides, titanium silicides ($Al_5Si_4$), and complex compounds — chromium alumosilicides $(Si, Al)_2Cr$. In this zone of second layer the least amount of the aluminium-containing component was noted (see Table 2).

Phase composition of the products of solid-phase chemical reaction between two components is predetermined by correspondence of thermodynamic conditions of equilibrium of phases of a certain composition and the conditions, established in a certain area of the reaction zone. Most frequently sequence of arrangement of the single-phase layers qualitatively corresponds to that of the phases along isothermal horizontal on the constitutional diagram. Such dependence is observed in diffusion of nickel, weight share of which prevails in the plasma coating (42.5 wt.%), into the metallized aluminium-base layer with formation of aluminides.

It is also necessary to take into account in the multicomponent systems ratio of the diffusion rate of different components, which jointly diffuse in the same direction, and chemical activity thereof. Both these factors may stipulate non-uniformity of distribution of concentration of components of a complex system in layers of the formed reaction products. This, in its turn, enables formation of the compounds, which do not correspond to sequence of arrangement of the phases along isothermal horizontal on the constitutional diagram. Exactly such effect was registered in formation of $Al_{23}Ti_9$ and $Al_3Ti$ titanium aluminides in the areas 2*b* and 2*c*.

According to the results of metallographic analysis and layer-by-layer XDPA and XSMA, principal differences in phase composition and structure of the coatings after their heat treatment at temperatures 700 and 750 °C, as well as in character of diffusion of nickel, titanium, chromium and similarly located layers and diffusion zones of these complex coatings, were not detected. But the tendency to microhardness decrease was observed at annealing temperature of 750 °C. Evidently further increase of the heat treatment temperature may enable reduction of microhardness of the layer, produced by metallization, due to coagulation of the dispersed strengthening particles formed due to the diffusion interaction between layers of the coating.

The character of kinetic dependence of the gas-abrasive wear intensity at 600 °C (Figure 3) is affected by the fact that this two-layer coating has after heat treatment phase composition that changes over the depth. Fractography investigations of the surface (Figure 4) and phase composition of the coatings at different stages of the tests showed that external dense zone 2*a*, consisting mainly from Al–Si alloy strengthened by dispersed inclusions of nickel aluminides and aluminium and silicon oxides, is most wear-resistant. Intensity of its wear does not exceed 1.5 mg / ($cm^2$·kg), whereby formation of cracks and shelling-out on surface in the process of tests was not detected (Figure 4, *b*).

After removal of surface zone 2*a* of about 100 μm thickness intensity of wear increases up to 3.0–

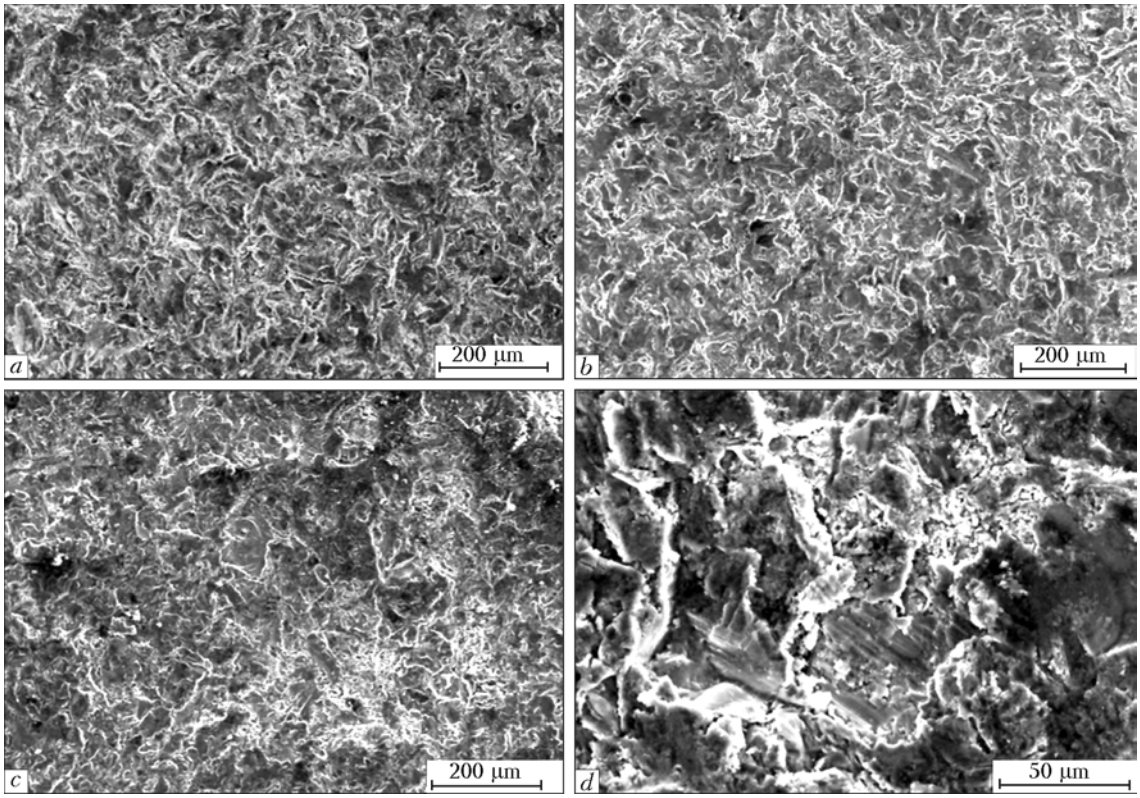


**Figure 4.** Topography of surface of modified multilayer coating before (*a*) and after (*b*) gas-abrasive wear at depth 100 (*b*) and 200 (*c*–*d*) μm at 600 °C

3.5 mg / ($cm^2$·kg) and remains constant up to full attrition of the metallization layer. At transition into the plasma-sprayed layer intensity of the gas-abrasive wear sharply increases up to 12.5 mg / ($cm^2$·kg).

Structure of zones 2*b* and 2*c* is less homogeneous; columnar crystals, containing according to XSMA data aluminium, titanium, nickel and silicon, which are nickel and titanium aluminides and titanium silicides, have formed in them (see Table 2). Wear of mentioned zones is accompanied by formation of cracks and cohesion destruction (Figure 4, *c*, *d*).

So, mechanical properties of the diffusion zones depend upon the shape and distribution of the strengthening particles. The most orbicular, uniformly distributed fine particles enable high ductility and relatively high strength of the layer; acicular (columnar) crystals significantly increase its hardness, but essentially reduce ductility. Wear resistance of zones 2*a* and 2*b* is higher than that of the plasma-sprayed layer 8.0 and 3.5 times, respectively.

## CONCLUSIONS

1. Processes of the diffusion interaction between layers of the two-layer thermal coating, lower layer of which is produced by the plasma spraying of composite powder $TiSi_2$·$Al_2O_3$·Ni·$CrC_2$ and upper one ---- by electric arc metallization of AlSi alloy at annealing in flow of argon at 700 °C within 1.5 h, were investigated.

2. It was established that annealing enabled significant changes in phase composition of the layers. In the compacted upper layer nickel and titanium aluminides, chromium alumosilicides and titanium silicides, formed in the process of diffusion of nickel, chromium and titanium of the plasma coating, were detected, whereby cross diffusion of aluminium was not registered, i.e. alitizing of the plasma coating did not occur.

3. It was determined that changes in morphology and phase composition of the coatings as a result of the diffusion interaction caused sharp increase (more than 3 times) of wear resistance at temperature 600 °C.

*The authors express their gratitude to Scientific-Technical Center of Ukraine for financial support of this work, carried out within framework of project G 046.*

1. Borisova, A.L., Adeeva, L.I., Tunik, A.Yu. (1994) *Influence of initial material characteristics and spraying conditions on structure and properties of thermal coatings.* Kiev: PWI.
2. Kerkush, I.P., Melnik, P.I. (1996) Improvement of properties of plasma-sprayed iron coatings by chrome plating. *Poroshk. Metallurgiya*, **1 / 2**, 58–61.
3. Vasiliev, R.A., Gonopolsky, A.M., Kopylova, I.L. et al. (1989) Development of technology of diffusion saturation of thermal coatings. In: *Abstr. of Conf. on Theory and Practice of Thermal Spraying of Coatings* (Dmitrov, Sept. 1988), Vol. IV, 119–121.
4. Zemskov, G.V., Sinkovsky, A.S., Balykov, V.S. et al. (1980) Structure and some properties of carburized plasma coatings. In: *Protective coatings on metals*, Issue 14, 43–55.
5. Nakamori, M., Harada, E. (1984) Resistance to high-temperature corrosion of combined coatings consisting from plasma sprayed layer and layer resultant of diffusion treatment. *Boshoku Gijutsu*, 33(**7**), 395–401.
6. Medyukh, R.M., Danilenko, V.A. (1990) Investigation of kinetics of diffusion chrome plating of steel and molybdenum plasma coatings. In: *Abstr. of Conf. on Deposition, Strengthening and Properties of Protective Coatings on Metals* (Ivano-Frankovsk, Oct. 1990), 17.

7. Epik, A.P., Stepanchuk, A.N., Vdovichenko, N.S. et al. (1990) Effect of borating on properties of thermal coatings. *Ibid.*, 18.
8. Zemskov, G.V., Slobodyanyuk, A.A., Glebov, V.I. et al. (1989) Comparative study of wear resistance of composite plasma and plasma-diffusion coatings. In: *Abstr. of Conf. on Theory and Practice of Thermal Coating Deposition* (Dmitrov, Sept. 1988), Vol. 11, Part 2, 51–52.
9. Medyukh, R.M. (1994) Structure and some properties of plasma and molybdenum coatings after diffusion chrome plating. In: *Protective coatings on metals*, Issue 28, 69–71.
10. Derkach, V.D., Yuga, A.I., Chevichelova, T.M. et al. (1990) Effect of chemical-heat treatment on tribotechnical properties of bronze-based plasma coatings. In: *Abstr. of Conf. on Deposition, Strengthening and Properties of Protective Coatings on Metals* (Ivano-Frankovsk, Oct. 1990), 34.
11. Zemskov, G.V., Kogan, R.L., Sinkovsky, A.S. et al. (1986) Heat resistance of steel with protective coatings. In: *Transact. on Heat-Resistant Coatings.* Leningrad: Nauka.
12. Slobodyanuk, A.A., Zemskov, G.V., Kogan, R.L. et al. (1985) Aluminium and chrome plating of plasma coatings on steel and titanium. In: *Protective coatings on metals*, Issue 19, 30–32.
13. Zemskov, G.V., Kogan, R.L., Slobodyanyuk, A.A. et al. (1980) Diffusion metallizing of plasma coatings. *Ibid.*, Issue 14, 69–70.
14. Zemskov, G.V., Kogan, R.L. Slobodyanyuk, A.A. et al. (1982) Investigation of aluminium plating of plasma coatings on titanium. *Ibid.*, Issue 16, 58–61.
15. Slobodyanyuk, A.A., Zemskov, G.V., Kogan, R.L. et al. (1980) Development and study of plasma and plasma-diffusion coatings on titanium and its alloys. In: *Abstr. of All-Union Meeting on Theory and Practice of Thermal Coating Deposition* (Riga, May 1980), Vol. 2, 70–72.
16. Takeuchi, J., Murata, Y., Harada, Y. et al. (1998) An improvement of $Cr_2C_3$–NiCr sprayed coatings followed by chromium diffusion treatment. In: *Proc. of ITSC*, Vol. 2, 1425–1430.
17. Ryazantsev, I.Ya., Goncharenko, I.V., Filatov, N.G. et al. (1986) Chromising using method of plasma-sprayed coating on steel surface. *Metallovedenie i Term. Obrab. Metallov*, **1**, 34–36.
18. Gauding, C., Jacquot, P., Prince, P. et al. (1998) Vacuum heat treatment and low pressure carburizing of APS NiCr coatings. In: *Proc. of ITSC*, Vol. 2, 1387–1392.
19. Oki, S., Veno, G., Gohda, S. (1998) Spray diffusion: new method for surface modification combined with thermal spray and heat treatment. *Surface Eng.*, 14(**2**), 155–158.
20. Titlyanov, A.E., Radyuk, A.G., Zakharov, A.S. et al. (1998) *Development of wear-resistant layers on surface of copper products*. Moscow: Materialovedenie.
21. Ohmori, A., Yoshida, K., Li, C.-L. (1997) Characterization of graded Ti silicide coating formed by thermal diffusion treatment of low pressure plasma sprayed silicon coating on titanium substrate. *Transact. of JWRI*, **2**, 35–41.
22. Minkevich, A.N. (1965) *Chemical-heat treatment of metals and alloys*. Moscow: Mashinostroenie.

# TITANIUM. PROBLEMS OF PRODUCTION. PROSPECTS. Analytical Review. Part 3*

**K.A. TSYKULENKO**
E.O. Paton Electric Welding Institute, NASU, Kiev, Ukraine

Different methods of the induction and electron beam remelting of titanium and significant difficulties of production of titanium ingots by these methods are considered. Possible ways of cost reduction of the titanium products and prospects of Ukraine in the world titanium industry are shown.

*Keywords: methods of the induction and electron beam remelting, factors of cost reduction of the titanium products, possible role and prospects of Ukraine in the world titanium industry*

Application of different electrodes in melting of ingots causes problems connected with their fabrication, stability, etc. Different methods of the induction and electron beam remelting allow refusing from application of both consumable and non-consumable electrodes.

In melting in the induction furnace heating and melting of the metal occurs due to induction of alternating electromotive force and creation of eddy currents, which are transformed into heat directly released in the metal. The melted metal is intensively mixed due to occurring electrodynamic forces in it. That's why within the whole mass of the melt the required temperature is maintained with the least melting loss in comparison with different methods of arc and electron beam melting.

The most important advantage of the induction furnaces, stipulated by generation of heat inside the melted metal, turns into disadvantage in case of their application for the refining melting. Slags with a comparatively low electric conductivity get heat in the induction furnaces from the molten metal, which hinders processes of the metal refining. This stipulates application of the induction melting furnaces mainly in foundries.

Vacuum-induction furnaces are mainly used for melting of the charge, protection of the melt from influence of atmosphere, bringing it up to the necessary condition (in general case the area of the interphase surface being the same, the content of impurities in the melt is proportional to duration of seasoning in vacuum), and for casting of metals and alloys in vacuum.

Vacuum-induction melting, as well as other methods, is used in production of titanium ingots [1]. In addition to triple VAR of a consumable electrode, it is possible to use the following schemes with partici-

*Parts 1, 2 see in Nos. 1, 2, 2007, respectively.

pation of the vacuum-induction melting as VIR + ESR + VAR or VIR + VAR + EBR. Here vacuum-induction melting is the process used for preliminary refining of the metal and compaction of the charge materials into the consumable electrode, which has maximal chemical homogeneity, for subsequent remelting by «quasi-equilibrium» processes –– VAR, ESR, and EBR.

Designs of the vacuum induction furnaces are simpler than of the vacuum arc ones [2, 3]. As a rule, in the jacket there are a chamber with a melting inductor and a crucible, a mechanism for its turning, and a casting chamber, in which one or several moulds are located. Because of interaction of the metal with material of the melting crucible lining, duration of the melt seasoning in VIR is limited by several minutes. Interaction of the metal being melted with the crucible material in VIR is more intensive than in open induction melting [4]. In the induction melting processes requirements to the crucible material are practically the same as in the skull melting processes.

The need in a fully chemically inert unit for melting of active metals, in particular titanium, enabled development of vacuum-arc, electroslag, electron beam and plasma-arc processes of remelting in copper water-cooled moulds. The induction method was not exception either.

As far back as in 1920s design of the induction furnace with a water-cooled crucible from electricity conducting metal was suggested. Later such units started to be called cold crucibles [5]. In order to ensure possibility to transfer energy from the inductor to the melt, the wall of the cooled crucible was made in the form of separate sections, electrically insulated from each other. Molten metal from the cold crucible was poured into moulds.

Development of the process of ingot production in cold crucibles with application of the induction heating is described in [6]. In this work the conclusion was drawn on principal possibility and prospects of using process of the titanium waste remelting in a sectional mould.

Induction remelting in the sectional mould has its peculiarities. In contrast to vacuum-induction and induction melting in conventional or cold crucibles, when an ingot is produced by casting the whole accumulated mass of the metal into the mould, in remelting in a sectional mould, like in all other kinds of remelting in a water-cooled mould, the process of simultaneous melting of the fed metal and solidification of the produced melt takes place. The ingot may be formed by means of relative movement of the inductor and the sectioned mould. Metal pool in the latter acquires because of influence of the electromagnetic forces and pressing-out of its upper part from the mould walls a shape of a cupola. Both consumable electrodes and different lumpy and loose materials may be subjected to remelting in such mould. The process may proceed under a layer of slag and in the atmosphere of inert gases or vacuum.

In first designs of the induction sectioned moulds special measures for isolation of the sections from each other were no envisaged. Into the interspaces between sections of the induction mould aluminous isolating caps for thermocouples were placed, which also acted as seals that prevented pouring out of the melt through the interspaces between the segments [7]. Such designs did not allow melting titanium ingots of more or less significant diameter.

Increase of the installation power and diameter of the mould from 63.5 to 355.6 mm caused constant emergencies because of occurrence of arc discharges in the interspaces between sections of the mould and short-circuiting of the latter by the molten metal, which showed impossibility of the process performance without reliable isolation of the sections from each other. Experience of the electroslag remelting, in which an ingot is formed in a thin crust of the slag skull, stipulated application for this purpose of the slag that allowed avoiding mentioned problems. Molten slag filled interspaces between the sections and, having solidified, acted as a reliable isolation of the section and the metal of the ingot being formed.

Induction-slag remelting was used in melting of titanium ingots of small diameter. It should be noted that presence of slag does allow performing remelting at reduced pressure. At the pressure below 75 mm Hg strong evaporation of slag was registered, that's why removal of hydrogen in this method of remelting occurs less efficiently than in VIR or VAR. In addition, it is inexpedient to use in induction-slag remelting the schemes with drawing of an ingot from the mould [5]. During movement of an ingot relative the mould wall tear of the slag crust is possible, due to which short-circuiting of the section by molten metal occurs.

State-of-the-art designs of the sectioned moulds envisage isolation of the section by a layer of glass cloth. In addition, external surface of the mould sleeve is covered by the glass cloth, which imparts to it additional rigidity and insulates the sleeve from the inductor. Prevention of break-downs between the sections because of their short-circuiting by melt of the metal being remelted is achieved by application of the matching high-frequency transformers, maintaining on the inductor of a reduced (80–100 V) voltage, and application of a big number of sections. While in design of the mould, described in [7], there are four such sections, in state-of-the-art sectioned moulds there may be 15, 20, and more sections [7]. In case of increase of the number of sections, voltage between them significantly (by one order) reduces. Moreover, the process is performed in such way that solidification front of the melt to be at the lower turn of the inductor. Molten metal, located above this level, is pressed-out from the mould walls and does not contact with them, forms a «cupola», and the ingot being formed finds itself located outside the area of the inductor influence and does not represent hazard from the viewpoint of a break-down between separate sections due to their short-circuiting by the ingot metal

at voltage 4–5 V. Such approach allows refusing from application of slag as an insulator and using possibility of operation at reduced pressure or in shielding gases. Because of a characteristic «cupola», area of the metal pool surface in induction remelting in the sectioned mould exceeds section of the ingot being melted, i.e. the metal pool has a developed surface. Intensive mixing of the melt and developed surface of the metal pool enable intensification of the melt degassing process.

As far as possibility of the induction remelting of titanium in a sectioned mould is concerned, remelting of the consumable electrodes, pressed from titanium sponge, is not used anymore because of clear advantage of the technology with application of the loose titanium sponge, when it is fed into the mould from aside. A promising direction is considered remelting of different kinds of wastes — chips, cuttings, parts, which got unfit for service, for example, flanges of the casting fitting-out of spun casting machines [6], and gas-saturated titanium sponge [8, 9].

By the induction remelting method in the sectioned mould ingots of small and medium diameter (up to 300–350 mm) are, as a rule, produced. Production of bigger ingots is inexpedient because of the need to use powerful generators supplying the induction remelting installations. And, while application of such generators in VIR, when capacity of the furnace constitutes dozens tons and melting of the metal is performed within a comparatively short time interval, is justified, in remelting in the sectioned mould in case of formation of an ingot at rates not more than several millimeters per minute, increase of the generator power above a certain value becomes economically disadvantages.

Big titanium ingots may be produced by the method of electron beam remelting, in the process of which heating and melting of the metal proceeds, like in VIR, due to generation of heat directly in the metal being remelted, but in this case owing to treatment of the surface by a flow of electrons, kinetic energy of which during their collision with surface of the material being radiated transforms into heat energy of movement of the particles.

Flow of electrons is produced due to the effect of thermoelectron emission of the heated cathode. As a rule, tungsten and tantalum are used as the cathode material of the electron beam gun. For imparting to the electrons necessary kinetic energy acceleration voltage from several kilowatts to several dozens kilowatts (the higher is voltage, the higher is energy of the electrons) is used, whereby positive lead-out of the high-voltage power source is electrically connected either with the material being radiated, or with a non-melting cooled anode.

For efficient application of the produced flow of electrons (the electron beam) high vacuum is required, as far as because of small mass of the electrons their flow on the way to the material being radiated dissipates as a result of collision with other particles. In the course of collision of the electrons with molecules of the residual gases a portion of the energy is lost, whereby the processes of ionization and recombination of the particles occur, which create visible radiation. Way of the beam gets visible.

Interaction of the electrons with ionized gas enables additional dissipation of the beam. All this takes 1–15 % of the beam energy. More significant (from 6 to 25 %) losses of energy occur in direct collision of the electrons with surface of the metal, and they are stipulated by reflection of a portion of the beam electrons from the metal surface and occurrence of secondary electron emission and X-ray radiation [10].

Power of X-ray radiation in EBR is low (several shares of a percent of the installation power), but its biological action represents a serious hazard for the operation personnel. That's why range of the acceleration voltage values is limited by 35–40 kV. Thickness of steel walls of the installation is selected, taking into account reliable shielding of the personnel against radiation (as a rule 10–15 mm).

At acceleration voltage up to 40 kV depth of penetration of the electrons into metals does not exceed several micrometers. But because of high density of the electron beam energy (by three orders higher than that of the electric arc) the radiated metal not just melts but intensively evaporates, due to which on way of the beam a thin channel is formed, depth of which exceeds several thousands times depth of the electron diffusion.

In electron beam melting and remelting of metals such effect is harmful. That's why for dispersion of the electron beam energy all over the treated surface electromagnetic systems are used, which deviate the beam according to the preset program and ensure necessary trajectory of the heat spot movement. For uniform heating of the surface and ensuring minimum melting loss it is necessary to scan the beam at the frequency above 50 and sometimes more than 100 Hz [11, 12], whereby overheating of the metal pool surface is approximately by 100–150 °C higher than in VAR [10].

Two principally different systems of electron guns for melting of metal are known: without an acceleration anode (with a ring cathode) and with it. In case of melting by the electron guns without the acceleration anode, when voltage is applied between the cathode and the material being heated, electron beam is formed in the space immediately adjacent to the surface being heated. This allows obtaining a powerful electron beam at relatively low acceleration voltage. Low values of the acceleration voltage (several kilowatts) determine lower levels of X-ray radiation and cost of the power source. The electron beam guns without the acceleration anode have simple design and are easy in servicing. In guns of this type distance between the cathode and surface of the billet being melted or of the metal pool in the mould should be comparatively small and correspond to the acceleration voltage.

Close location of the cathode unit to the surface of the metal being remelted causes getting on the cathode and the focusing electrode of the molten metal vapors and spatter [10, 11]. Presence of the electrical field in the area of melting causes intensified ion bombardment of the cathode unit and frequently occurrence of glow discharges. As a result stability of the process is disturbed, and service life of the cathode usually does not exceed several hours.

Common for formation of the beam and vacuum treatment of the melt chamber stipulates necessity to maintain in it significantly lower values of the residual pressure of the gas-vapor phase than it is necessary in performance of the degassing and melt distillation processes. For ensuring of stable operation of the electron beam guns one should not allow even for a comparatively short time increase of pressure in the chamber above $1 \cdot 10^{-4}$ mm Hg [11]. That's why invariable attribute of EBR is a highly productive vacuum system, consisting of a great number of valves, gates, and pumps of different types (diffusion, booster, and roughing-down ones). As power of the electron beam guns and productivity of the melting installation grows up, requirements to productivity of the vacuum system sharply increase. An important parameter in this case is ratio of the rate of pumping out of the diffusion pumps of the installation to power of the latter. For installations of different types this ratio constitutes 50–200 l / (s·kW).

Application of a more perfect system of the guns with the acceleration anode, which makes it possible to use so called system of differential pumping-out, at which degassing of a small space before the acceleration anode and of the melting chamber proper (behind the anode) is performed separately, allows reducing load on the vacuum system. Pressure levels in the melting chamber and in the chamber, in which the cathode is located, may differ by 2–3 orders [12].

For efficient application of the produced electron beam and vacuum treatment of the melt, pressure in the melting chamber of the installations with differential pumping-out may be significantly higher than in the installations without the acceleration anode, however in this case it should not exceed $1 \cdot 10^{-2}$ mm Hg either.

Electron beam guns with the acceleration anode may be placed at a significant distance from the melting metal (usually at 800–1500 mm). It enables reduction of the amount of vapors and spatter of the molten metal getting on the anode unit. Absence of electric field in the melting zone and significant reduction of influence of sudden gas releases on operation of the cathode–anode system significantly reduce influence of the glow discharge occurrence. As a result service life of the cathode of such guns equals 100 h and more [11].

In the space behind the anode one can easily control the electron beam by means of electromagnetic fields (focalize, deviate, move it according to a preset program) and ensure in this way required conditions of heating. There are three varieties of electron beam guns with the acceleration anode: annular, axial, and flat-beam ones. Their principal difference consists in the form of a generated beam. Electromagnetic systems of such guns deviate the electron beam, when it is directed at the metal, at the angle 45, 60 and sometimes up to 180–270°. This makes it possible to place guns sideways and even from below from the heated surface, protecting the cathode unit from vapors and spatter of the metal. It should be noted that axial and flat-beam guns as the most perfect units allow implementing to the greatest degree principle of the heat source independence, which radically distinguishes EBR from VAR.

By means of the independent heat source one may regulate duration of the melt stay in the molten state that affects efficiency of its refining. Moreover, the melt is subjected in EBR to the action of a deeper vacuum and higher temperature than in VAR. Big depth of the furnace melting space pumping-out in EBR improves conditions of the degassing, distillation and dissociation processes of the non-metal inclusions. Increase of the melt temperature significantly affects mainly processes of evaporation of the elements. However, overheating and long seasoning of the melt parallel with removal of harmful impurities causes losses of the metal (the base and the alloying elements). Dependence of these losses upon power of the electron beam installation and specific consumption of electric power is practically a linear one [10].

Electron beam melting of the titanium sponge does not render significant influence on content of main impurities [11]. Concentration of oxygen and nitrogen is at the level of the initial metal [12]. This is connection with high pressure of the titanium vapor and thermodynamic stability of titanium oxides. Hydrogen, weight share of which in EBR reduces 3–6 times, i.e. significantly higher than in VAR, is the exclusion. As a result impact toughness of the EBR metal is 2 times higher than that of the VAR metal. In melting of the titanium alloys significant reduction of content of the alloying components with a higher pressure of vapor than that of titanium, for example, manganese, aluminium, chromium, etc. occurs, especially in melting of the lumpy charge. First of al it concerns aluminium, because it is an alloying element of practically all titanium alloys. The evaporation loss may be reduced by application of a consumable billet instead of the charge or addition of respective hardeners in melting.

Intensification of the processes of titanium refining from nitrogen and oxygen is enabled by increase of the reduced reaction surface that is implemented in the remelting schemes with an intermediate unit. Application of the latter envisages longer stay of the melt in molten state, whereby averaging of the chemical composition, removal of the refractory inclusions from the melt due to their deposition on bottom of the unit, floatation of the non-metal inclusions of low density and their dissociation under the electron beam

action take place. In addition, such scheme allows using as an initial charge the scrap (up to 100 %) and spongy titanium of somewhat poorer quality and melting of ingots-slabs [13, 14] and hollow ingots [15].

Application of such complex and expensive process as EBR should be justified either by impossibility of producing high-quality metal by some other method or achievement of advantages at the process stage [10]. As one can see, there are many other methods besides EBR for production of titanium, but the latter one showed nowadays its efficiency in reprocessing of the titanium scrap and production of secondary titanium [12]. Possibility of refusing from application of the consumable electrodes (which would require for establishment of the respective production) has predetermined predominated role of this process in titanium industry of Ukraine.

Comparative characteristic of the parameters and qualitative estimation of different methods of melting and remelting of metals and alloys, presented in [4], showed that the most productive are vacuum-induction and plasma-arc skull melting processes (up to 5 t / h); the least productive are plasma-arc and electron beam remelting processes (up to 1.2 t / h); electroslag and vacuum-arc remelting have intermediate value (up to 2 t / h). From the viewpoint of power consumption the most economical is the process of vacuum-arc remelting (about 1 kW·h / kg), while vacuum induction melting is the most power consuming (about 4 kW·h / kg). Effect of evaporation of the melt components was registered in all processes, whereby intensity of evaporation increases along the chain VIR–VAR–EBR.

Selection of a process for production of titanium ingots is rather individual and depends upon many factors (existing infrastructure of the accompanying production; requirements to quality of the metal; designation of the latter, required volumes of its production, etc.).

Reduction of cost of the titanium products and wider application of titanium in the industry can occur due to the following factors:

- perfection and development of new technological processes of titanium processing (new low-cost methods of the titanium sponge production and reprocessing of the gas-saturated, having increased content of technogenic impurities, sponge, and new methods of melting and remelting);
- organizational-technological measures connected with unification of different processing stages, organization of the vertically integrated production, and involvement into reprocessing of different wastes of the titanium industry;
- respective quality of the metal and its designation.

Establishment of a big titanium company VSMPO-Avisma in Russia is a bright example. Unification of two stages of the metallurgical processing allowed reducing production cost of the products by 10–12 % [16]. The VSMPO-Avisma and Boeing companies announced in 2006 about establishment of the joint venture, which will perform machining of the stamped items from titanium for their subsequent application in the «Boeing» passenger aircraft [17]. Waste metal of the production (titanium chips) will be returned to VSMPO-Avisma for their subsequent reprocessing and involvement into the production cycle.

For ensuring of the required properties content of impurities in titanium and its alloys is limited. So, weight share of oxygen in the deformable titanium alloys does not exceed 0.30, of nitrogen 0.15 and of hydrogen 0.015 %. The most gas-saturated is VT1-2 alloy (general content of these impurities in it equals 0.46 %) designed for fabrication of different bars. Because of high content of impurities this alloy has approximately 2 times higher value of ultimate tensile strength than similar to it VT1-00 and VT1-0 alloys (commercial titanium). Lately it is sometimes required to supply to the consumers ingots of titanium alloys with increased content of oxygen, i.e. with somewhat increased due to this strength of the alloy (Figure).

Evidently, both producers and consumer of titanium started to understand necessity of the compromise between purity of the alloy and its designation and, therefore, the method of production and cost. High cost of the titanium products at low cost of the initial feedstock is determined by expenses of the process stages. And, probably, there is no need at early stages of production to achieve high purity of the metal, spending for this purpose significant resources, and then to get in the ready metal increased contents of various kinds of impurities. It is more expedient to arrange the production chain in such way that required quality of the metal, for example, increased content of oxygen, be achieved at once at minimal expenses.

Such situation exists in production of steel, when after development of the blast furnace and the acid Bessemer converter, terminated thousand-year epoch of «pure» steel. Replacement of charcoal for coke caused contamination of the cast iron and, therefore, produced from it steel by sulfur; blowing of the molten metal by air caused in addition its contamination with nitrogen [20]. One learned to impart necessary properties to «dirty» steel by means of various alloying additives, because the consumer is interested not in the composition of a produced alloy, but in its properties. Content of harmful impurities in steels, as well as in titanium alloys, is limited. So, for example, for ensuring high reliability and long service life of ball bearings the content of sulfur in the steel, from which they are manufactured, was brought to ten thousand's shares of a percent. It needed high expenses. But it turned out that not just content of sulfur itself was important, but the ratio of oxygen and sulfur in the metal.

Metallurgy of titanium, in comparison with metallurgy of steel, is still very young, and, possibly, in

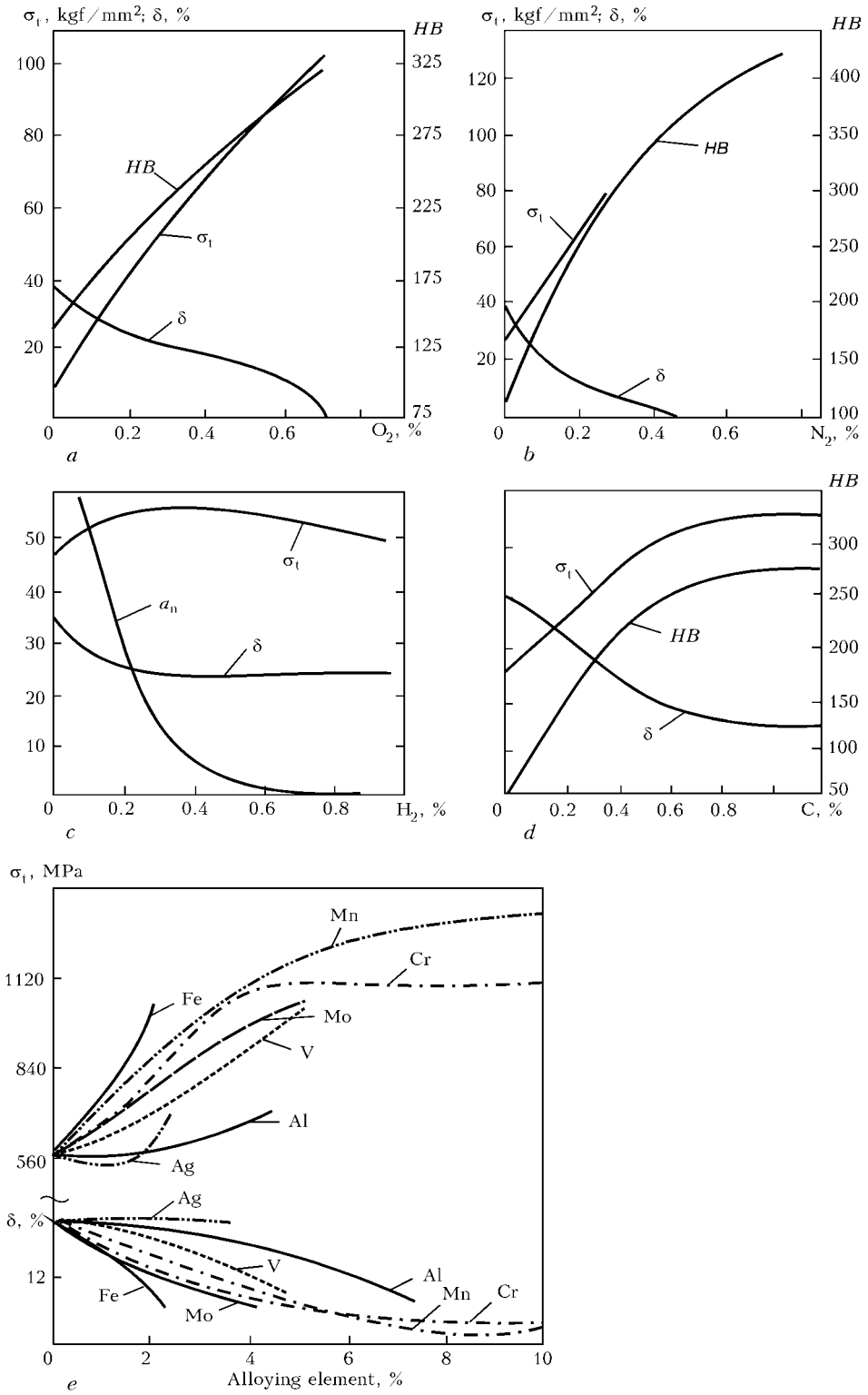


Influence of oxygen (*a*), nitrogen (*b*), hydrogen (*c*), carbon (*d*) and alloying elements (*e*) on mechanical properties of titanium [18, 19]

future low-cost titanium alloys will appear, in which negative influence of increased content of impurities will be compensated by a respective system of alloying. Evidently, alloying metals contained in VT3, VT3-1 and VT4 titanium alloys, affect their mechanical properties to greater extent than hydrogen [21]. At present one has to pay attention to classification of new titanium alloys, which are being developed, depending upon their possible application. Of course, in military and airspace fields, as ever, high-purity alloys are needed. Their cost may be reduced only due to new technological solutions. But in other fields, for example, jewelry business, manufacturing of rims for glasses, substrates of hard disks for computers, housings of watches, etc., «space» purity, evidently, is not required, but just high specific strength or just corrosion resistance, or absence of magnetism, etc. That's why such titanium alloys may be produced

**Table 1.** Chemical composition of ferrotitanium according to GOST 4761–80 (ST SEV 989–89)

| Grade | Weight share of elements, % | | | | | | | | | | |
|---|---|---|---|---|---|---|---|---|---|---|---|
| | Ti | Al | Si | C | P | S | Cu | V | Mo | Zr | Sn |
| | not less than | not more than | | | | | | | | | |
| FTi70S05 | 68–75 | 5.0 | 0.5 | 0.2 | 0.05 | 0.05 | 0.2 | 0.6 | 0.6 | 0.6 | 0.10 |
| FTi70S08 | 68–75 | 4.0 | 0.8 | 0.3 | 0.03 | 0.03 | 0.3 | 1.8 | 2.0 | 1.5 | 0.15 |
| FTi70S1 | 65–75 | 5.0 | 1.0 | 0.4 | 0.05 | 0.05 | 0.4 | 3.0 | 2.5 | 2.0 | 0.15 |
| FTi35S5 | 28–40 | 8.0 | 5.0 | 0.2 | 0.04 | 0.04 | 2.0 | 0.4 | 0.4 | 0.2 | 0.04 |
| FTi35S7 | 28–40 | 9.0 | 7.0 | 0.2 | 0.07 | 0.05 | 2.0 | 0.8 | 0.5 | 0.2 | 0.05 |
| FTi35S8 | 28–40 | 14.0 | 8.0 | 0.2 | 0.07 | 0.07 | 3.0 | 1.0 | 1.0 | 0.7 | 0.08 |
| FTi30 | 28–37 | 8.0 | 4.0 | 0.12 | 0.04 | 0.03 | 0.4 | 0.8 | 0.4 | 0.2 | 0.01 |
| FTi25 | 20–30 | 5.0–25.0 | 5.0–30.0 | 1.0 | 0.08 | 0.03 | – | – | – | – | – |

*Note*. Ferrotitanium of FT and 70S08 grades contains additionally 0.8 % Mn and 0.8 % Cr.

according to a simplified technology (without application of vacuum or from off-grade sponge, waste, etc.), which will allow significant reducing of their cost. The need in compromise between purity of the alloy and its designation and in ensuring of minimal production cost had, evidently, given impetus to companies «Allegheny Technologies» (USA) and VSMPO (Russia) to establish the joint venture UNITI, which is specialized in production of titanium alloys of just civil designation. UNITI will be engaged in development of the titanium markets of non-airspace and non-military designation [22].

**Role of Ukraine and its prospects in world titanium industry.** In addition to production, fabrication and supply of the titanium feedstock (the concentrates and the sponge), Ukraine started to produce titanium ingots. Establishment of production of titanium ingots became a first step on the way to increase of Ukraine's part in the world titanium industry. This production is mainly based on electron beam remelting, which is rather expensive method. Despite the possibility of melting by this method ingots from the charge materials containing up to 100 % of the titanium waste, such approach to reduction of the production cost is not always justified. Contained in the charge oxygen and nitrogen impurities, which are not removed in EBR, do not allow producing high-quality titanium ingot. The highest efficiency of this method of production of the ingots may be achieved in reprocessing of the high-quality sponge for production of the airspace and military designation titanium.

**Table 2.** Content of main impurities in sponge and produced ingots

| Object of analysis (melting conditions) | Weight share of main impurities, $\%\cdot10^{-4}$ | | | |
|---|---|---|---|---|
| | Ñ | N | O | H |
| Sponge (cleaned in vacuum) | 91 | 47 | 685 | 47 |
| VAR ingot | 64 | 113 | 713 | 17 |
| ESR ingot (chemically pure $CaF_2$, He, direct polarity) | 108 | 115 | 955 | 22 |
| The same (unrefined $CaF_2$) | 89 | 63 | 811 | 20 |

The next step could be increase of the volumes of production with simultaneous reduction of cost of titanium products due to establishment of the vertically integrated chain for production of titanium. However, attempts to establish such chains for the time being have failed, and without necessary investments one should not count on them in near future. Share of Ukraine in world production of titanium ingots is still small and constitutes approximately 1 %. While volumes of production gradually increase, consumption of the titanium ingots in Ukraine is insignificant and has lately reduced. Produced ingots go mainly for export. That's why the way of the titanium cost reduction through organizational-technological measures and unification of different technological process stages is in the meanwhile closed.

Reduction of cost of the titanium products due to application of cheaper methods of production of the ingots also envisages certain worsening of the titanium alloy purity. So, electroslag method, which did not find practical application in production of titanium and its alloys in airspace and military fields, is successfully used for production of ferrotitanium, because requirements to ferrotitanium, designed for deoxidizing and alloying of steel, alloys and cast iron, as wel as for production of welding materials, do not at all regulate content in it of such harmful impurities as hydrogen, oxygen, and nitrogen (Table 1).

Ferrotitanium and titanium alloys for airspace industry occupy two opposite positions in regard to purity of the titanium alloys. However, certain compromises between them are possible relative price and quality of titanium for so called non-special purpose designation, i.e. used in jewelry business, manufacturing of rims for glasses, substrates of hard disks for computers, housings of watches, sport items, etc. This, for the time being insufficiently developed segment of the world titanium market, can give Ukraine

a real chance to increase its role in the world titanium industry. Ukrainian industry, which has high capacities for production of the ESR metal, can relatively quickly reorient itself at production of low-cost titanium alloys of non-special purpose designation. It should be noted once more that quality of titanium, produced by the ESR method, is sufficiently high. At the beginning of development of the titanium market in former USSR a struggle was waged between supporters of the ESR and the VAR processes for possession of the aviation market. Of course, the ESR method practically excludes possibility of removal of gases from titanium and in this respect can not compete with any vacuum process. However, as it is noted in many investigations, the main factor, which determines purity of the ESR ingot metal, is purity of the initial material to be remelted (electrode, sponge, and other charge materials). Content of impurities in the electroslag titanium, depending upon the used slag, kind and polarity of current, and composition of the remelting atmosphere, may noticeably vary [23]. So, minimal content of oxygen in the electroslag titanium is achieved in remelting in the stagnation helium atmosphere or in remelting at reverse polarity current; minimal amount of nitrogen ---- at reduced pressure or at alternative current. In addition, in case of use of unrefined fluoric calcium as a slag, content of nitrogen in the ESR ingot is even lower than in the VAR ingot (Table 2). Depending upon allowable contamination of titanium by various impurities one can select respective technological scheme of ESR.

Comparative investigations of quality of the cast and deformed ESR and double VAR titanium showed that both in cast and deformed state the ESR and the VAR titanium has rather close mechanical characteristics. Only in case of application as an initial material of high-quality sponge, subjected to vacuum separation, the ESR titanium is noticeably inferior to the VAR titanium in respect to such parameter as impact toughness. Exactly this fact did not allow the ESR process occupying its niche in the titanium industry of former USSR, where practically the whole production went for needs of the defense complex. However, high values of toughness characteristics are needed not in all cases; for example, in jewelry business they are not of great significance.

After development of new equipment and technological solutions (a current-conducting mould, double-circuit scheme of remelting, magnet-controlled melting, etc.) possibilities of ESR as a whole and ESR of titanium, in particular, have expanded. And these possibilities have to be used with maximum efficiency. For development of market of titanium of the non-special purpose parts, which may consume up to 45 % of titanium products, coordination of efforts of many specialists will be needed. This will include development of new titanium alloys, respective slag systems, estimation of applicability of a specific alloy for various fields, development of respective standards, and many other activities. In order to move forward one has to make steps in the chosen direction. Ukraine, having big feedstock resources and means of production, will try to occupy worthy position in the world titanium industry.


1. Medovar, B.I. (1996) New developments in field of electroslag technology. *Problemy Spets. Elektrometallurgii*, **2**, 3–6.
2. (1968) *Induction furnaces for melting of metals and alloys*. Moscow: Metallurgiya.
3. Tselikov, A.I. (1997) *Metallurgical machines and units*. Moscow: Metallurgiya.
4. Gritsianov, Yu.A., Putimtsev, B.N., Molotilov, B.V. et al. (1975) *Metallurgy of precision alloys*. Moscow: Metallurgiya.
5. Petrov, Yu.B., Ratnikov, D.G. (1972) *Cold crucibles*. Moscow: Metallurgiya.
6. Latash, Yu.V., Shejko, I.V., Bernadsky, V.N. et al. (1986) Induction remelting in sectional mould, feasibilities and prospects of its application for remelting of titanium waste. *Problemy Spets. Elektrometallurgii*, **2**, 64–70.
7. Kleites, P.J. (1973) Induction-slag remelting of titanium. In: *Vacuum metallurgy*. Moscow: Metallurgiya.
8. Zhadkevich, M.L., Latash, Yu.V., Shejko, I.V. et al. (1997) On problem of feasibility of remelting of sponge titanium with higher content of man-caused impurities. Report 1. *Problemy Spets. Elektrometallurgii*, **1**, 55–60.
9. Zhadkevich, M.L., Latash, Yu.V., Konstantinov, V.S. et al. (1998) On problem of feasibility of remelting of sponge titanium with higher content of man-caused impurities. Report 2. *Problemy Spets. Elektrometallurgii*, **3**, 43–45.
10. Latash, Yu.V., Matyakh, V.N. (1987) *Current methods of production of superhigh quality ingots*. Kiev: Naukova Dumka.
11. Movchan, B.A., Tikhonovsky, A.L., Kurapov, Yu.A. (1973) *Electron beam melting and refining of metals and alloys*. Kiev: Naukova Dumka.
12. Paton, B.E., Trigub, N.P., Kozlitin, D.A. et al. (1997) *Electron beam melting*. Kiev: Naukova Dumka.
13. Paton, B.E., Trigub, N.P., Akhonin, S.V. et al. (1996) Some tendencies of development of titanium metallurgical refining. *Problemy Spets. Elektrometallurgii*, **1**, 25–31.
14. Zhuk, G.V., Kalinyuk, A.N., Trigub, N.P. (2004) Production of titanium ingots-slabs using method of EBCHM. *Advances in Electrometallurgy*, **3**, 20–22.
15. Paton, B.E., Trigub, N.P., Zhuk, G.V. et al. (2004) Producing hollow titanium ingots using EBCHM. *Ibid*., **3**, 16–19.
16. Rubanov, I. (2005) Is wrong with titanium. *Ekspert*, 14.11.2005. www.infogeo.ru / metals / press /
17. www.vsmpo.ru
18. Gurevich, S.M. (1981) *Reference book on welding of nonferrous metals*. Kiev: Naukova Dumka.
19. (2003) *Metals and alloys*: Refer. Book. Ed. by Yu.P. Solntsev. St.-Petersburg: Professional.
20. Medovar, B.I. (1990) *Metallurgy yesterday, today, tomorrow*. Kiev: Naukova Dumka.
21. Garmata, V.A., Gulyanitsky, B.S., Kramnik, V.Yu. et al. (1967) *Metallurgy of titanium*. Moscow: Metallurgiya.
22. Aleksandrov, A.V., Prudkovsky, B.A. (2003) Different sides of titanium and its alloys. *Titan*, **2**, 66--71.
23. (1981) *Electroslag metal*. Ed. by B.E. Paton, B.I. Medovar. Kiev: Naukova Dumka.

# ALTERNATIVE TECHNOLOGIES OF REMELTING OF INDUSTRIAL WASTES OF TITANIUM AND ALLOYS THEREOF

**I.V. SHEJKO, V.A. SHAPOVALOV** and **V.S. KONSTANTINOV**
E.O. Paton Electric Welding Institute, NASU, Kiev, Ukraine

Data on application of the induction melting in a sectional mould for refining and disposal of the titanium and wastes thereof are presented.

*Keywords: inductor, electromagnetic field, titanium, metal pool, ingot, sectional mould, titanium sponge*

Titanium and its alloys are irreplaceable structural materials in many fields of new engineering, for example in cases, when reduction of mass is of great importance, and in chemical machine building and ship building, where high corrosion resistance is needed in chemically corrosive environment, including sea water. That's why, despite high cost of the titanium metal products, its consumption by the industry annually increases.

Production of metal titanium (titanium sponge), which is the basis for production of the alloys and cast and deformed items, is a multistage and rather power-intensive chemical-metallurgical process, requiring application of expensive equipment and reagents. As a result, from a comparatively low-price and rather distributed natural raw materials the metal is produced, cost of which is significantly higher than that of steel, aluminium, copper and other non-ferrous metals.

Main stages of the metal titanium production are as follows:

- melting of titanium slag in an ore heat-treating furnace from the ilmenite concentrate;
- chlorination of the produced slag in the chlorinators with the melt of salts;
- cleaning of titanium tetrachloride $TiCl_4$ by means of chemical treatment, rectification and distillation;
- magnesium-heat reduction with production of the primary metal product (spongy titanium);
- vacuum distillation (separation) of the spongy titanium from technogenic impurities (mainly magnesium chlorides);
- pressing of the consumable electrodes from the cleaned spongy titanium;
- remelting of the electrodes in the vacuum-arc furnaces with production of ingots of commercially pure titanium and alloys on its basis.

The most power-intensive stage in the technological chain of the titanium sponge production is vacuum distillation, which envisages heating of the produced mass up to the temperature 1000–1020 °C in vacuum and its seasoning at this temperature for several tens of hours [1–4].

Residual content of chlorine and other impurities in titanium sponge is regulated by respective standards (GOST 17746–72), according to which content of chlorine in the sponge of TG90–TP20 grades should not exceed 0.08 wt.%. In order to obtain such amount of chlorine in the titanium sponge it is necessary to season the reaction mass in the apparatuses at high temperature for a long time, which causes significant consumption of power, reduction of productivity and service life of the vacuum distillation units [4].

In the process of the titanium sponge production about 10 % of wastes are formed, which have different fraction composition and increased content of gas and technogenic impurities [1, 3, 5]. Analysis of different lots of the titanium sponge of the TG-TB grade proves that part of it (about 60 %) may be used for melting of titanium ingots and later as consumable electrodes, for example, in casting of bodies and components of the valving for chemical machine building [6]. Data on content of impurities in the titanium sponge according to GOST 17746–72 are presented in Table 1.

One can see from Table 1 that content of impurities in the off-grade TG-TB sponge, produced at Zaporozhie Titanium-Magnesium Works (ZTMW), is rather high, although it is lower than the level allowed by the standard. So, sponge of this grade may be used as the charge for melting of ingots and production of non-special purpose cast items.

In addition, significant amounts of titanium wastes in the form of chips and cuttings are formed at the enterprises of chemical machine building. Majority of them are the conditioned metal, chemical composition of which corresponds to the grade one. So, the wastes may be involved into the charge in production of ingots and cast items.

Limited amount of the wastes in the form of chips, scrap, etc. (not more than 30 %) may be mixed with the metal titanium sponge and compacted into briquettes or consumable electrodes for their subsequent remelting. This technology is widely used in industry, but it is complex, expensive, and significantly in-

**Table 1.** Chemical composition and hardness of spongy titanium (GOST 17746–72)

| Grade of titanium | Weight share of impurities, %, not more than | | | | | | *HB*, not more than |
|---|---|---|---|---|---|---|---|
| | Fe | Si | Ñ | Ñl | [N] | [ Î ] | |
| TG-90 | 0.06 | 0.01 | 0.02 | 0.08 | 0.02 | 0.04 | 90 |
| TG-100 | 0.07 | 0.02 | 0.03 | 0.08 | 0.02 | 0.04 | 100 |
| TG-110 | 0.09 | 0.03 | 0.03 | 0.08 | 0.03 | 0.05 | 110 |
| TG-120 | 0.11 | 0.03 | 0.04 | 0.08 | 0.03 | 0.06 | 120 |
| TG-130 | 0.13 | 0.04 | 0.04 | 0.10 | 0.03 | 0.08 | 130 |
| TG-150 | 0.20 | 0.04 | 0.05 | 0.20 | 0.04 | 0.10 | 150 |
| TG-TB | 2.00 | -- | 0.05 | 0.30 | 0.30 | -- | -- |
| TG-TB (ZTMW)* | 0.34 | 0.026 | 0.025 | 0.07 | 0.105 | 0.125 | -- |

*Mean statistical data, based on 20 lots of the ZTMW-produced titanium sponge, are presented.

creases cost of the titanium products. And the main shortcoming consists in impossibility of full involvement of the wastes into melting of the ingots, especially at the enterprises of the machine-building complex. Rather tempting are attempts of many researchers to use process of the induction melting in the sectional mould (IMSM) for production of titanium ingots with application of different kinds of charge, including those, which previously were not used for melting of the titanium-containing ferroalloys [7–10].

The induction melting with formation of an ingot in the sectional mould, as well as cold-crucible induction melting, have not still occupied stable niche in the area of special electrometallurgy. Available in the literature data may be characterized as a search of possible ways for application of this method for refining of different metals and alloys (mainly highly-reaction ones in the molten state), disposal of different kinds of the expensive metal wastes, and melting of the high-quality complex alloys from the components, having sharp physical differences (density, melting and boiling points, etc.).

Important peculiarity of IMSM is the fact that melting of the charge and solidification of the ingot occurs in the electromagnetic field of high intensity, which causes vigorous mixing of the metal melt. Intensive circulation of the metal is one of the most important advantages of this process, because it ensures equalizing of temperature and chemical composition within the pool volume, accelerates melting of the charge, and enables active interaction of the metal with the slag.

First information on application of IMSM for melting of the titanium alloys relates to 1960–1970s. In the laboratory «Bureau of Mines» (USA) under guidance of P. Clites and R. Beall melting of ingots from the titanium scrap with application of the oxygen-free flux (fluoric calcium), fed in the course of melting into the mould together with the titanium sponge, was tested [8]. In the process of melting fluoric calcium formed in the pressing-out zone of the metal pool an annular slag pool, which enabled production of a thin slag skull on the cooled wall of the mould. This skull prevented shunting of the mould section by the metal, and (like in electroslag remelting) isolated an ingot from the cooled wall of the mould.

General amount of calcium fluoride constituted about 4 % of mass of the metal charge. Used in this process fluoric calcium not just failed to ensure removal of impurities from titanium but, vise versa, the available in it impurities transferred into the ingot. That's why the latter was subjected to remelting in vacuum in order to bring to minimum contamination of titanium.

Comparative chemical analysis of the melted ingots with the vacuum-arc melting metal showed that the former ones had high content of controllable impurities, especially silicon, iron, and hydrogen [8]. As a result values of such physical-mechanical characteristics as hardness, tensile strength and yield strength were somewhat higher, while relative elongation and reduction in area lower than those of titanium melted with application of the induction-slag technology. Peculiar feature of the induction-slag melting metal is its reduced impact toughness. Unfortunately the authors did not check if this peculiarity is preserved after remelting of the produced consumable electrodes in the VAR furnaces.

More detailed investigation of the behavior of main alloying elements and impurities in titanium in IMSM was carried out at the E.O. Paton Electric Welding Institute of the NAS of Ukraine [11–14]. The fulfilled works are mainly directed at disposal of the wastes of titanium production (titanium sponge of the TG-TB grade) and machine-building enterprises.

One may judge about quality of the titanium ingots, produced on the IMSM installation, by the data presented in Table 2.

It follows from Table 2 that such impurities as iron, carbon and silicon are distributed in the ingots rather uniformly, and their content depends upon their initial amount in the titanium sponge, i.e. no change of the weight share of these elements in the ingot in comparison with their content in the charge as a result of remelting was detected.

**Table 2.** Content of impurities in ingots melted from titanium sponge of TG-TB grade ($D_{ingot}$ = 105 mm)

| Charge characteristics | Place of sampling | Weight share of elements, % | | | Volume share of elements, % | | | *Í Â* |
|---|---|---|---|---|---|---|---|---|
| | | Fe | Ñ | Si | [N] | [ Î ] | [N] | |
| TG-TB sponge (fraction 2–12) | Top | 0.33 | 0.022 | 0.020 | 0.098 | 0.117 | 0.010 | 201 |
| | Middle | 0.33 | 0.020 | 0.018 | 0.094 | 0.110 | 0.008 | 104 |
| | Bottom | 0.34 | 0.024 | 0.025 | 0.102 | 0.124 | 0.012 | 212 |

Gas impurities are also distributed within the ingot volume rather uniformly. Increased content of oxygen and hydrogen in bottom part of the ingots is explained by their absorption by the molten metal from the melting chamber atmosphere at the initial period of melting as a result of evaporation of the adsorbed on the melting chamber walls moisture after beginning of radiation from the metal pool surface.

Interesting results were obtained in melting of titanium ingots from the off-grade TG-TB titanium sponge, which was diluted by the high-grade sponge of the TG-100 grade at different ratios (Table 3).

The results obtained (Table 3) prove that the IMSM process allows melting ingots, which fully meet requirements of the specifications even when content of the TG-TB titanium off-grade sponge in the charge constitutes 50 %. This is by 20 % higher than in the charge, used in pressing of consumable electrodes for VAR.

The most power-intensive stage in production of spongy titanium is vacuum refining (separation) of spongy titanium from magnesium chlorides.

In case of reduction of the duration of this stage, in the spongy titanium may remain increased content of chlorine and magnesium, which can significantly exceed the level established by the state standard.

In order to assess possibilities of the IMSM process in removal of mentioned impurities the titanium sponge was used, containing definitely significant amount of chlorine (0.15, 0.30 and 0.52 %) [3].

The results of investigation of chemical composition of the ingots, melted from this sponge, are presented in Table 4.

One can see from Table 4 that content of iron and nitrogen in the ingots remains at the same level as in the initial titanium sponge. At the same time, in the process of melting oxygen is removed to great degree, which, in opinion of the authors, occurs as a result of evaporation of the adsorbed on the sponge surface moisture due to degassing of the installation melting chamber, as well as heating of the charge on spout of the feeder.

Melting of the spongy titanium with increased content of magnesium chlorides is accompanied by vigorous gas release, which is proved by bubbling of the metal pool, and in certain cases ---- by local outburst of the melt in the places, where pieces of sponge were immersed to the bottom of the pressed-out portion of the pool.

In remelting of the sponge with 0.52 % $Cl_2$, formation of condensate on the mould wall above the molten titanium level in the form of a film of chlorides, occurs.

In certain areas of surface of the ingots a thin layer of fine-dispersed sublimates was detected (Figure 1), which could be easily removed by a metal brush. As a whole, surface of the ingots is satisfactory, it has no apparent defects.

Special difficulties are connected with remelting of the titanium chips, having extraordinary developed surface, in which a thin layer of oxides is formed during cutting, and which, in addition, is soiled by the lubrication materials (emulsion) used in machining. Such chips, as a rule, are sent to the ore heat-treating furnaces for melting of ferrotitanium and are used for pressing of briquettes used in the process of deoxidizing of steel.

Technological investigations showed that in case of remelting of the cleaned in proper way chips of commercially pure VT1-0 titanium and VT5 alloy (washing in hot solution of alkaline with subsequent defatting in the aviation petrol), it is possible to melt ingots with content of impurities, corresponding to requirements of the standard (Table 5).

**Table 3.** Content of impurities in ingots melted from titanium sponge of different grades ($D_{ingot}$ = 67 mm)

| Charge composition | Weight share of impurities, % | | | | |
|---|---|---|---|---|---|
| | Fe | Ñ | [N] | [O] | [ Í ] |
| 80 TG-100<br>20 TG-ÒÂ | 0.058 | 0.035 | 0.012 | 0.068 | 0.007 |
| 70 TG-100<br>30 TG-ÒÂ | 0.100 | 0.045 | 0.018 | 0.085 | 0.007 |
| 60 TG-100<br>40 TG-ÒÂ | 0.150 | 0.057 | 0.025 | 0.120 | 0.008 |
| 50 TG-100<br>50 TG-ÒÂ | 0.250 | 0.070 | 0.035 | 0.160 | 0.008 |
| Regulated by specifications for VT1-0 alloy | 0.300 | 0.070 | 0.040 | 0.200 | 0.010 |

**Table 4.** Content of impurities in ingots melted from spongy titanium with increased content of magnesium chloride ($D_{ingot}$ = = 67 mm)

| Place of sampling | Weight share of impurities, % | | | |
|---|---|---|---|---|
| | Ñl | Fe | [N] | [ Î ] |
| Spongy titanium | 0.15 | 0.28 | 0.22 | 1.05 |
| Ingot | 0 | 0.28 | 0.22 | 0.24 |
| Spongy titanium | 0.30 | 0.32 | 0.14 | 1.10 |
| Ingot | 0 | 0.32 | 0.15 | 0.22 |
| Spongy titanium | 0.52 | 0.15 | 0.14 | 0.68 |
| Ingot | 0 | 0.17 | 0.15 | 0.25 |

Significant amounts of conditioned wastes of the titanium alloys are formed in the granular technology, which was developed comparatively recently and is used in aviation and missile-space engineering for manufacturing of special-purpose parts, like impellers, turbines, housings of different complexity from refractory alloys, including those on the basis of titanium.

High rate of solidification of the granulated powders of $4 \cdot 10^3$–$2 \cdot 10^4$ deg / s, produced mainly by the method of centrifugal spraying of the consumable ingots, melted by the low-temperature plasma in inert gas, ensures production of a homogeneous fine-grain structure, uniformity of distribution of phase components of the alloys, and possibility of introduction into them of the alloying components in the amount, not achievable by traditional methods of casting.

One of the problems is complexity of production of the granulated powders, and in a number of cases also absence of efficient technologies for processing of the formed wastes, which represent a conditioned by chemical composition but not corresponding to the granulometry metal [15–18]. The share of these wastes in general balance of the metal consumption equals 35–40 %.

In this connection remelting of the granulated powder wastes from the VT5-1kt titanium alloy on the IMSM installation (67 mm diameter) was tested. Such diameter of the ingots corresponded to the diameter of consumable billets (with small allowance for machining) used in the centrifugal spraying installations (CSI). Results of the investigation are presented in Table 6.

As it follows from presented data, remelting according to the IMSM technology practically does not affect weight share of main alloying elements in the melt (aluminium and tin). Content of gas impurities (oxygen and nitrogen) in the ingot metal is higher than in the granules used as the charge. It is stipulated not so much by gas environment in the melting chamber, as by presence of the adsorbed gases and moisture on the charge surface, which is extraordinary developed, whereby it is impossible to remove adsorbed impurities by conventional degassing of the melting chamber because of high compacting ability of the charge in the hopper.

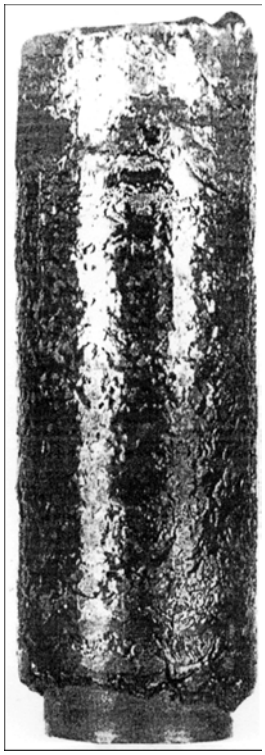

**Figure 1.** General view of ingot melted from spongy titanium with 0.3 % Cl ($D_{ingot}$ = 67 mm)

Soft dispersed heating of the melt, characteristic of the induction source of heating, in combination with mixing of the melt prevents local overheating of its surface, thus not causing evaporation of even such alloying elements as aluminium and tin, which have rather high values of vapor pressure.

Melted from the wastes ingots have good quality of surface, any defects on the surface are absent (Figure 2).

Investigation of macrostructure of the ingots showed that they have structure, characteristic of the ingots produced by the VAR, ESR, EBR and PAR methods (Figure 3).

At the E.O. Paton Electric Welding Institute of the NAS of Ukraine for the first time under industrial conditions at PA «Kievtraktorodetal» remelting of the consumable billets from the OT4-2 titanium alloy assembled from the waste elements of fitting-out of

**Table 5.** Content of impurities in IMSM ingots melted from chips

| Grade of alloy | Atmosphere in melting chamber | Weight share of impurities, % | | | | |
|---|---|---|---|---|---|---|
| | | Fe | Ñ | [N] | [Î] | [Í] |
| VT1-0 (initial) | -- | 0.22 | 0.056 | 0.04 | 0.16 | 0.012 |
| VT1-0 | Argon | 0.20 | 0.055 | 0.04 | 0.15 | 0.008 |
| VT1-0 | Helium | 0.12 | 0.048 | 0.03 | 0.12 | 0.006 |
| Regulated by specifications | -- | 0.30 | 0.070 | 0.03 | 0.20 | 0.010 |
| VT5 (initial) | -- | 0.23 | 0.052 | 0.04 | 0.25 | 0.009 |
| VT5 | Argon | 0.23 | 0.059 | 0.04 | 0.25 | 0.008 |
| VT5 | Helium | 0.16 | 0.045 | 0.03 | 0.21 | 0.007 |
| Regulated by specifications | -- | 0.30 | 0.100 | 0.05 | 0.30 | 0.015 |

**Table 6.** Chemical composition of ingots melted from wastes of granulated powder of VT5-1kt alloy

| Gas atmosphere in melting chamber | Pressure in melting chamber, MPa | Weight share, % | | | | | | | |
|---|---|---|---|---|---|---|---|---|---|
| | | Alloying elements | | Impurities | | | | | |
| | | Àl | Sn | Ñ | Fe | Si | [ Î ] | [N] | [ Í ] |
| Argon | 0.05 | 5.40 | 2.64 | 0.018 | 0.078 | Traces | 0.086 | 0.023 | 0.0045 |
| Argon | 0.10 | 5.41 | 2.67 | 0.018 | 0.080 | Same | 0.088 | 0.025 | 0.0046 |
| Helium | 0.05 | 5.40 | 2.63 | 0.017 | 0.078 | » | 0.082 | 0.016 | 0.0037 |
| Helium | 0.10 | 5.41 | 2.65 | 0.018 | 0.079 | » | 0.085 | 0.019 | 0.0430 |
| Initial metal | – | 5.42 | 2.68 | 0.018 | 0.080 | 0.01 | 0.080 | 0.011 | 0.0050 |
| TU 91-1-192–87 | – | 4.0–5.5 | 2.0–3.0 | 0.005 | 0.200 | 0.10 | 0.120 | 0.040 | 0.0080 |

the machines for centrifugal casting of sleeves, was implemented.

In the foundry of this Association the flanges from the OT4-2 titanium alloy were used as heat-insulating inserts in chill moulds of the machines for centrifugal casting of sleeves for tractor engines, which allowed excluding the cast iron chilling in edge (end) zones of the castings. Titanium inserts (flanges) operate under tense thermal conditions ---- quick heating during casting of the cast iron into the rotating chill mould alternates with their sharp cooling in water pool after removal of the cast iron sleeve from the chill mould. So, after casting of several hundreds of sleeves, big amount of radial cracks are formed on working surface of the flanges, which quickly deepen in the process of subsequent castings. Later one can not use such flanges anymore (Figure 4). Annually at the plant up to 15 t of expensive rolled titanium sheet were used for manufacturing of new flanges.

It is impossible to use titanium flanges as the charge in IMSM because of their big dimensions, and their crushing or cutting into smaller pieces is not economically justified. Remelting of such wastes of the same overall dimensions became possible due to application of the consumable billets assembled from the waste flanges.

For production of the consumable billets the treated on the shot-blasting installation titanium rings were assembled into a stack of 20–25 rings and welded with each other by the argon-arc method (Figure 5). Additionally outside strips from titanium sheet of 15–20 mm width were welded for prevention of the ring break during melting.

In IMSM protection of the plate against action of highly concentrated source of the heat energy, like in VAR, is not required. The role of inoculation in IMSM is brought down to formation after its melting of the metal pool, sufficient for normal progress of the process. In melting of ingots on the OP117 installation (Figure 6) 2–3 waste flanges, placed before the melting in the form of a stack on the bottom plate, were used as inoculation. Internal cavity of the flanges was filled by titanium cuttings or chips.

Melted ingots of 220 mm diameter have characteristic peculiarities ---- on surface of the ingots longitudinal thin ribs were registered of 0.5–2.0 mm height, formed as a result of filling of the joints between sections of the mould by the molten metal. These ribs do not affect structure of the ingot and its

**Figure 2.** IMSM ingots melted from wastes of granulated powders of VT5-1kt alloy

**Figure 3.** Macrostructure of IMSM ingot of VT5-1kt alloy

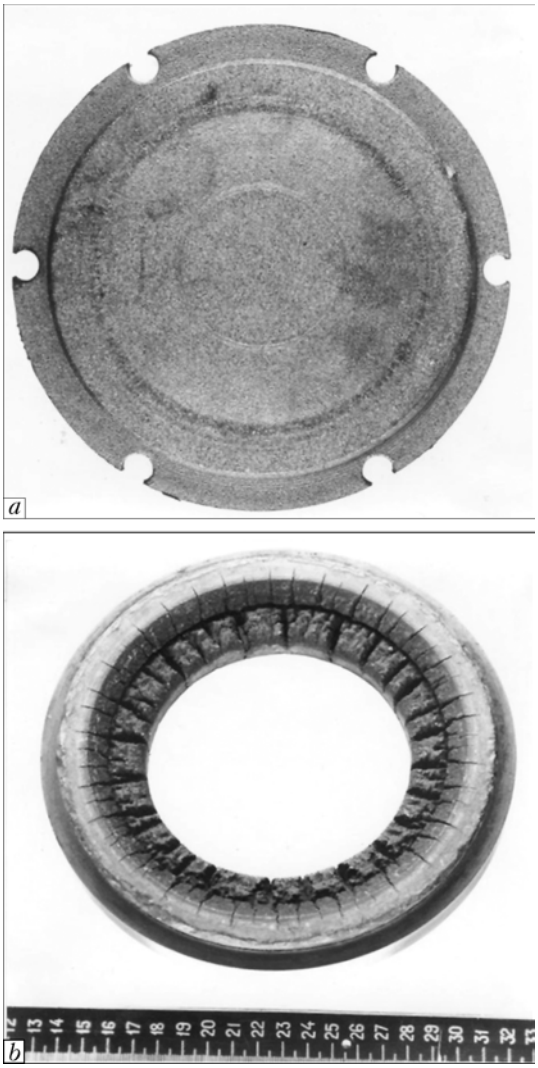

**Figure 4.** General view of waste flanges from OT4-2 titanium alloy: *a*, *b* — front and rear flanges of chill mould, respectively

subsequent machining, that's why they should not be considered as defects of the surface (Figure 7).

In surface layer of the ingots torsions or subcrustal porosity were not detected. In case of observance of the technological conditions at final stages of melting, shrinkage cavity in the IMSM ingots is absent (Figure 8). All this increases the efficient metal yield up to 96 %.

As a whole crystalline structure of the IMSM ingots in regard to direction of crystals is the same as in other remelting processes, but size of the crystals, as showed metallographic investigations, is by 1.0–1.5 points smaller, which is stipulated by intensive mixing of the metal pool in electromagnetic field.

Chemical composition of metal of the ingots, melted from waste elements of the casting fitting-out, is presented in Table 7.

As to the content of main alloying elements, metal of the ingot corresponds to requirements of the standard for the OT4-2 alloy, and in regard to the content of regulated impurities it does not exceed requirements of the specifications for secondary alloys.

Results of investigation of the influence of methods of preparation for remelting of waste titanium

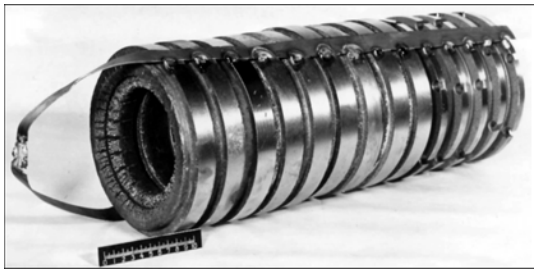

**Figure 5.** Consumable billet assembled from waste flanges of OT4-2 titanium alloy

flanges on weight share of gas impurities in metal of the ingots are of interest (Table 8).

Amount of gas impurities in the metal of ingots, melted from the preliminary non-cleaned flanges, somewhat exceeds allowable norms. Preliminary cleaning by shot-blasting of the flanges before assembly of the consumable billets allows reducing content of gas impurities down to the level, which meets requirements of the specifications. Even more clean gets metal of the ingots, melted from the flanges additionally scrubbed in hot solution of soda, then flushed by water, and dried at the temperature 380–400 K. Higher quality results may be achieved if the flanges to be remelted are subjected to etching in the solution of acids.

As it follows from data of Table 8, in remelting of consumable billets from the non-cleaned flanges noticeably increases in the metal content of nitrogen and oxygen, in contrast to the ingots melted from the preliminarily cleaned flanges, where increase of gas impurities, is insignificant. The data obtained prove that the main share of impurities is brought in the course of remelting into the molten metal together with oxide films, covering surface of the flanges. Shot-blasting of the flanges sharply reduces arrival of nitrogen and oxygen into the metal, and content of gas impurities gets within established by the regulated limits.

Weight share of hydrogen in the ingots is significantly lower in comparison with the initial content irrespective of the quality of preparation of the flanges for remelting.

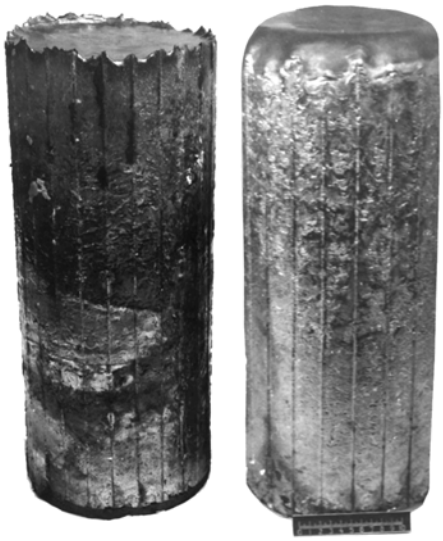

**Figure 6.** Ingots melted from OT4-2 titanium alloy wastes ($D_{ingot}$ = = 220 mm)

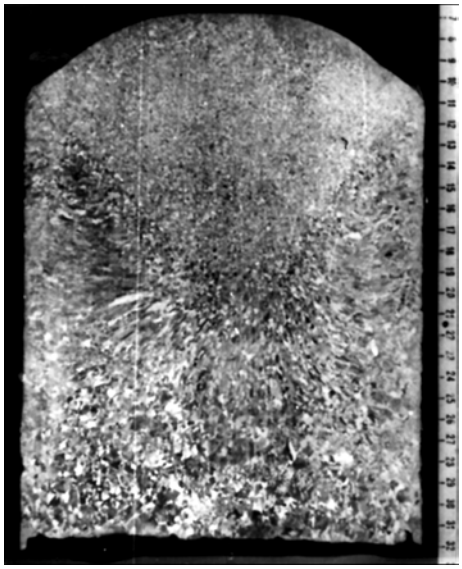

**Figure 7.** Macrostructure of head part of ingot melted with removal of shrinkage cavity

It should be noted that in bottom part of the ingots a higher concentration of gas impurities was registered. Such character of their distribution is stipulated by the fact that at the start period of melting, during temperature increase, in the melting chamber the adsorbed on its walls nitrogen and oxygen transit into the furnace atmosphere and are then dissolved in the molten metal. Further build up of the ingot occurs in the scrubbed in this way atmosphere.

Results of the hardness measurement showed that the metal melted from the non-cleaned flanges had, as one should have expected, higher hardness than the initial metal (Table 9). Surface cleaning of the flanges enabled production of the metal, hardness of which did not exceed the initial one.

Majority of titanium alloys, including the OT4-2 alloy, contain aluminium and manganese, which have high vapor pressure at the titanium melting point, as alloying components. That's why melting of the alloys, which include these elements, as well disposal of the formed wastes by remelting thereof are connected with certain difficulties, stipulated by significant losses of aluminium and manganese under conditions of vacuum melting. The IMSM process is performed, as a rule, in inert gas at atmospheric pressure in the melting chamber. That's why even rather long seasoning (up to 25 min) of the metal melt in argon at atmospheric pressure does not cause significant losses of aluminium and manganese in the titanium alloys (Table 10).

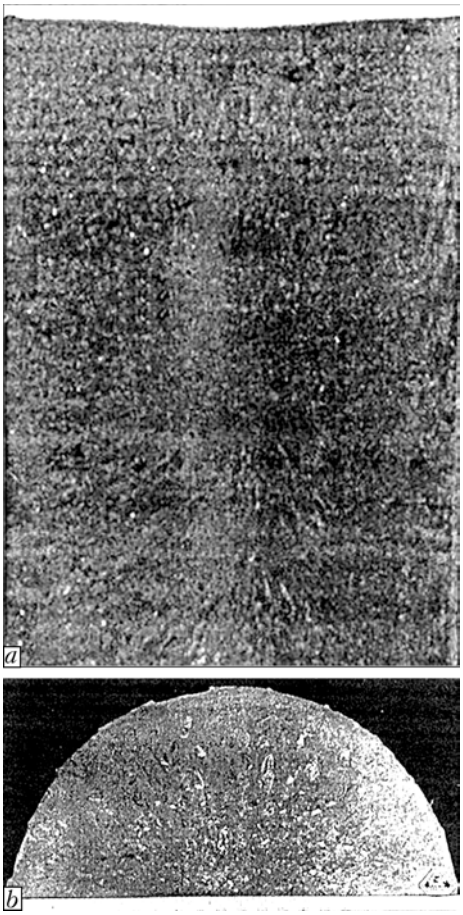


**Figure 8.** Macrostructure of IMSM ingots of 200 mm diameter from OT4-2 alloy: *a*, *b* — longitudinal and cross sections, respectively

Losses of these elements do not exceed 3.5 (aluminium) and 2.8 rel.% (manganese) at seasoning of the melts in molten state for 25 min. Under real conditions of remelting duration of a portion of the metal stay in molten state does not exceed 10–15 min and, therefore, losses of these elements are even less.

Effect of multiplicity of the induction remelting of the OT4-2 alloy wastes on content of gas impurities may be judged by the data presented in Table 11.

As one can see from presented data, at each stage of remelting increase of content of such impurities as oxygen and nitrogen occurs, which allows repeated remelting of the casting fitting-out elements from the titanium alloy, which got unfit for operation.

**Table 7.** Chemical composition of metal of OT4-2 alloy ingots

| Place of sampling | Weight share, % | | | | |
|---|---|---|---|---|---|
| | Alloying elements | | Impurities | | |
| | Àl | Ì ï | Fe | Si | Ñ |
| Initial metal | 3.69 | 1.27 | 0.22 | 0.13 | 0.07 |
| Ingots | 3.62 | 1.06 | 0.41 | 0.19 | 0.12 |
| Regulated by standard and specifications | 0.5--4.0 | 0.5--2.0 | ≤ 0.6 | ≤ 0.3 | ≤ 0.15 |

**Table 8.** Content of gas impurities in IMSM ingots of OT4-2 alloy

| Kind of charge | Place of sampling in ingots | Weight share of gases, % | | |
|---|---|---|---|---|
| | | [Î] | [N] | [Í] |
| Flanges without cleaning | Head | 0.224–0.227 | 0.047–0.051 | 0.012–0.014 |
| | Middle | 0.280–0.234 | 0.050–0.056 | 0.013–0.016 |
| | Bottom | 0.292–0.328 | 0.051–0.062 | 0.013–0.017 |
| Flanges after shot-blasting | Head | 0.218–0.225 | 0.034–0.039 | 0.008–0.009 |
| | Middle | 0.218–0.224 | 0.035–0.039 | 0.010–0.012 |
| | Bottom | 0.231–0.244 | 0.038–0.044 | 0.010–0.012 |
| Flanges after shot-blasting and scrubbing | Head | 0.183–0.191 | 0.030–0.033 | 0.007–0.009 |
| | Middle | 0.194–0.198 | 0.029–0.033 | 0.007–0.009 |
| | Bottom | 0.213–0.218 | 0.036–0.041 | 0.009–0.012 |
| Initial metal | Flanges | 0.177–0.225 | 0.029–0.043 | 0.018–0.038 |
| Regulated according to specifications | – | ≤ 0.30 | ≤ 0.06 | ≤ 0.015 |

**Table 9.** Hardness values of OT4-2 titanium alloy

| Object of investigation | *Í Â* | | |
|---|---|---|---|
| | Bottom part | Middle | Head part |
| Ingot from flanges: | | | |
| non-cleaned | 375–385 | 370–380 | 360–375 |
| cleaned | 253–277 | 251–263 | 228–248 |
| Initial metal | – | 270–285 | – |
| Regulated hardness of alloy according to specifications | – | ≤ 300 | – |

**Table 10.** Change of content of aluminium and manganese in titanium alloys depending upon duration of seasoning in molten state

| Alloying elements | Initial weight share of elements in alloy, % | Change of weight share of elements, %, at duration of seasoning, min | | | | |
|---|---|---|---|---|---|---|
| | | 5 | 10 | 15 | 20 | 25 |
| Aluminium | 2.97 | 2.96 | 2.96 | 2.96 | 2.93 | 2.90 |
| Manganese | 2.09 | 2.08 | 2.06 | 2.05 | 2.03 | 2.01 |
| Aluminium | 3.83 | 3.82 | 3.80 | 3.76 | 3.74 | 3.71 |
| Manganese | 1.82 | 1.82 | 1.80 | 1.79 | 1.77 | 1.76 |

**Table 11.** Content of gas impurities in OT4-2 titanium alloy after IMSM

| Number of remelts | Weight share of elements, % | | |
|---|---|---|---|
| | [Î] | [N] | [H] |
| Initial metal | 0.182 | 0.034 | 0.018 |
| First remelt | 0.218 | 0.039 | 0.013 |
| Second remelt | 0.242 | 0.045 | 0.010 |
| Third remelt | 0.255 | 0.052 | 0.009 |
| Regulated by specifications | ≤ 0.300 | ≤ 0.060 | ≤ 0.015 |

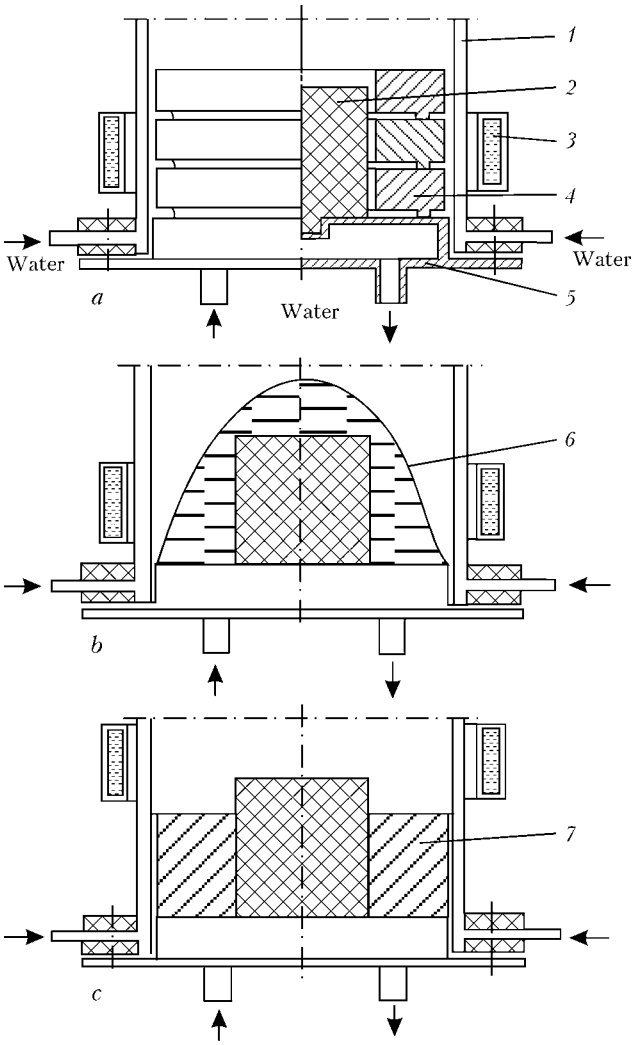


**Figure 9.** Operation-by-operation scheme of melting of hollow ingots-billets (of washer type) on OP117 installation: *a* — arrangement of charge and rod in sectional mould; *b* — charge melting; *c* — hardening of metal; *1* — mould; *2* — graphite rod; *3* — inductor; *4* — scrap of titanium items; *5* — bottom plate; *6* — molten metal; *7* — cast

**Figure 10.** Appearance of hollow ingot-billet (of washer type) of 220 mm diameter with graphite rod

Content of hydrogen in the alloy even after repeated remelting practically remains at the same level. Moreover, trend to its reduction is noted.

For the purpose of the machining volume reduction in manufacturing of the casting fitting-out from secondary OT4-2 titanium alloy, the technology of melting on the OP117 installation of billets with the dimensions close to those of the items, was developed. For this purpose the previously used mould of 800 mm height was replaced for a shorter one of 40 mm height. Due to this volume of the melting chamber filled by argon, reduced by more than 30 %, which enabled saving of the inert gas and reduction of melting cycle of the billets.

In addition, the OP117 installation was equipped with a pneumatic device, on which the bottom plate was fixed. Using pneumatic device, air-tight pressing of the bottom plate to the lower flange of the sectional mould was performed, which made it possible to significantly reduce time for preparatory operations, connected with loading of the titanium charge into the mould and removal of the ingot.

A cylindrical recess was made axially in the bottom plate, into which a graphite rod of 80–85 mm diameter was installed before each melting. Installation of the rod allowed melting a billet in the shape of a ring, which sharply reduced volume of machining and amount of wasted metal in the form of chips.

Scheme of melting of the ring billets from titanium alloy on the OP117 installation is presented in Figure 9. Appearance of the produced ring billet is shown in Figure 10.

In melting of the ring billets each melt is actually brought to the start period of a conventional melting, whereby full melting of the charge (waste flanges) occurs within 10–12 min, and the whole cycle of the ring billet melting (from loading of the charge to removal of the billet) lasts for about 20–22 min.

Small overheating of the melt and its short contact with surface of the graphite rod do not cause significant increase of carbon content in the alloy and can not be a reason for rejection of the produced items.

## CONCLUSIONS

1. In the course of fulfilled at the E.O. Paton Electric Welding Institute technological investigations and industrial application it was shown that the IMSM method may be successfully used for disposal of industrial wastes of titanium and its alloys at the machine building and metallurgical enterprises.

2. It was established that the design of melting installations for IMSM and their maintenance make them competitive in comparison with the electron beam melting and, in a number of cases, the only economically justified method of the titanium waste remelting under conditions of a machine-building enterprise.


1. Garmata, V.L., Petrunko, A.N., Galitsky, N.V. et al. (1983) *Titanium*. Moscow: Metallurgiya.
2. Rodyakin, V.V., Kushkin, B.N., Arutyunov, E.L. et al. (1967) *Influence of technology of magnesium-thermic reduction process on residual content of chlorine in titanium spongy:* Transact. Vol. 1. Moscow: Metallurgiya, 112–122.
3. Rodyakin, V.V. (1977) *Magnesium-thermic production of spongy titanium*. Moscow: Metallurgiya.
4. Sandler, R.A., Petrunko, A.N., Likhterman, V.A. et al. (1987) *Refining of spongy titanium blocks*. Moscow: Metallurgiya.
5. Rodyakin, V.V., Geger, V.E., Skripnyuk, V.M. (1971) *Magnesium-thermic production of spongy titanium*. Moscow: Metallurgiya.
6. Latash, Yu.V., Konstantinov, V.S., Gorbenko, V.A. et al. (1989) Industrial application of low-temperature plasma in melting of electrode ingots from low-grade spongy titanium for production of stop-valve titanium bodies. *Problemy Spets. Elektrometallurgii*, **3**, 71–75.
7. Shippereit, G.H., Zethepman, A.F., Evers, D. (1961) Cold-crucible induction melting of reactive metals. *J. of Metals*, 13(**2**), 140–144.
8. Clites, P.G., Beall R.A. (1969) Inductoslag melting of titanium. *Kept. Investig. Bur. Mines. Dept. Interior*, **7268**, 1–20.
9. Chonister, D. (1986) Induction melting of titanium. Zirconium and reactive metals. In: *Proc. of AVS/ASM Conf. on Vacuum Metallurgy* (Pittsburgh, June, 1986), 2–4.
10. Latash, Yu.V., Shejko, I.V., Konstantinov, V.S. (1990) Melting of high-reactive, noble and rare-earth metals and alloys in plasma and induction units with cold crucible-mould. In: *Problems of welding and special electrometallurgy*. Kiev: Naukova Dumka.
11. Latash, Yu.V., Shejko, I.V., Bernadsky, V.N. et al. (1986) Induction remelting in sectional mould, possibilities and prospects of its application for remelting of titanium waste. *Problemy Spets. Elektrometallurgii*, **2**, 64–70.
12. Zhadkevich, M.L., Latash, Yu.V., Konstantinov, V.S. et al. (1997) On problem of feasibility of remelting of spongy titanium with higher content of man-caused impurities. Report 1. *Ibid.*, **1**, 55–60.
13. Zhadkevich, M.L., Latash, Yu.V., Konstantinov, V.S. et al. (1998) On problem of feasibility of remelting of spongy titanium with higher content of man-caused impurities. Report 2. *Ibid.*, **2**, 43–45.
14. Zhadkevich, M.L., Latash, Yu.V., Konstantinov, V.S. et al. (2001) On problem of application of independent heating source for recycling of wastes of titanium and its alloy. *Ibid.*, **1**, 27–31.
15. (1985) *Powder metallurgy of titanium alloys*. Ed. by A.S. Frous. Moscow: Metallurgiya.
16. (1979) *Dispersion powders and materials on their base*. Ed. by V.V. Skorokhod. Kiev: IPM.
17. (1986) *Ultrarapid tempering of molten alloys*. Ed. by G. German. Moscow: Metallurgiya.
18. (1983) Powder metallurgy. In: *Results of science and engineering*. Vol. 1. Moscow: VINITI.

# Prof. M.L. ZHADKEVICH IS 70

Prof. L.M. Zhadkevich, Doctor of Technical Sciences, corresponding member of the NAS of Ukraine, noted specialist in the field of materials science, metals technology and special electrometallurgy, and Deputy Director of the E.O. Paton Electric Welding Institute, was 70 on the 12th of July, 2007.

He started to be involved into problems of the technology of metals in 1955 at the Kujbyshev Metallurgical Works, whereto he was appointed after graduating from a technical school. There he passed the path from a pressman to a chief of the country-largest pressing workshop. Then he completed education at the All-Union Correspondence Polytechnic Institute, and became one of the leading specialists in the field of materials science and pressure treatment of metals. Production of blanks and assemblies of high-strength aluminium and other alloys for machine- and ship-building, aircraft engineering and rocket construction was arranged under the leadership of M.L. Zhadkevich.

In 1977, M.L. Zhadkevich was appointed to the Kiev Zonal Research Institute for standard and experimental design of residential and public buildings, where he headed a division for experimental aluminium constructions and developed technologies for production of aluminium parts. He was leading the activity on mastering the technologies for pressing and fabrication of standard and unique building aluminium structures in Brovary, Voronezh, Khabarovsk and Kishinyov.

M.L. Zhadkevich has been working at the E.O. Paton Electric Welding Institute since 1984. He was a director of the Pilot Plant for Special Electrometallurgy from 1985. Under difficult conditions of restructuring of the economy of the country, by handling organisational and research problems he managed to provide successful functioning of the Plant in building of a new generation of equipment and technologies for electroslag casting of billets for heavy and power engineering, electron beam welding of large-size units of rockets from super strong aluminium alloys, hardening and repair spraying of blades for gas turbine and other power generation parts and units, ship building and defence industry.

Since 1993 L.M. Zhadkevich has been the Deputy Director in research activities at the E.O. Paton Electric Welding Institute, and Head of Department «New Physical-Technical Methods for Welding and Special Electrometallurgy». He was the first to develop new multi-component nickel- and cobalt-base alloys for hardening and repair technologies. He elaborated scientific principles of simulation of complex electrometallurgy processes, as well as production of nanocrystalline and other materials with high service properties.

Theoretical and experimental studies performed by L.M. Zhadkevich at a high scientific level are of interest to specialists involved in development of welding and related technologies. Being a supervisor of a research area, he trained 4 doctors and 3 candidates of technical sciences. M.L. Zhadkevich is the author of over 420 scientific papers, including 8 monographs. Equipment, materials and technologies developed under the leadership of M.L. Zhadkevich have been widely applied in fabrication of critical aerospace

structures, power generation equipment, parts used in defence industry, instrument making, etc. They are covered by dozens of patents and author's certificates, and noted with many medals and diplomas.

M.L. Zhadkevich combines to advantage the research and scientific-organizational activities. He is a member of the Inter-Departmental Commission on State Program «Titanium of Ukraine», member of the Inter-Departmental Commission on non-ferrous metallurgy, member of the Scientific Board of the E.O. Paton Electric Welding Institute, Thesis Defence Board of the E.O. Paton Electric Welding Institute, Board of Directors of the Joint Ukrainian-American Experimental Centre «Pratt & Whitney–Paton», and member of the editorial boards of a number of publications.

For his contribution to the progress of materials science, and development of high-efficiency technologies for production and processing of new materials in particular, as well as for his fruitful scientific-organisational activity, M.L. Zhadkevich was awarded the Order of the Red Banner of Labour, medals, honorary title «Honoured Scientist and Technician», and State Prize of Ukraine in the field of science and technology. He is a corresponding member of the National Academy of Sciences of Ukraine, and a full member of the Academy of Technological Sciences.

*We cordially congratulate the hero of the jubilee and wish him from the bottom of our hearts good health, personal happiness and great success in accomplishment of his creative plans.*

*E.O. Paton Electric Welding Institute of the NAS of Ukraine*
*Editorial boards of «Sovremennaya Elektrometallurgiya» and «Advances in Electrometallurgy» journals*